Wave Forces on Vertical and Composite Breakwaters

N W H Allsop
D Vicinanza
J E McKenna

Report SR 443
March 1995, revised March 1996

HR Wallingford

Address and Registered Office: **HR Wallingford Ltd.** Howbery Park, Wallingford, Oxon OX10 8BA
Tel: + 44 (0)1491 835381 Fax: + 44 (0)1491 832233

Registered in England No. 2562099. HR Wallingford is a wholly owned subsidiary of HR Wallingford Group Ltd.

Contract

The work described in this report was part-funded by the Department of Environment Construction Sponsorship Directorate under research contracts PECD 7/6/263 and 7/6/312, and part by the European Union MAST programme under contracts MAS2-CT92-0047 and MAS3-CT95-0041. Additional research support was given by the University of Sheffield, Queen's University Belfast, and by the Department of Hydraulics of the University of Naples, with further funding for visiting researchers at Wallingford from the Department of Education of Northern Ireland, DENI, the TECHWARE programme of COMETT, and the National Council for Research in Italy, CNR.

The project co-ordinator for the MAST II MCS-Project under contract MAS2-CT92-0047 was Dr-Ing H. Oumeraci of Franzius Institute of Hannover University. The project officer for European Commission Directorate General XII was Mr C. Fragakis.

The project co-ordinator for the MAST III project PROVERBS under contract MAS3-CT95-0041 was Professor H. Oumeraci of Leichtweiss Institute of University of Braunschweig. The project officer for European Commission Directorate General XII was Mr C. Fragakis.

The DOE nominated officer for research contracts PECD 7/6/263 and 7/6/312 was Mr P.B. Woodhead and HR Wallingford's nominated officers were Dr W.R. White and Professor N.W.H. Allsop. This report is published by HR Wallingford on behalf of the DOE, but any opinions expressed are those of the authors, and not necessarily those of the funding department.

The research described in this report was conducted within the Coastal Group of HR Wallingford, at Queen's University of Belfast, and at the University of Naples, under the overall supervision of Professor N.W.H. Allsop. The HR Wallingford job numbers were CAS 41, CAS 58, and CAS 169. The HR Wallingford file was C/E/1/3.

Prepared by N.W.H. Allsop (name) Manager Coastal Structures (job title)

Approved by K.Atwell Director, HR Wallingford

Date 16 October 1996

Summary

Wave Forces on Vertical and Composite Breakwaters

N W H Allsop
D Vicinanza
J E McKenna

Report SR 443
March 1995, revised March 1996

This report gives information on wave loadings on vertical and composite breakwaters and related harbour or coastal structures. The report reviews types of vertical breakwaters used around the UK, in Europe, and further overseas, and identifies design methods in use in the UK, Europe, and Japan. Analysis of performance in service, and of research studies, shows that present design methods underpredict wave loads under wave impact conditions, and are not able to identify reliably geometric / wave conditions which lead to such impacts.

Comprehensive 2-dimensional hydraulic model tests were conducted in a random wave flume at HR Wallingford to measure wave pressures on a wide range of simple and composite vertical walls, under normal wave attack ($\beta=0°$). The test results have been used to:

- Assess the reliability of existing prediction methods;
- Identify the ranges of geometric and wave conditions which lead to wave impacts;
- Develop simple methods to estimate wave forces under impact conditions.

The results of the tests have been compared with predictions by a number of different methods. Analysis of the percentage of impacts relative to all waves has been used to define a new decision diagram which summarises parameter regions in which wave conditions and wall / mound geometries lead to breaking wave impacts. For pulsating wave conditions, Goda's method has been found to be generally appropriate, but for wave impact conditions, it under-estimates loads significantly, even when extended by Takahashi. Up-lift forces are generally well predicted by Goda's method for pulsating conditions, but again under-estimated for impact conditions. For wall configurations that most resemble crown wall sections, the method in the CIRIA Rock Manual developed by Bradbury & Allsop gives generally safe predictions.

The results of these studies are intended to be of direct use to engineers analysing the stability of vertical or composite walls in deep water, in harbours, or along the shoreline. The prediction methods derived here, and/or the test results themselves, may be used to estimate wave loadings on a wide variety of structures, existing or in design. The report is also written for other researchers working in this field, to illustrate the range of data available for more detailed analysis, identify regions of continuing uncertainties, and to assist set priorities for future studies.

The work reported here was part-funded by the Department of Environment Construction Sponsorship Directorate under research contracts PECD 7/6/263, PECD 7/6/312 and CI 39/5/96, and part by the European Union MAST programme under the MCS-Project, contract MAS2-CT92-0047, and later the PROVERBS project, contract MAS3-CT95-0041. Additional support was given by the University of Sheffield, Queen's University Belfast, and by the Department of Hydraulics of the University of Naples, with further funding for visiting researchers at Wallingford from the Department of Education of Northern Ireland, DENI, the TECHWARE programme of COMETT, and the National Council for Research in Italy, CNR.

For any further information on these and related studies, please contact N.W.H. Allsop, in the Coastal Group at HR Wallingford.

Notation

A_c	Armour crest freeboard
a	Empirical coefficient
B_b	Crest width of rubble mound berm
B_c	Width of caisson
B_{cw}	Width of crown wall
B_{eq}	Equivalent width of rubble mound in front of wall, averaged over height of mound
B_{wl}	Structure width at static water level
B_t	Width of rubble mound at toe level
b	Empirical coefficient
C_r	Coefficient of wave reflection
$C_r(f)$	Reflection coefficient function
C_t	Coefficient of wave transmission
D	Particle size or typical diameter
D_n	Nominal particle diameter, defined $(M/\rho_r)^{1/3}$) for rock and $(M/\rho_c)^{1/3}$ for concrete armour
D_{n50}	Nominal particle diameter calculated from the median particle mass M_{50}
d	Water depth over toe mound in front of wall
E_i	Incident wave energy
E_r	Reflected wave energy
E_t	Transmitted wave energy
F_B	Buoyant up-thrust on a caisson or related element
F_F	Earth pressure force on a caisson from the seaward part of the mound
F_R	Earth pressure force on the caisson from the harbour side of the mound
F_S	Factor of safety
F_h	Horizontal force on caisson or crown wall element
$F_{h99.8\%}$	Horizontal force at 99.8% non-exceedance level
$F_{h1/250}$	Mean of highest 1/250 horizontal wave forces
F_u	Up-lift force on caisson or crown wall element
$F_{u99.8\%}$	Up-lift force at 99.8% non-exceedance level
$F_{u1/250}$	Mean of highest 1/250 up-lift wave forces
f	Wave frequency
f_m	Frequency of peak of wave energy spectrum, = $1/T_p$
g	Gravitational acceleration
H_{max}	Maximum wave height in a record
H_{m0}	Significant wave height from spectral analysis, defined $4.0m_0^{0.5}$
H_{so}	Offshore significant wave height, un-affected by shallow water processes
H_s	Significant wave height, average of highest one-third of wave heights
$H_{2\%}$	Wave height exceeded by 2% of waves in a record
$H_{1/10}$	Mean height of highest 1/10 of waves in a record
h	Water depth
h_b	Height of berm above sea bed
h_c	Height of rubble mound / core beneath caisson / wall
h_f	Exposed height of caisson or crown wall over which wave pressures act
h_s	Water depth at toe of structure
k	Permeability (Darcy), also used as wave number = $2\pi/L$

L	Wave length, in the direction of propagation
L_m	Offshore wave length of mean (T_m) period
L_o	Deep water or offshore wave length - $gT^2/2\pi$
L_p	Offshore wave length of peak (T_p) period
L_{Ps}	Wave length of peak period at structure
M_h	Overturning moment due to horizontal wave force
M_u	Overturning moment due to up-lift force
M_t	Overturning moment due to all wave loads
M_{50}	Median mass of armour unit derived from the mass distribution curve
m_0	Zeroth moment of the wave energy density spectrum
m_2	Second moment of the wave energy density spectrum
N_{wo}	Number of waves overtopping expressed as proportion or % of total incident
N_z	Number of zero-crossing waves in a record = T_R/T_m
n_v	Volumetric porosity, volume of voids expressed as proportion of total volume
P	Encounter probability
P_f	Target probability of failure
p	Wave pressure
q	Mean overtopping discharge, per unit length of structure
q_s	Superficial velocity; or specific discharge, discharge per unit area, usually through a porous matrix
R_c	Crest freeboard, height of crest above static water level
R_u	Run-up level, relative to static water level
R_{us}	Run-up level of significant wave
$R_{u2\%}$	Run-up level exceeded by 2% of run-up crests
r	Roughness or run-up reduction coefficient, usually relative to smooth slopes
S_F	Shear force at caisson / rubble boundary
$S(f)$	Spectral density
s_m	Steepness of mean wave period = $2\pi H/gT_m^2$
s_p	Steepness of peak wave period = $2\pi H/gT_p^2$
T_m	Mean wave period
T_{Pf}	Return period = $(1 - (1 - P_f)^{1/T})^{-1}$
T_p	Wave period of spectral peak, inverse of peak frequency
T_R	Length of wave record, duration of sea state
T_s	Wave period associated with H_s, not statistically significant
u, v, w	Components of velocity along x, y, z axes
x, y, z	Orthogonal axes, distance along each axis
z	Level in water, usually above seabed
α (alpha)	Structure front slope angle to horizontal
β (Beta)	Angle of wave attack to breakwater alignment
ρ (rho)	Mass density, usually of fresh water
ρ_w	Mass density of sea water
ρ_r, ρ_c, ρ_a	Mass density of rock, concrete, armour units
Δ (delta)	Reduced relative density, eg. $(\rho_r/\rho_w)-1$
λ (lambda)	Model / prototype scale ratio (Froude); also used as fraction of aeration
μ (mu)	Coefficient of friction, particularly between concrete elements and rock; also $\mu(x)$ = mean of x
ξ (xi)	Iribarren number or surf similarity parameter, = $\tan\alpha/s^{1/2}$

ξ_m, ξ_p	Iribarren number calculated in terms of s_m or s_p
ϕ (phi)	Angle of internal friction of rock or soil
τ (tau)	Shear strength of rock mound or soil, also used as the time interval between samples
σ (sigma)	Stress
$\sigma(x)$	Standard deviation of x
σ'	Normalised standard deviation σ/μ
σ_n	Normal stress

Contents

Contents continued

Tables

Figures

Contents *continued*

1 Introduction

Harbour breakwaters and related marine structures may be of two general forms:

a) Impermeable and solid with vertical or very steep faces;
b) Rubble mound with permeable and rough side slopes.

Much research effort has addressed the stability and hydraulic performance of rubble mound breakwaters, but relatively less effort has been directed towards the stability of vertical walls. Relatively little reliable information is available on wave forces / pressures on vertical / composite walls.

This report presents results from new research studies to derive information on wave forces acting on vertical and composite walls and related maritime structures, Figure 1.1. The studies were targeted primarily at vertical breakwaters, especially those formed by monolithic caissons, or by large concrete or stone blocks joined to act monolithically. Some results of these studies can also be applied to coastal seawalls or other steep or vertically faced structures, and some results can be applied to crown walls on rubble mound breakwaters or seawalls, although the experimental work was not specifically configured to address those structures.

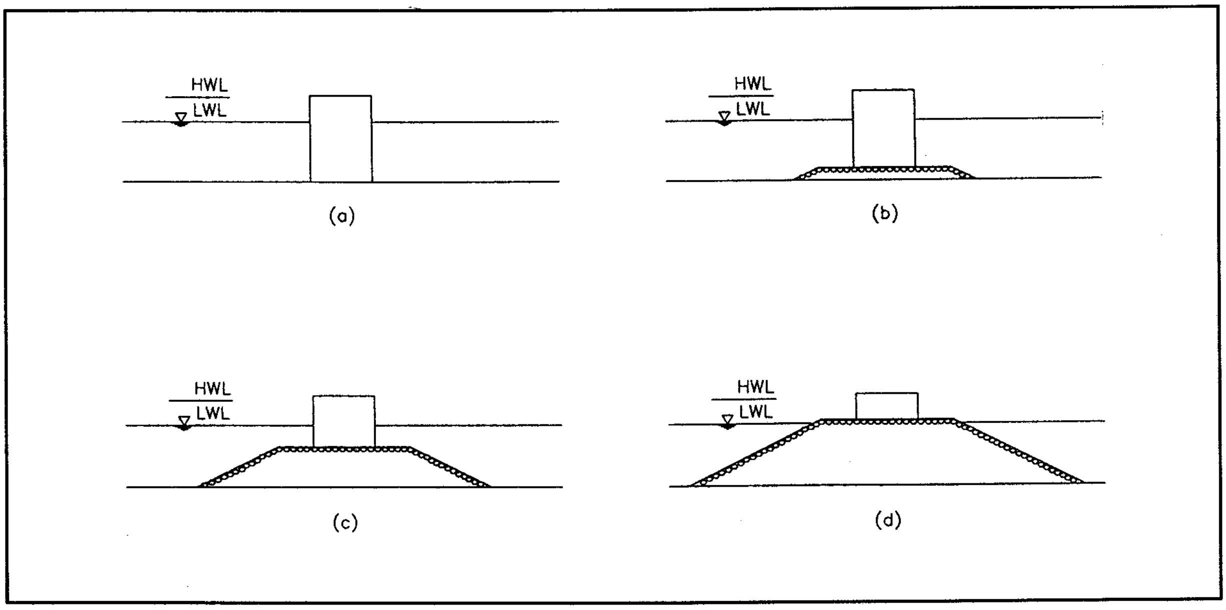

Figure 1.1 Vertical and composite breakwater configurations

1.1 The problem

Breakwaters and related structures are built primarily to give protection against wave attack on ship moorings, manoeuvring areas, port facilities, and adjoining areas of land. Design methods for such structures are generally well established, but some important aspects of those design methods are now seen to be uncertain or of limited application for some configurations. Recent research studies in Europe have confirmed that design methods for wave forces based on studies in Japan on caisson breakwaters are limited in their application; give little data on local wave pressures; and may severely under- or over-estimate loadings in some important cases. Using such methods, some structures may be over-designed, and hence too expensive. For others risks of failure may be under-estimated, leading to danger to personnel and property.

European engineers including UK consultants and contractors are involved in analysis, design, rehabilitation, and construction of harbour and coastal structures worldwide. UK design methods / codes are used internationally. It is therefore particularly important that such methods are well-based and reliable.

1.2 Terms of reference for the study

The primary objective of the work commissioned by DOE under contract 7/6/312 was to provide design data for vertical faced breakwaters and related structures on the stability response under wave attack. The programme of work described at the start of the studies was summarised:

a) describe the strength and hydraulic properties of the principal structure types and component elements;
b) identify the principal failure modes for such structures, and each of the main elements;
c) describe the design methods used internationally;
d) carry out parametric model studies to quantify the responses of selected structure cross-sections to the appropriate range of input conditions;
e) identify the remaining areas of uncertainty, specification of future work needed for further improvement in economy and/or safety;
f) describe general design rules for vertical wall structures, identifying the range of application, and suggesting target factors of safety.

These terms of reference were expanded to allow the basic test set-up to be shared with two related projects. Studies under the Harbour Entrance project supported by DOE under contract 7/6/263 addressed the hydraulic performance of vertical walls. Under the European Union MAST research programme on Monolithic Coastal Structures (MCS-Project), HR Wallingford assisted by other European researchers extended those studies on hydraulic performance of simple vertical walls to include a range of "low reflection" alternative structure types. These included caissons with voided chambers, perforated wave screens, and armoured slopes in front of vertical walls. Results of those studies have been presented separately, see Allsop (1995), Allsop et al (1995b), McBride et al (1995a), and McBride & Watson (1995).

The studies on wave loadings and breakwater stability discussed here were expanded to include contributions from researchers from Belfast and Naples developed in collaboration with HR and University of Sheffield. The Ph.D project by McKenna at Queen's University Belfast was intended to address in more detail wave up-lift pressures on caisson breakwaters and related elements on permeable foundations, but the final project title adopted was slightly less specific as "Wave forces on caissons and breakwater crown walls". This study was started in October 1993, and is to be completed in September 1996. A further Ph.D project by Vicinanza at the University of Naples addressed temporal and spatial variation of wave impact pressures on vertical and composite walls with a project title of "Pressioni e forze di impatto di onde frangenti su dighe a paramento verticale e composte". Vicinanza's collaboration in these research studies started in November 1994, and his Ph.D studies are due to be reported in 1997.

The studies discussed in this report were conducted in a 2-dimensional (2-d) wave flume under normal wave attack. A later project supported by Department of Environment under contract CI 39/5/96 and EU MAST III under contract MAS3-CT95-0041, extended work reported here to cover effects of oblique and short-crested wave attack using a 3-dimensional wave basin, the UK national Coastal Research Facility. These tests are reported in HR report SR 465 by Banyard et al (1996).

1.3 Outline of the studies

Division of experimental work within this project was relatively straight-forward. Design of the model studies, the test sections, measurement systems, and the test programme were completed at Wallingford with assistance from Sheffield and Belfast during 1993 / 94. Model tests by the HR / Sheffield / Belfast team were completed in December 1994.

Expansion of the project to meet requirements of the other partners had however increased the number / complexity of tests substantially, and therefore the volume of data collected. Analysis therefore took more resources than anticipated, but did generate both more data and more reliable information than could otherwise have been expected. The main activities of each partner may be summarised:

HR Wallingford - overall design of studies; provision of test facility, measurement equipment, test structures, technical and computing support; lead analysis and reporting; and overall supervision. McKenna from Belfast supervised by Whittaker and Allsop extended the study to include more detailed analysis of up-lift pressures; assisted in test design; conducted many of the tests; and analysed up-lift forces and overall forces / stability.

Vicinanza supervised by Benassai and Calabrese from Naples modified and extended the analysis programs, and assisted in detailed analysis of wave pressures / forces and statistical analysis of wave forces, of pressure gradients and impulses.

Allsop at Sheffield reviewed much of the historical information on vertical breakwaters in the UK; provided support and supervision for the visiting researchers at Wallingford particularly in analysis of wave forces; and compiled and edited research papers and this report.

Studies under the MAST MCS project were divided into four areas covering: Task 1, impact forces and structure / foundation interaction; Task 2, scaling problems and air entrainment; Task 3, local morphological changes; and Task 4, wave overtopping and constructional measures. HR Wallingford were contracted to contribute to Task 3.1 on wave reflections, Task 3.3 on scour at vertical walls, and was scheduled to lead Task 4.3 on constructional measures to reduce reflections and overtopping.

During early stages in the MCS-Project, it became apparent that additional work was needed on impact forces / pressures. Analysis by Oumeraci et al (1995) demonstrated that impact loads are of critical importance in the stability of caisson breakwaters against progressive movements, and Allsop & Bray (1994) demonstrated that short duration impacts are of considerable importance to the integrity of blockwork walls. In the light of these findings, the Wallingford / Sheffield / Belfast / Naples team expanded their contribution to the MCS project with new studies on wave impact pressures added to Task 1 and discussed here. Work under Task 4.3 was also expanded, and has been reported in detail in the MCS and Harbour Entrances reports, see McBride et al (1996) for a summary.

1.4 Outline of this report

The main types of vertical walls in use in harbours or along coastlines are described in Chapter 2, and design methods available to determine the main hydraulic and structural responses are discussed in Chapter 3.

The design of research studies developed under this project, the structure configurations tested, and the test equipment and procedures are described in Chapter 4.

Results of the wave pressure / force measurements are first described in Chapter 5, which discusses the form and handling of the data collected, and definitions of wave pressure / force events needed to reduce the large volumes of data to more manageable proportions. The detailed analysis of these measurements are then discussed in Chapter 6, covering the distinctions between pulsating and impact conditions, and exploring the different prediction methods needed for these different response regions.

Application of the wave force results, and the prediction methods derived from them are discussed in Chapter 7, including a discussion on the effects of any scale corrections needed for wave pressures. Overall conclusions, and recommendations for design / analysis practice, and for future research, are addressed in Chapter 8.

2 Vertical breakwaters and related structures

This chapter describes the types and purposes of vertical and composite walls / breakwaters in use in the UK, in Italy and Japan, and elsewhere. The historical development of such structures is reviewed, illustrated by examples drawn from UK and overseas. Key features are identified from existing structures around the UK using stone or concrete blockwork, as well as for monolithic structures using concrete caissons around Italy and Japan.

The review draws on a number of sources identified below, but particularly on previous reviews by Allsop & Bray (1994), Franco (1994), Lamberti & Franco (1994), Oumeraci (1994c), and Tanimoto & Takahashi (1994a, b).

2.1 Purpose and form of structures

Breakwaters or seawalls have been built since the earliest development of the coastal zone. The primary purposes of such structures are to protect areas of water for navigation, anchorages or sheltered moorings; to protect working areas within and around harbours; or to defend land against erosion or flooding. Many such structures are required to serve a number of different purposes, and these may often change in time. The composition and construction of these structures owes much to local practice, taking particular account of local conditions and/or materials. The main types of harbour and coastal structure may be summarised:

- harbour breakwaters
- entrance channel breakwaters or moles
- cooling water breakwaters
- nearshore breakwaters, reefs, or sills
- groynes, bastions, and other beach control structures
- coastal seawalls
- coastal or shoreline revetments

These structures may be of three general forms:

a) impermeable / solid with vertical or steeply battered faces;
b) rubble mound with permeable and rough side slopes; or
c) composite construction incorporating a caisson or wall section on or behind a mound of armour.

The principal concern in the design process for a breakwater is to achieve required levels of wave protection in the harbour during service and extreme wave conditions. The degree of shelter required will depend on harbour usage, and will be most strongly influenced by the economics of the port operation. Wave protection is achieved by ensuring that the plan configuration, breakwater length and height, are sufficient to limit wave penetration to sensitive areas of the harbour at selected return periods or probabilities. These considerations influence the position and length of the breakwater, principally set by levels of wave diffraction, and its freeboard, generally set so that wave transmission over the structure is not excessive.

The main requirements for seawalls are essentially similar, with the structure required to limit to acceptable levels any wave overtopping, but also to protect the material behind or below the wall from erosion by direct or indirect wave forces.

A secondary consideration, but often presented as the major design case, is that any such structure should remain stable up to a given design condition, and/or that any damage should be restricted to given limits. Again different levels of damage / movement or safety factor may be accepted at different probability levels.

Around the UK, seawalls and revetments have been constructed to defend parts of the coastline against erosion, termed "coast protection"; or to reduce the level and/or risk of flooding of low-lying land by inundation from the sea, termed "sea defence". Seawalls may be generally vertical or steeply sloping, or they may be formed by embankments protected against erosion by armouring. Structures such as seawalls are substantially more numerous than large breakwaters, but many of the design methods and much of the technology derive from studies for breakwaters. Analysis / design methods in this report therefore focus primarily on larger structures used to defend coastlines and harbours, primarily harbour breakwaters for commercial / naval harbours or marinas; sometimes entrance channels for lagoons; or cooling water basins for power stations. They may be constructed in 5 to 50m of water and, where exposed to severe waves, rubble or composite breakwaters may be armoured by special concrete armour in sizes from 1 to 200 tonnes, although rarely above 40 tonne. Caissons may be constructed in sizes up to 3,000 tonnes, or even up to 10,000 tonnes.

Choices between different configurations are influenced by economics and availability of materials; by local construction practice and availability of plant; performance standards required from the structure and local environmental concerns; and client / designer preferences. In the UK, blockwork walls on rubble foundations were preferred during the last century, but rubble mounds have been more strongly favoured over the last 50 years. Caisson breakwaters are rare in the UK, although some structures use slice blockwork or sheet piles to form vertical walls. Designers elsewhere in Europe have also generally preferred rubble breakwaters for their relative ease of construction, less brittle failure modes, reduced susceptibility to wave impacts, and potentially reduced environmental impact, except in Italy where construction of vertical blockwork and caisson breakwaters dates back to the Roman era, and remains prevalent today. Engineers in Japan also strongly favour vertical caissons or, where wave forces may be particularly strong, horizontally composite breakwaters with a mound of armour units in front of the caisson.

2.2 Development of vertical breakwaters

In analysing the performance of vertical breakwaters or seawalls in the United Kingdom, it is useful to consider the design and construction of many historic structures, particularly those built during the major period of harbour development in and around the UK between 1830 and 1900. Many breakwaters constructed during that period still survive, and their stability is important to the continuing operation of the harbours protected.

The more common types of breakwater or seawall around the UK are of simple vertical or battered slope, with walls formed of stone or concrete blocks. Such structures were relatively cheap to construct when labour costs were low, and used a minimum of material. Breakwater walls were usually double-sided, but many quays or seawalls are backed by natural or imported materials. An example breakwater section from St Catherine's harbour on Jersey, constructed at about 1856, shows the dry masonry walls, the rubble filling between the walls, and the rubble mound on which the walls are founded, Figure 2.1.

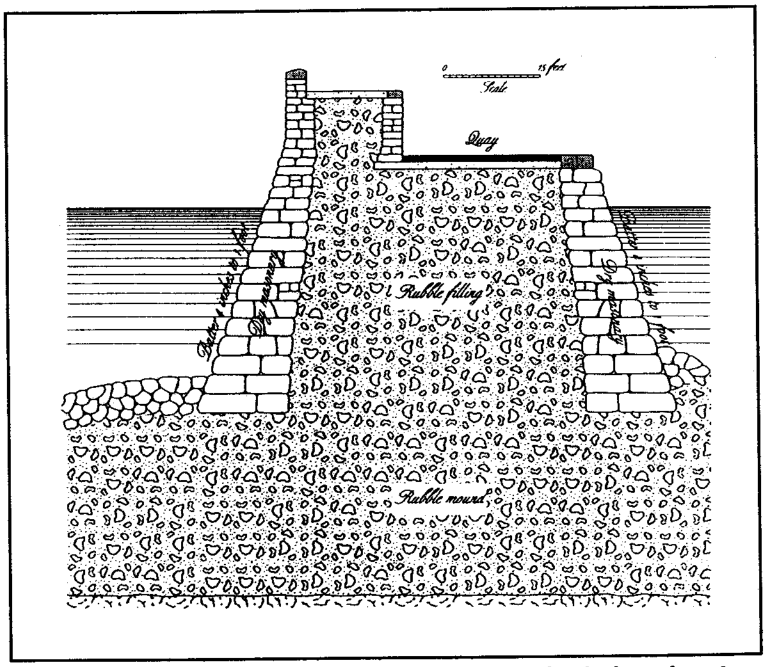

Figure 2.1 Stone blockwork, St Catherine's breakwater, Jersey 1996

Quarried stone is not naturally available in the rectangular shapes needed to form a coherent and stable wall. Production of stone blocks to acceptable sizes and tolerances used to be a routine task in civil engineering, but became significantly less economic as labour costs increased. Many breakwaters before 1900 therefore used large stone blocks to form the outer skin of the wall, with the core formed from smaller blocks and/or rubble infill. The use of concrete blocks to replace dressed stone blocks became more prevalent in the UK after 1850, see section of Dover breakwater in Figure 2.2.

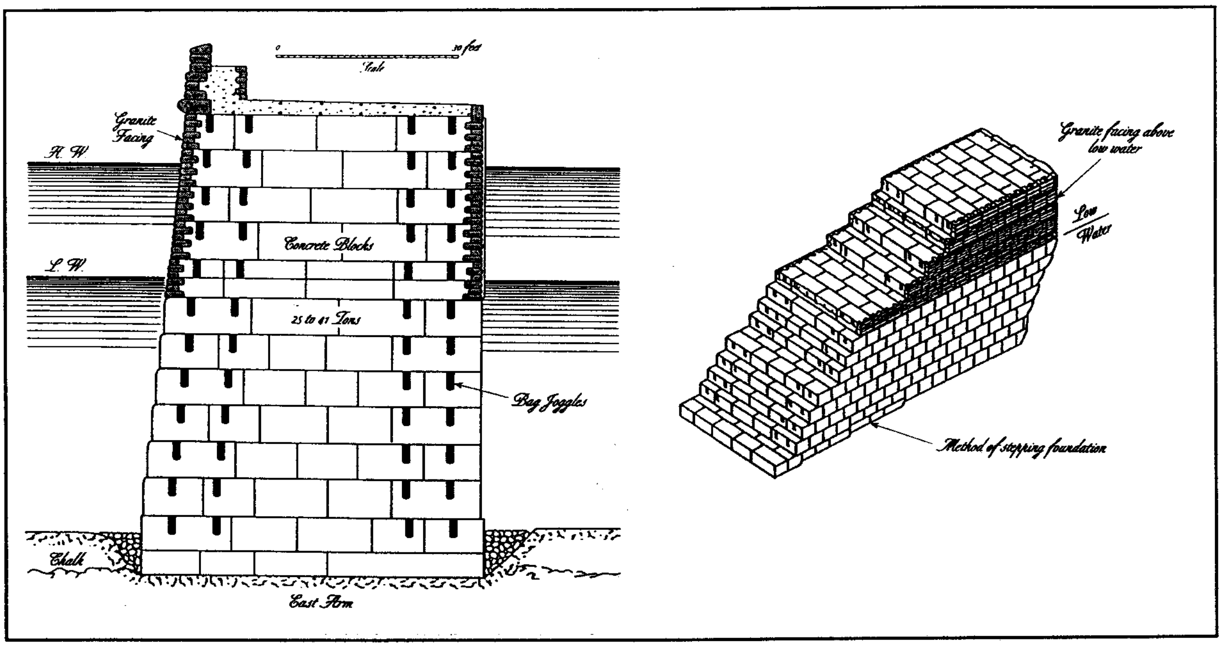

Figure 2.2 Concrete blockwork, East Arm Breakwater, Dover

Blockwork walls were constructed widely around the UK to form breakwaters, dock or quay walls, and seawalls. Whilst the main purposes of the breakwaters were to give quiet water for moored or manoeuvring vessels; and provide shelter for cargo handling operations, they were also often used as quays, support for cranes and other equipment, and additional space for cargo. Some breakwaters known as "Moles" or "Piers", Figure 2.3, also acted as training walls at the mouth of a river or estuary.

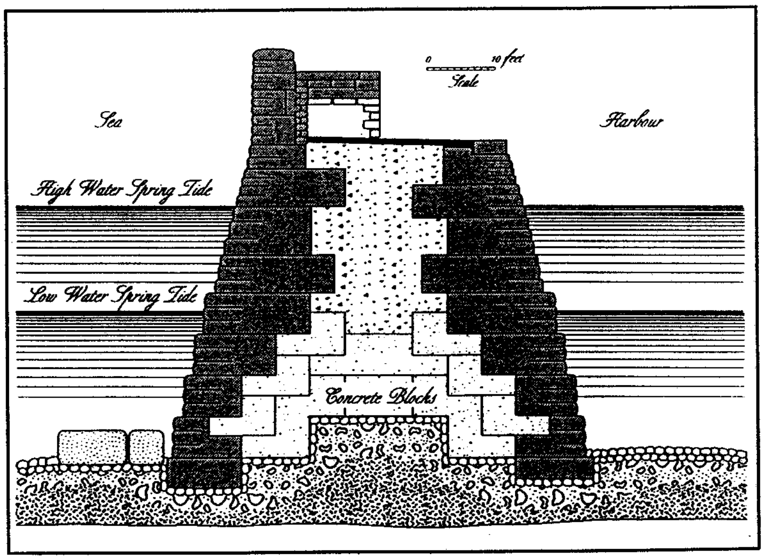

Figure 2.3 Training wall/breakwater, North Tyne

Seawalls around the UK were also constructed using similar techniques to halt erosion of beaches, dunes, or soft cliffs, and/or to limit wave overtopping and flooding during storms. Such structures are not the primary interest of this report, but examples are cited where they give particular information on design techniques or construction methods.

2.2.1 *Historical background*

Ancient breakwaters around the Mediterranean were constructed of stone blocks, sometimes with concrete or cementitous infill. Roman engineers used underwater construction with timber forms (sometimes sunken ships), and filling with cement, pozzolana, and brick. Franco & Verdesi (1993) describe a version of caisson construction used by Herod the Great's engineers at Caesarea around 20 BC, where wooden forms were filled by concrete / mortar lowered in baskets into the forms.

Little evidence remains of such construction around the UK, although some foundations of quay walls have been dated to Roman times. The use of concrete to form blocks in the UK was probably started by the Romans, but disappeared again from UK construction practice for marine / coastal structures until about 1850. Few details of construction of breakwaters or coastal walls are recorded before the late 1600's, and much of the information available to Bray & Tatham (1992) dates from the 1700 and 1800s. One notable exception is provided by the account of the construction by British engineers of the Greate Mole at Tangier by Routh (1912), discussed in section 2.2.2 below.

The main purpose of many harbours in the most exposed areas around the UK was defence, with naval requirements setting the position, orientation and plan for harbours at Dover, Portland, Plymouth, Holyhead, St Catherine's and Alderney, see layout in Figure 2.4. Other harbours were constructed as "harbours of refuge", to be used by fishing boats and trading vessels during storms. These new, and often much larger, harbours were much easier to enter than the small coastal harbours. Then, as now, narrow entrances and reflective walls of these small harbours caused very dangerous conditions close to the harbour entrance, problems that still persist for many harbours in the UK. These aspects are discussed in more detail in the harbour Entrances project, see particularly McBride et al (1996).

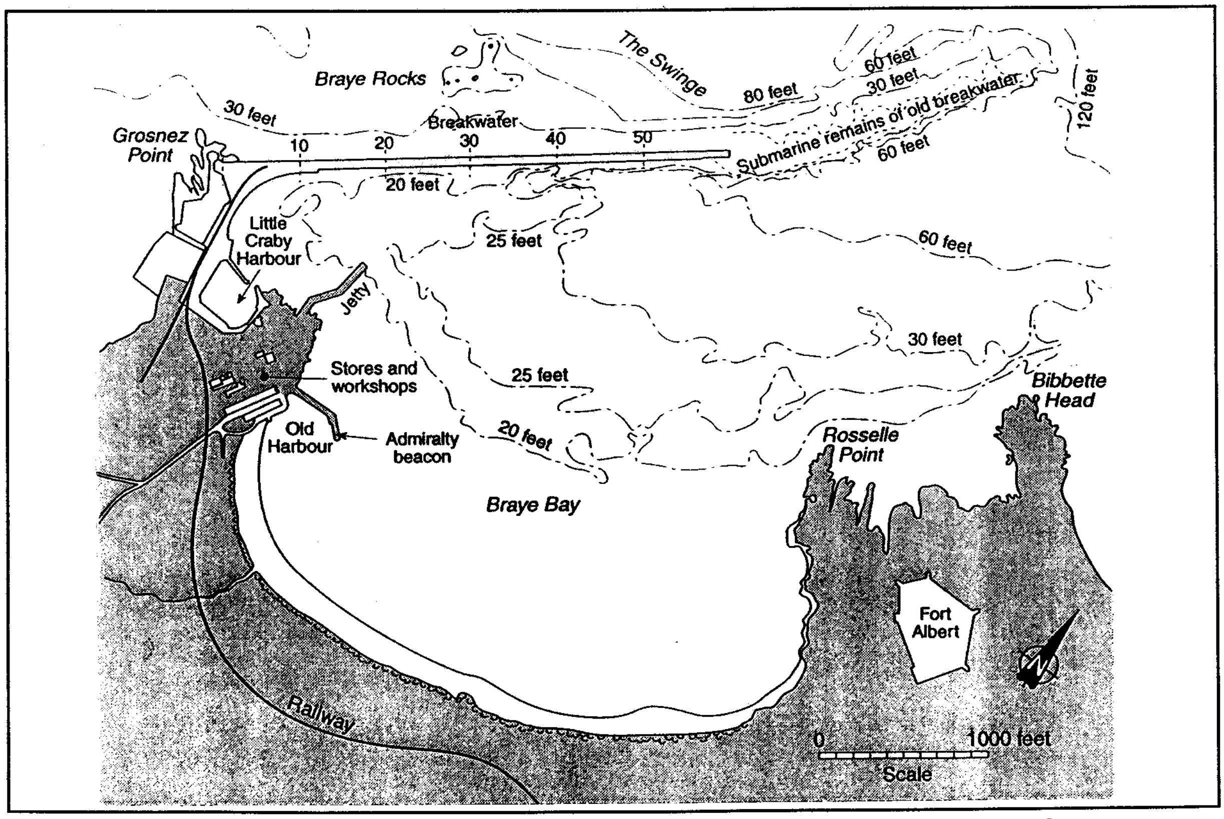

Figure 2.4 Layout of Alderney harbour, after collapse of breakwater outer section

Many vertical breakwaters or piers were constructed between 1830 and 1900, including Alderney started in 1846, Dover started in 1847, Tynmouth 1855, Holyhead 1876, Fraserburgh 1877. Most of these have survived in their original form, except Alderney which is discussed more by Allsop & Bray (1994) and Allsop et al (1991). Many of the naval harbours constructed in this period have since been abandoned by the navy, and are now used for commercial, fishing or leisure activities.

2.2.2 *Construction of breakwaters, piers, and seawalls*

The most common form of construction used in the UK for breakwaters or piers was a rubble mound brought up to a level slightly below low water, and surmounted by blockwork walls. Hewn stone, often granite, was laid in bond, generally at a slight batter off vertical. Blocks were laid dry or in lime or pozzolana mortar up to about 1900. Concrete filling was rarely used, and cement mortars became widely available only after about 1900, although lime and other mortars were used at least from 1650. Concrete rather than stone blocks was more widely used after about 1880. Various methods were developed to assist transfer tensile, bending, or shear loads between adjoining blocks, or between courses of blockwork, including iron cramps, keys or joggle joints between blocks.

Caissons were rarely used in the UK before 1900. One of the first uses by British engineers of caissons is described by Routh (1912) who relates the construction of the main breakwater or Greate Mole to shelter a harbour at Tangier from the Atlantic. The town was occupied by British troops, and protection was urgently needed for the vessels supplying the garrison. The Mole was started in conventional fashion, with rubble foundations placed ahead of blockwork construction. Construction started in August 1663, but had only reached 350m by August 1668 due to adverse wave conditions at the site; loss of rubble fill into the sand bed; the small and occasional nature of the workforce who were often diverted to other (military) duties; difficulties in obtaining materials; and significant delays in payment for work completed.

After the contract had been re-negotiated, the contractor returned in April 1670 to find the blockwork walls damaged and breached in at least two places. The construction method was re-considered, and a type of caisson construction used at Genoa was proposed using "great wooden chests" bound in iron, and filled with stones and mortar or concrete. After much debate, some of it reported in Samuel Pepys' diaries, a new contractor was appointed to extend the existing structure using caissons.

Wooden caissons of 500 to 2000 tons (Figure 2.5) were towed out from England, and once on site they were sunk onto the foundation by being filled with stone bound in a local mortar of Roman Tarras. Progress on the new construction was more rapid and less subject to damage than the earlier blockwork sections, and the prognostications were for a longer life than the earlier sections.

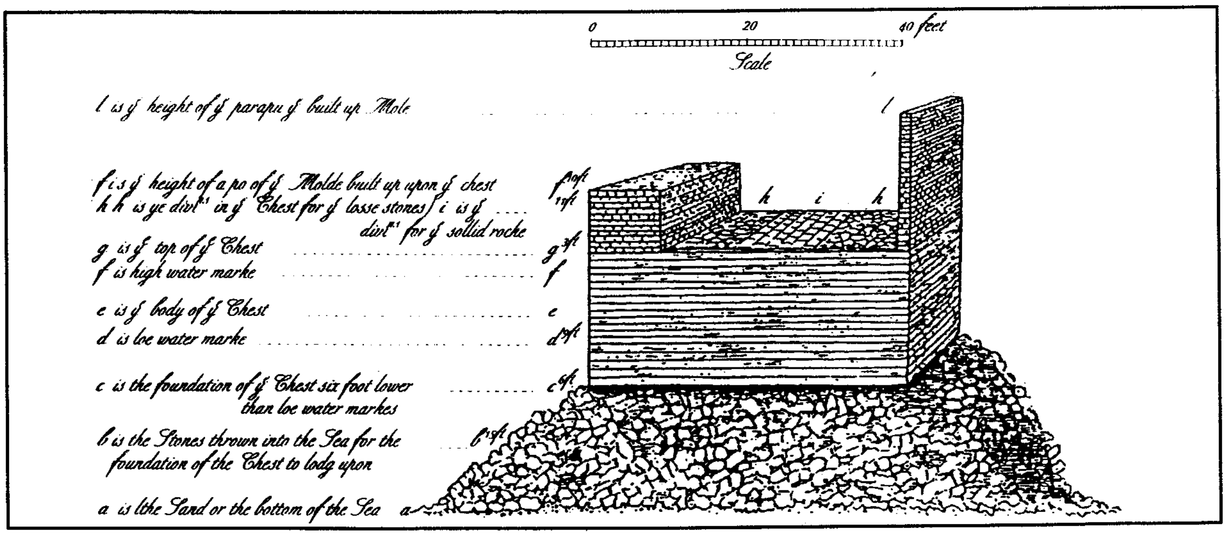

Figure 2.5 Timber caisson or Greate Chest used for the Mole, Tangier, 1677

Work on the Mole continued until 1678 when Tangier was attacked and all energies were diverted to its defence. Peace was concluded in 1680, and it was then decided that the breakwater should be destroyed lest it provide shelter to a later enemy. This was completed in 1684 with more difficulty than anticipated, and marked an apparent halt in significant breakwater construction by British engineers, and certainly in the use of caissons, until the early 1800's.

The use of concrete for filling breakwater walls, and/or to form the facing started to be used occasionally again after about 1830, becoming more prevalent after about 1870. There is no record of concrete being used for the North Pier at Eyemouth, 1767; the Old Pier at Wick, 1823; the piers at Hynish, 1843, Buckie, 1855, and West Hartlepool, 1858.

Pre-cast concrete blocks were however used at North Tyne in 1855, Figure 2.3; for Dover breakwater, 1866, Figure 2.2; and at Cork in 1877. Concrete filled bags formed a foundation to Fraserburgh breakwater in 1877, and for the Winton Pier, Ardrossan in 1892. Concrete filling was used for the later stages of Alderney breakwater 1849-1866, the South Breakwater at Aberdeen, 1873; for the North Pier at Aberdeen, and the Fraserburgh breakwater, both in 1877. It is interesting to note that Lamberti & Franco (1994) credit the Italian engineer Coen Cagli with re-introducing vertical wall breakwaters to Italy after a visit to Britain in 1896 where he saw the blockwork breakwaters at Dover, Sunderland, North Tyne, Peterhead, and Wick.

The development of so many harbours around the UK between 1850 and 1900, and survival of many of those breakwaters, have significantly reduced the need to construct new harbours around the UK, and has thus resulted in relatively few breakwaters being constructed since 1900. Those new structures have generally been formed as rubble mounds to their full height, protected by rock or concrete armour units, see particularly Port Talbot, Douglas, Bangor, and Peterhead. Many similar structures have also been designed and constructed by British engineers working overseas.

Exceptions to this were the new harbour at Brighton, protected by breakwaters using circular concrete caissons, Figure 2.6, based on the design used at Hanstholm in Denmark; and the vertical wave screen breakwaters at Sutton Harbour, Plymouth, and Cardiff Bay Barrage.

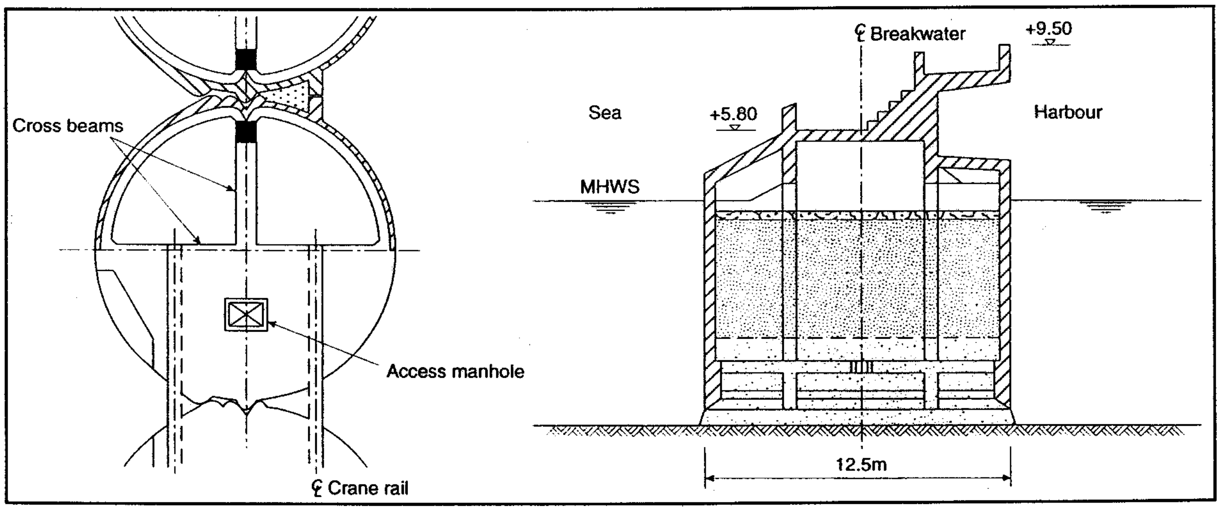

Figure 2.6 Circular caissons used at Hantsholm and Brighton Marina

2.2.3 Construction of vertically-composite breakwaters

<u>Stone or concrete blockwork</u>

Before the advent of advanced underwater working, construction of blockwork walls was chiefly limited by the depth to which diver-assisted placement of closely-fitted blocks was possible, and by the knowledge and equipment available for placing mass concrete. Rubble material was placed by barge, allowed to consolidate, then trimmed to accept the foundation stones.

In 1850, the water depth at which the foundation stones could be laid was usually limited to 12ft (3-4m) below low water level, but by 1900, depths of up to 50ft (15m) had been reached. After dressing the mound by divers, blockwork was then founded using the largest blocks available. The breakwater wall was carried upwards in plain or mortared blocks to the top of the wave wall. The block size often reduced as construction climbed, as increased time between immersion allowed more time to fit together smaller blocks, and/or in laying the mortar bedding / jointing. Individual blocks were often bonded together by keys, by iron or steel dowels in holes through the blocks, or by lead or mortar poured to form keys between blocks, although these complications were more often reserved for the outer end of the breakwater. The use of iron or steel rail cramps to hold together the outer end of a breakwater is discussed by Bray & Tatham (1992). Timber piles were sometimes used to take bending or tensile forces, and were occasionally incorporated within the breakwater structure.

The sections of St Catherine and Alderney Breakwaters shown in Figures 2.1 and 2.7-8 are relatively typical of the larger breakwaters constructed between 1850 and 1880. Of these two, Alderney is exposed to substantially more severe wave conditions, has suffered significant, provides us with more information on failure modes and responses, and has therefore been given more attention, recently by Allsop et al (1991) and Allsop & Bray (1994).

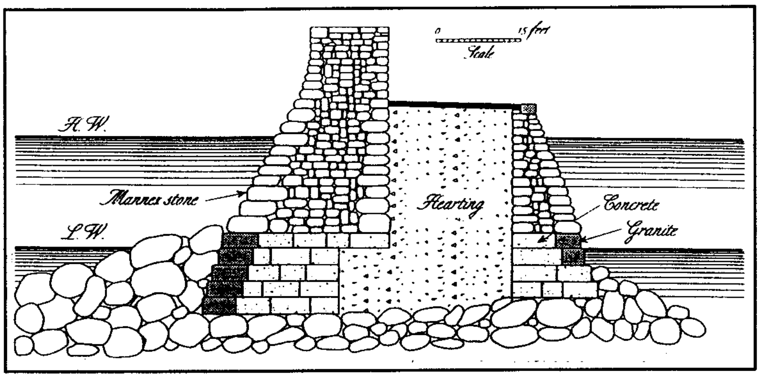

Figure 2.7 Cross-section of Alderney breakwater during construction, 1855

At the landward end of the Alderney breakwater, the foundation was set no more than 3.5m below low water level on spring tides. Along the outer sections, the lowest intended level was 7.3m (24ft) below low water, but consolidation of the mound increased this to 9.1m (30ft) towards the seaward end. Large blocks of stone, later of concrete, were laid on the rubble after it had been allowed to settle for about 6 months. The batter of the wall of 2 (vertical) :1 (horizontal) at the inner end is rather shallower than for many contemporary breakwaters, and was steepened for the outer sections. Walls at St Catherine's were battered at 3:1, and at Aberdeen at 8:1.

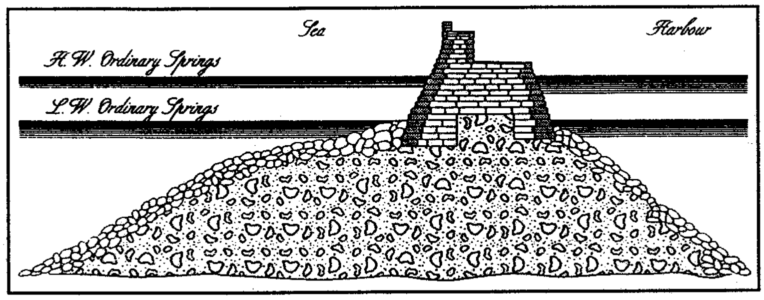

Figure 2.8 Cross-section of Alderney breakwater, completed, 1864

Blocks facing most of the breakwaters considered here were generally of dressed stone. Typical sizes are in the ranges 1m x 0.3m x 0.5m up to 2.5m x 1m x 1.5m. The sizes used were strongly dependent on the stone available, and the stone-working skills available. Very fine tolerances were possible, but would generally have been reserved for elements on the top of the breakwater, those that could easily be seen. Stone used as facing on the breakwater wall could be dressed to give joint gaps typically of no more than 1-2", about 25-50mm. At lower levels, where inspection was more difficult, and placing times shorter, tolerances may have been wider, and joint gaps of up to 75mm might be expected.

The gaps between adjoining blocks would generally have been negligible where blocks were laid in mortar. The mortar will however deteriorate over the structure life, the joints then open up, allowing water into the hearting or core, and sometimes allowing the blocks to move. Many failures of such walls have been associated with the loss of bond / filling between blocks. The use of concrete blocks, eg at Dover shown in Figure 2.2, avoided many of the problems of bonding stonework, and made it much easier to make special provisions for joining blocks, such as keyways or other stepped joints, or cut-outs for key blocks.

Once production of concrete blocks became economic, block sizes increased dramatically, sometimes to sizes approaching 400 tons. Stoney (1874) records the use of blocks of approximately 3.5m x 6m x 7m for quay construction in 1871, and suggests their use at Alderney. It was however agreed that the capital costs of the equipment needed to produce, move and place such blocks, would restrict their use to large projects.

Concrete caissons

Over the last 40-50 years, there have been considerable advances in design methods for vertical breakwaters; in construction technology for prefabricated concrete caissons; in placement of rubble foundations at depth; and these changes have altered the balance of advantages and disadvantages between rubble and vertical breakwaters.

The most common form of caisson is rectangular (or square) in plan and front elevation, and rectangular or near square in end elevation. Caissons may typically be 15-30m long, divided internally into cells. An example Italian caisson is shown in Figure 2.9. The caisson itself is designed to be floated out, ballasted with water to sink it into position, then filled by sand. In this low tidal range, the low crest section is then cast insitu.

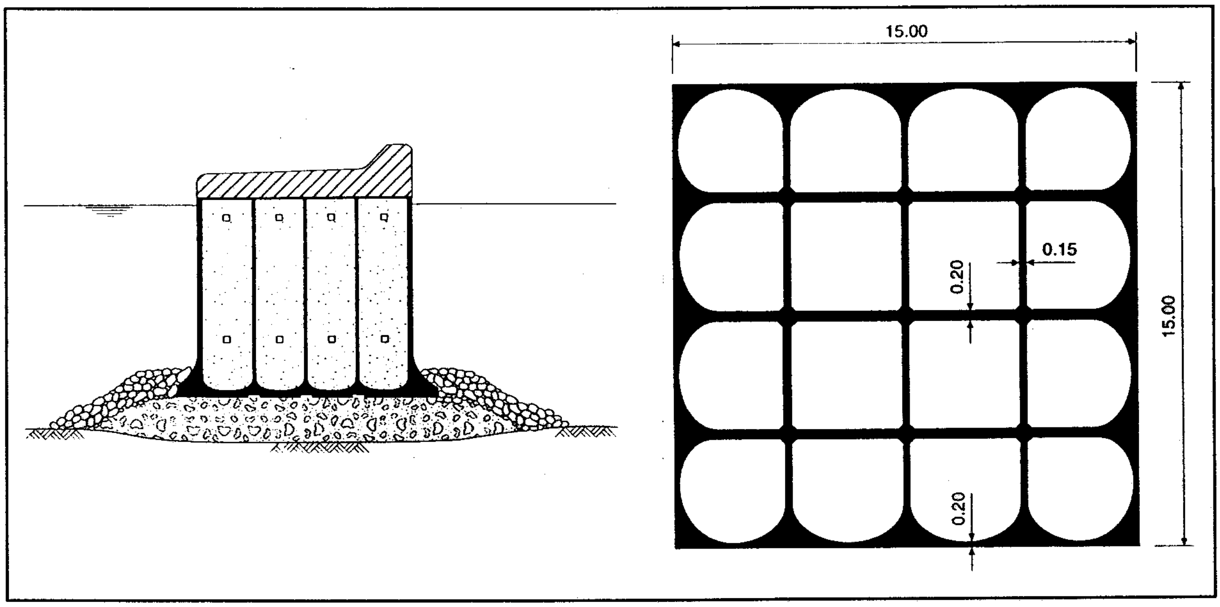

Figure 2.9 Concrete caissons for protection of Sestri Industrial Airport, 1938

The slightly more complex breakwater at Bagnara (1985) is shown in Figure 2.10. The crest wall is shaped to return any overtopping waves, and is set back to reduce impact forces and overtopping. The toe armour to this breakwater was damaged in 1991, but only along its most outer end where Tetrapod armour was used at the toe. The toe armour along the main trunk was 5 t modified cubes.

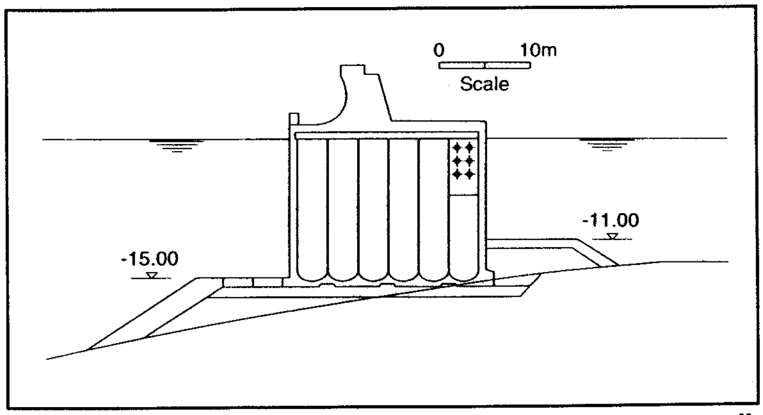

Figure 2.10 Caisson breakwater with set-back crest wall, Bagnara, 1985

One of the main disadvantages of a vertical wall breakwater is the high level of reflections. This problem, and potential solutions have been studied in the companion Harbour Entrance and MCS projects, see discussions by McBride et al (1996), Allsop (1995), Allsop et al (1995b), McBride et al (1995a), and McBride & Watson (1995). One approach is to modify the seawrd chambers of the caisson to allow wave energy dissipation in the first row of chambers, or in a few instances in the first 2 or even 3 chambers. An example of a 2-chamber perforated caisson is shown in Figure 2.11. This illustrates the higher floor levels in the inner perforated chambers, the vent through the crown wall to reduce air pressures within the rear chamber, and the use of concrete fill to increase strength and density in the seaward cells. In a few instances, perforated chambers are also used on the harbour side to reduce reflected wave action within the harbour, see the section of Bagnara breakwater in Figure 2.10. It should however be noted that caissons with a single perforated chamber are unlikely to achieve reflections below C_r=0.5 for any significant range of wave periods.

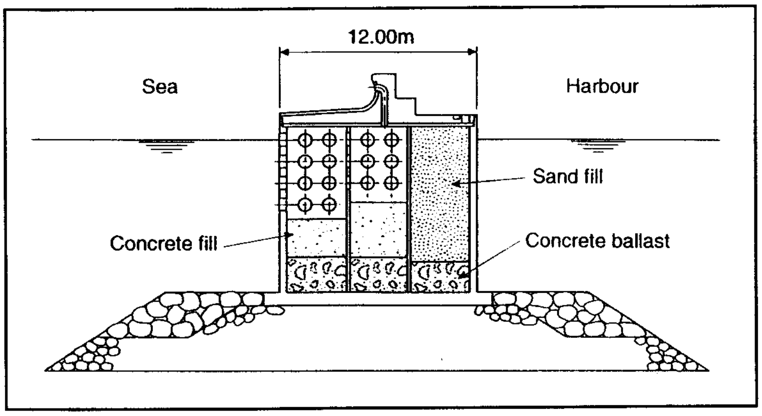

Figure 2.11 Perforated chamber caisson breakwater at Ponza

High wave reflections may combine with currents along the structure increased by interruption of tidal or wave-induced currents. These may precipitate local scour of the sea bed, a problem that has afflicted a number of caisson breakwaters. In the UK, Ganly (1983) reports that the circular caissons at Brighton placed directly onto chalk bedrock, Figure 2.6, were subject to substantial early scour leading to settlement of 3 caissons by up to 0.65m during construction. Extensive scour protection measures were then included during the remainder of the construction period. Despite these measures, scour holes have continued at Brighton, with significant expenditure being needed to reinforce the toe detail by pumping concrete into flexible bags at the seaward edge of and beneath the caissons. Elsewhere, scour remains one of the more difficult design problems, and substantial anti-scour measures have often been required to avoid local collapse or loss of support. The hydro-dynamic processes involved in scour are reviewed by Oumeraci (1994a), but little information is given on potential prevention measures. Practical advice derived from analysis of service performance is given by Funakoshi et al (1994), and is discussed in 2.3 below.

Most vertical breakwaters in Europe have been constructed around Italy. Comprehensive reviews of many Italian breakwaters, design, construction, failures and repairs, have been described by Franco (1994) and Lamberti & Franco (1994). Around the world, more harbours and breakwatershave been constructed recently in Japan than anywhere else, perhaps even more than in the rest of the world together. The scale of such construction is illustrated by the port of Onahama where the caisson construction yards completed 1500 caissons in 1932 - 1992, with 131 constructed in 1971. Much further information on caisson breakwaters in Japan is given by Tanimoto & Takahashi (1994a, b) who describe the development and historical progress of vertical breakwaters in Japan, and give details of many example structures. Of those relevant to this report, three examples are shown in Figures 2.12 - 2.14.

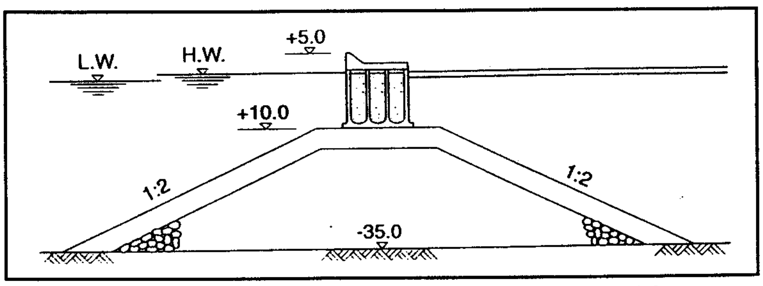

Figure 2.12 Tsunami protection breakwater at Ofunato

The tsunami protection breakwater at Ofunato, 1967, shown in Figure 2.12 is in relatively deep water at 35m, but is required to resist relatively low wave heights. The perforated chamber caissons used at Kamaishi, Figure 2.13, is built in 60m of water using a mound of 35m, and is the deepest breakwater built in Japan. This structure again serves as tsunami protection so the design wave heights are relatively low.

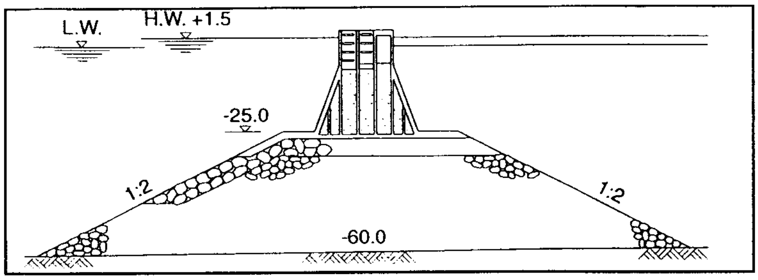

Figure 2.13 Tsunami protection breakwater at Kamaishi

The widest caisson in Japan at 38m is shown in Figure 2.14. This breakwater at Hedono port is in less than 30m of water, but is designed to resist a design wave of H_s = 9.7m. Here the toe armour uses 64t Tetrapod units in a layer about 6m thick. The longest caisson built in Japan up to 1994, was 100m long, about 20m wide, and was used as a temporary breakwater at Kochi port. This caisson was cast in a ship dock, and towed 370 km to site.

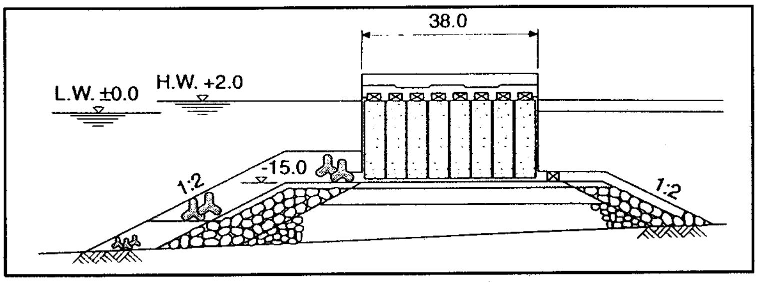

Figure 2.14 Harbour breakwater with wide caisson at Hedono

More details on vertical breakwaters based on work up to 1992 were presented in a special edition of Coastal Engineering by Oumeraci (1994), Franco (1994), Tanimoto & Takahashi (1994b), Hattori et al (1994), Chan (1994) and Oumeraci & Kortenhaus (1994). These papers concentrate on information from research studies, with some comments on design, and with a little information on practical examples. More practical information is given in the Workshop on Wave Barriers in Deep Waters presented at the Port and Harbour Research Institute in Japan, see particularly Tanimoto & Takahashi (1994a), Lamberti & Franco (1994), Allsop & Bray (1994), Xie (1994), Juhl (1994) and Ligteringen (1994).

2.3 Performance in service

Analysis of reports of damage or failure of breakwaters suggests that there are three main periods of potential concern during the life of the structure: the construction period; initial service; and the extended service period, often well beyond the normal economic life used in present design life calculations. Much of the damage reported appears to occur early in the life of the structure, even during construction, so it would appear that if a breakwater survives the first 5 years without damage it is generally likely to survive the next 40-50 years. This confirms the premise that damage / failures are generally avoidable if sufficient information is available on the main failure processes.

Relatively little information on service performance of breakwaters was derived from the CIRIA project reported by Bray & Tatham (1992). Of those owners from whom information on breakwaters was requested, only 8% responded, perhaps suggesting that these structures have given little obvious cause for concern in recent years. In their report however, Bray & Tatham note that incremental degradation of such walls is often overlooked, and that the apparent lack of problems may be due primarily to lack of inspection. In some instances, it might be concluded that damage occurred so early that the structure was abandoned, or was replaced at a relatively early stage in its life. In other instances, it might be concluded that historical rates of deterioration have been so slow that the need for maintenance expenditure is small. This would ignore the brittleness of the failure modes for many of these structures, and Bray & Tatham concluded that there is a significant requirement for inspection and monitoring to avoid those sudden failures that occur when the structure has degraded to a failure point.

Various publications between 1850 and 1900 give details of breakwater performance, but often fail to distinguish clearly between cause and response. A good example of this problem is given by reports of damage to Wick breakwater. Stevenson (1874) describes the start of breakwater construction in 1863 using dry-placed blocks of 5 to 10 tons. During storms in 1870, a section of about 380 ft (115m) of the breakwater was destroyed, presumably by breaching the breakwater wall. This section was then rebuilt using Portland cement to bond the block facing, and iron dowels between courses. A storm in February 1872 gave wave impact pressures so severe that facing stones were shattered, although Stevenson's report does not identify whether this was by direct wave impact, or could have been by stones from the mound being hurled against the face, see discussion by Allsop et al (1991) on Alderney. In December 1872 a section of blockwork bonded together and estimated as weighing 1350 tons slid into the harbour. This was followed by a similar fate to another section weighing 2600 tons in 1873. These are cited by other authors including Cornick (1969) as evidence of impact forces from breaking waves. Shield (1895) however refers to informal discussions at Wick, and suggests that damage was strongly influenced by foundation failure, but gives little other data.

Instances are rarer now where the design or construction seems to have incorporated a significant flaw from the start, and severe damage or failure has become apparent during the construction period. The prime historical example of this in the UK is the Alderney breakwater where a design that had worked well in a low wave environment at St Catherines on the sheltered side of Jersey was used again for an extremely exposed site, subject to frequent and severe storms. Potential weaknesses of the Alderney breakwater were noted during the construction period, leading to steepening of the front face to increase restraining loads on individual blocks; use of mortar / concrete to fill between blocks to reduce internal pressures; reduction of the mound level to place the foundation at greater depth.

Also during construction of the breakwater at Catania in Sicily in 1930, very large blocks slid backwards into the harbour under wave attack. This weakness was ascribed to the absence of the crest blocks, and no changes were made to the design. The damage was however repeated in 1933 when much of the upper part of the breakwater slid backwards. Analysis of this failure identified the lack of horizontal connectivity between layers, hence the relative ease with which successive layers slid over that beneath. All later structures built in Italy include keys, or other connections to resist horizontal forces. Despite this, few if any existing structures were re-appraised or strengthened, and collapses of such breakwaters continued at Genoa (1955), Ventotene(1966), Palermo (1973), Bari (1974), and Naples (1987).

One of the major durability problems of these types of structures arises from scour along the seaward face of the breakwater. Lamberti & Franco (1994) ascribe collapse of the Mustapha breakwater at Algiers primarily to foundation failure, initiated or aggravated by local scour. Funakoshi et al (1994) analysed breakwaters of total length 77km at 13 Japanese ports, and found scour up to 2m in nearly all examples, including examples where scour prevention / alleviation measures had been included from the start of construction. Generally such scour abated after the first 1-2 years. Funakoshi et al (1994) recommend repeated bed surveys, and that scour protection measures for the toe mound should be staged over the first 2 years after construction.

In the use of most practical design methods, it is assumed that wave impacts will either not occur, or that the pressures will be so brief as not to allow time for massive caisson sections to respond. Limitations of these assumptions are exposed by the examples of breakwater damage by impacts described for Mutsu-Ogawara by Hitachi (1994), for Sakata and Mutsu-Ogawara by Takahshi et al (1994a), and for Amlwch by Allsop & Vicinanza (1996).

Mutsu-Ogawara port on the Pacific coast of Japan was under construction in February 1991, when it was hit by waves which at H_s=9.9m substantially exceeded both the construction period design condition (1:10 year) of H_s=7m, and the 1:50 year design condition of H_{sd}=7.6m. Damage was particularly severe where mounds of armour blocks intended to cover the front face were incomplete and/or had been damaged. These part-height mounds acted to trip the waves causing impact forces so severe that two 24m long caissons suffered structural damage, one of them losing most of its upper part. Photographs taken during the storm show breaking waves being thrown many tens of metres into the air above the breakwater, very similar to the process seen at Alderney under severe waves

Sakata port is on the Japan Sea, and is therefore in theory less exposed than the Pacific coast. Even so, wave conditions during the winter of 1973 / 74 reached H_{so}=7.2m and exceeded H_{so}=4.5m on 4 other occasions. In a water depth no more than 9-10m, these conditions would have reached or exceeded the breaking limit, and a high toe mound to protect against possible scour would also have increased the probability of impacts. Nearly all of the 39 caissons, each 20m long and 17m deep, slid during these storms, some by nearly 4m.

In a storm in 7 December 1990, a small breakwater was damaged at Amlwch port on Anglesey, north Wales. The breakwater is about 60m long, runs out approximately eastwards from the coastline, and the breakwater axis is slightly curved. The structure was constructed before 1977 using concrete blocks laid in slices onto a mass concrete foundation plate into the rockhead. Each block is thus interlocked with its neighbours by keyways. The breakwater crest wall is at +7.7mODN, and the structure toe at approximately -11mODN. During the storm, the outer end of the breakwater slid backwards by about 0.1-0.2m, leaving cracks down through the slice blockwork in three places of up to 0.075m width.

Wave conditions at Amlwch during this storm are not known, but are estimated as at least H_{so}=4m, probably with a mean wave period of T_m=9s. The foreshore approaching the structure is very steep, approximately 1:13, so falls outside of any established design method. The water level during the storm probably reached at least +3.4mODN, giving water depths at the toe of 11-14m. Allsop & Vicinanza (1996) estimated limiting inshore wave conditions as H_{si}=4m at MHWS, but reducing to H_{si}=3.6m at MLWS. Using the simple method of Vicinanza et al (1995), the horizontal force was calculated as 1040kN/m at MHWS. With no up-lift, for the blocks direct on concrete, and μ=0.5, these give a factor of safety of F_s = 0.9 at high water, contrasted by predictions using the Goda method which gives F_s = 1.2 at high water, and F_s = 2.3 at low water. These factors of safety would be reduced if uplift pressures could act on or beneath the blocks.

It is claimed by many researchers, particularly in Italy, Japan and Germany that vertical breakwaters with pre-cast caissons have lower construction costs and much shorter installation times when compared with rubble mounds. The form of their installation may also reduce environmental impact in the form of noise or dust pollution, on site, at the quarry, and in transport to the site. Once constructed, vertical breakwaters often have less visual and spatial impact which is particularly attractive to navigators who strongly dislike navigating close to rubble slopes. Caisson breakwater sections also have the potential to be removed at the end of the project life by simply emptying the fill material and re-floating the empty caisson sections for re-use elsewhere.

It is clear from the examples of damage reviewed above, and the many other examples described in the literature, that there remain significant uncertainties in methods to analyse and design vertical and composite breakwaters. The arguments in favour of these types of structure suggest however that it is now appropriate to re-examine the relative advantages and disadvantages of vertical breakwaters, and particularly to re-examine methods to determine wave loadings on such structures.

3 Design methods

3.1 Design considerations and failure modes

The main activities in the design process, strictly the analysis process, are to identify the main failure processes, and then to dimension the selected structure type to ensure that the principal loadings remain below the structure's resistance when suitably factored. In the design of vertical breakwaters and related walls, the main emphasis has historically been on balancing the horizontal (and perhaps up-lift) forces against the caisson weight and hence friction forces. This chapter generally follows that approach.

3.1.1 Structural failures

The main failure modes for these types of structures may be summarised:

Sliding (backwards) of the wall elements relative to the foundation;
Rotation or overturning, backwards, of the wall;
Forward rotation of the wall;
Gross settlement of wall;
Structural failure of breakwater elements;
Loss of integrity / continuity of structure.

The main loadings acting on these types of walls arise from direct wave pressures; up-lift forces; quasi-hydrostatic forces from internal water pressures; and geotechnical forces / reactions from backing or supporting materials. Some of the failure modes above may themselves be initiated or accelerated by contributing failures, including particularly local or global foundation failures. These structures resist wave and geotechnical forces essentially by their own weight, and by friction with the underlying materials. Under local pressures / gradients, interlock or bonding forces between component elements maintain continuity and avoid movement or loss of elements and/or fill.

The most commonly addressed failure mode for monolithic vertical structures is sliding backwards under direct wave forces. This depends primarily on the horizontal loads, but may also be influenced by up-lift forces. Failure by overturning (backwards) may theoretically be examined by assuming rotation about the rear heel of the caisson / wall. In practice, the point of rotation is not fixed, depending upon the bearing capacity and geotechnical characteristics of the rubble mound and foundation. Analysis of foundation failure modes has been studied under the MAST II MCS research project, summarised by de Groot et al (1995), and constitutes a major part of the MAST III project PROVERBS, so further discussion on these issues within this report will be very limited.

Blockwork breakwaters may also fail by loss of integrity where a block is removed (seaward) by net suction forces, followed by progressive damage and then catastrophic collapse. Detailed analysis of the high local pressures / pressure gradients that may influence this failure mode will be described by the Naples / Sheffield / Wallingford team in forthcoming reports to PROVERBS.

This report is therefore primarily concerned with the (horizontal) wave loads acting on the seaward face of the wall, and with the contribution of up-lift forces to overall stability of caisson or similar elements. Peak local pressures will also be discussed, but detailed analysis of these effects will be limited in this report, as they are discussed more fully in the Ph.D theses of McKenna (1996) and Vicinanza (1996).

3.1.2 Functional failures

Vertical or composite walls may alternatively suffer functional failures when they fail to give adequate protection despite surviving structurally. In harbours, such a functional failure will generally be due to excessive wave overtopping which leads to transmission of wave activity into the (previously) sheltered parts of the harbour. A related functional failure may occur if the breakwater structure is adopted to serve other functions as well. This often leads to requirements to limit wave overtopping under frequently occurring conditions to allow safe working on / behind the breakwater, vehicle of pedestrian access, and perhaps avoidance of damage to buildings or other fixtures on the breakwater.

A particular disadvantage of vertical walls is these structures do not themselves dissipate any significant proportion of the incident wave energy. Plain vertical walls will either reflect or transmit wave energy, primarily depending on the relative crest freeboard, and as such structures are primarily intended to reduce wave transmission, the majority of wave energy incident on the structure is reflected back away from the structure. These increases in wave activity may cause problems to navigation, or may initiate / accelerate local bed scour or beach movement. This area is not considered further in this report as it has been covered very fully in the accompanying Harbour Entrances project, summarised by McBride et al (1996), and under the MAST MCS project. Results of those and related studies have been presented by Allsop (1995), Allsop et al (1995a, 1995b), Allsop et al (1994a, 1994b), Allsop & McBride (1994), Bennett et al (1992), McBride et al (1996), McBride et al (1995a, 1995b), McBride et al (1994), McBride et al (1993), and McBride & Watson (1995).

3.1.3 Design approaches

The analysis of stability of such structures requires the identification of all significant failure modes, and the derivation or use of appropriate analysis methods for each failure mode. These analysis methods may be conducted at widely different levels of complexity or rigour. They may include detailed calculations of loadings and structure resistance; calculation of a given response parameter and testing that it falls below some given limit; comparison of the main features / dimensions of the proposed structure against those of similar structures in the geographic region, or in the experience of the engineer.

Considerable design information on the stability and hydraulic performance of rubble mound breakwaters has been derived from research at HR Wallingford and elsewhere, and has been included in design manuals such as the CIRIA / CUR rock manual edited by Simm (1991), and in parts of British Standard BS6349, BSI (1984, 1991). There is however substantially less information available in Europe on the stability and hydraulic performance of vertical breakwaters, despite their historical preponderance around the UK and elsewhere. BS6349 Pt 1 (1984) as amended summarises Goda's method for predicting non-impulsive wave forces. The CIRIA rock manual notes however that vertical or composite walls can suffer high impulsive or impact forces, with local pressures substantially greater than suggested by some design formulae. These impact pressures are limited spatially and temporally, and have usually been regarded as of relatively little effect on the overall stability of the structure. Damage to breakwaters in the UK, and to others in Italy and Japan, and recent studies under the European Union MAST research programme on the dynamic responses of caissons to impact pressures, have illustrated that there are circumstances where present design methods for wave forces are insufficient.

The failure modes which vertical walls are required to resist may be re-presented under four headings:

a) Sliding or overturning of the breakwater wall as a single entity;
b) Removal of elements from the (blockwork) wall, resulting in a loss of continuity, and hence destruction of the wall;
c) Gross failure of the rubble mound and/or foundation, allowing movement of the wall;
d) Local failure of the mound or supporting seabed, allowing movement of blocks, loss of fill and/or continuity of the blockwork.

Of these, sliding or overturning of single elements a), and gross foundation failure c), have been relatively rare in the UK in recent years, but have been more common in Italy and Japan. Local failures leading to loss of continuity, and thence to overall failure b) or d), may have been more common in the UK, although records of early failure of minor breakwaters are sparse and incomplete.

Aspects of scour leading to mode d) relate principally to the design of any armour to the seaward face and berm of the rubble mound, and to the stability of the seabed material in front of the structure.

Scour is not considered further in this project, but has been addressed separately under the MAST II MCS project, see particularly Oumeraci (1994a).

Breakage of (small) elements, and/or the loss of integrity of blockwork walls, have not been much studied, and few if any data are available on local pressures / pressure gradients. Allsop & Bray (1994) noted failures of Alderney breakwater, and other related walls in the UK, and suggested that local failures of the wall, may perhaps be caused by extreme local pressures / pressure gradients. Allsop & Bray suggested an idealised stability analysis for a single block within a wall, but noted that no information is available to identify the magnitudes and frequencies of occurrence of severe local pressures and/or pressure gradients. Individual blocks or other small elements are much more likely to respond to rapidly changing pressures, both spatially and temporally than are large elements / caissons, so more detailed data are needed to analyse the stability of small elements.

3.2 Design formulae for wave forces / pressures

It is often convenient to treat pressures or forces that act on these structures under wave action in two categories:

Quasi-static, or pulsating;
Dynamic, impulsive or impact

Quasi-static or pulsating wave pressures change relatively slowly, varying at rates of the same order of magnitude as the wave crest. Two principal quasi-static forces may be considered here. In the first, a wave crest impinges directly against the structure applying a hydro-static pressure difference. The obstruction of the momentum of the wave causes the wave surface to rise up the wall, increasing the pressure difference across the wall. The net force is approximately proportional to the wave height, and can be estimated using relatively simple methods.

The second case is the opposite of that above, arising as the wave reflects back from the structure, inducing a net negative force or suction on the wall. Again the magnitudes of the forces are relatively low, and the process is relatively easy to predict.

Dynamic or impact pressures are caused by the special conditions that arise where a wave breaks onto the structure. Impact pressures associated with breaking waves are of substantially greater intensity than pulsating pressures, but are of shorter duration. The detailed processes of wave breaking are not well understood, the occurrence of breaking cannot be predicted with reliability, and these pressures are therefore extremely difficult to calculate.

It has generally been accepted that dynamic loads can be very important, but it has been argued that many structures are substantially un-affected by such short duration, high intensity loads. Schmidt et al (1992) remind us that despite more than 80 years of research work on impact loading on vertical structures subject to breaking waves, there are two basic attitudes related to the role of wave impact loadings in the design of such structures. The first attitude simply assumes that impact pressures are not important and thus should not be adopted in the design. The second attitude is to skip the problem of evaluating the design impact load by assuming that the structure can be designed in such a way that impact pressure will not occur.

A third approach is to conduct a dynamic analysis of the structure, and its foundation, and of the applied loads. This approach is strongly argued by Oumeraci (1995a), Oumeraci et al (1994a & b) and Oumeraci & Kortenhaus (1994). Problems arise in the high level of data required, both on the time series of loadings, but also on the geotechnical characteristics of the mound and foundation. The development of these overall stability models are at relatively early stages. This approach therefore presently remains the purview of researchers, although it is to be expected that dynamic design methods and example data will become available during or after the completion of the PROVERBS research project, (1996 -1999).

These problems are compounded by uncertainties in defining those conditions that lead to wave impacts. Schmidt et al (1992) and later Oumeraci (1994a) define 7 different breaker classifications in terms of H_b/d. Unfortunately, the breaker height H_b is extremely difficult to predict with any certainty, so these classifications are of limited practical use. Goda (1985) describes a number of rules to identify whether particular structures or sea states will cause a risk of impulsive wave conditions, and that method is reinterpreted here as the flow diagram in Figure 3.1.

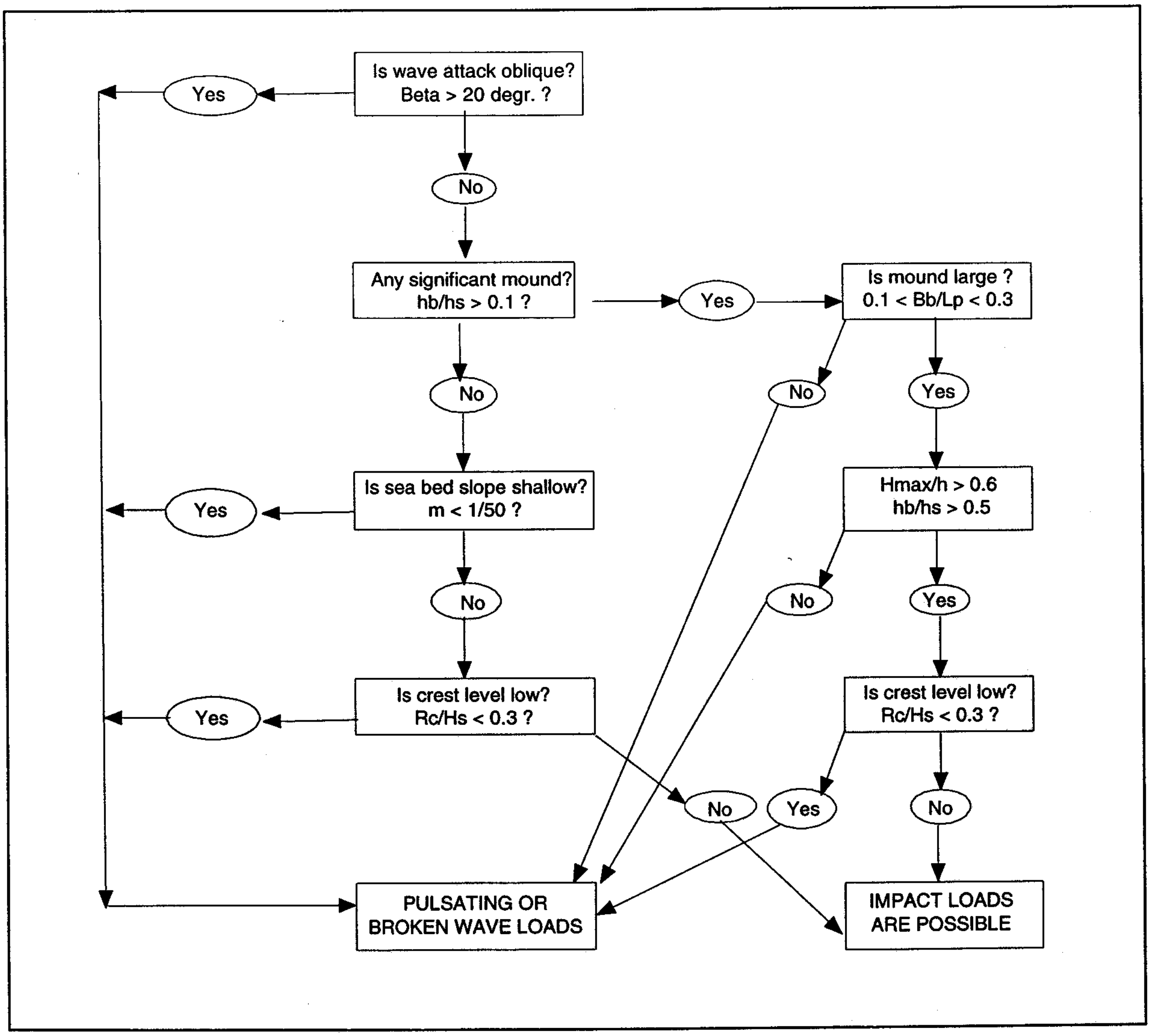

Figure 3.1 **Decision tree for impulsive breaking conditions**

The review of design methods below will therefore concentrate primarily on methods used in design manuals and codes, but will include information on dynamic of impact effects, on the definition of the onset of impact conditions, and on dynamic responses where generally available. This review draws on material also considered by McKenna (1996) and by Vicinanza (1996), and in some instances refers the readers to those reviews for greater detail.

3.2.1 Horizontal forces

The main methods used in design manuals to estimate wave forces on upright walls, breakwaters or seawalls, have been derived by:

Goda for simple walls
Goda / Takahshi for composite breakwaters
Minikin for composite breakwaters
Jensen / Bradbury & Allsop for crown walls

The most widely used prediction method for wave forces on vertical walls was developed by Goda (1974, 1985). This method was primarily developed to calculate the horizontal force for concrete caissons on rubble mound foundations, and was calibrated against laboratory tests and back-analysis of historic failures. It assumes that wave pressures on the wall can be represented by a trapezoidal distribution, see Figure 3.2, with the highest value at still water level, regardless of whether waves are breaking or non-breaking. In Europe, Goda's method is cited by British Standard BS6349 Pt 1, BSI (1984), and by the CIRIA / CUR rock manual edited by Simm (1991). Before considering Goda's method in detail, it is however useful to review briefly previous methods, particularly those by Ito, Hiroi and Sainflou, see Ito (1971), and by Minikin (1963).

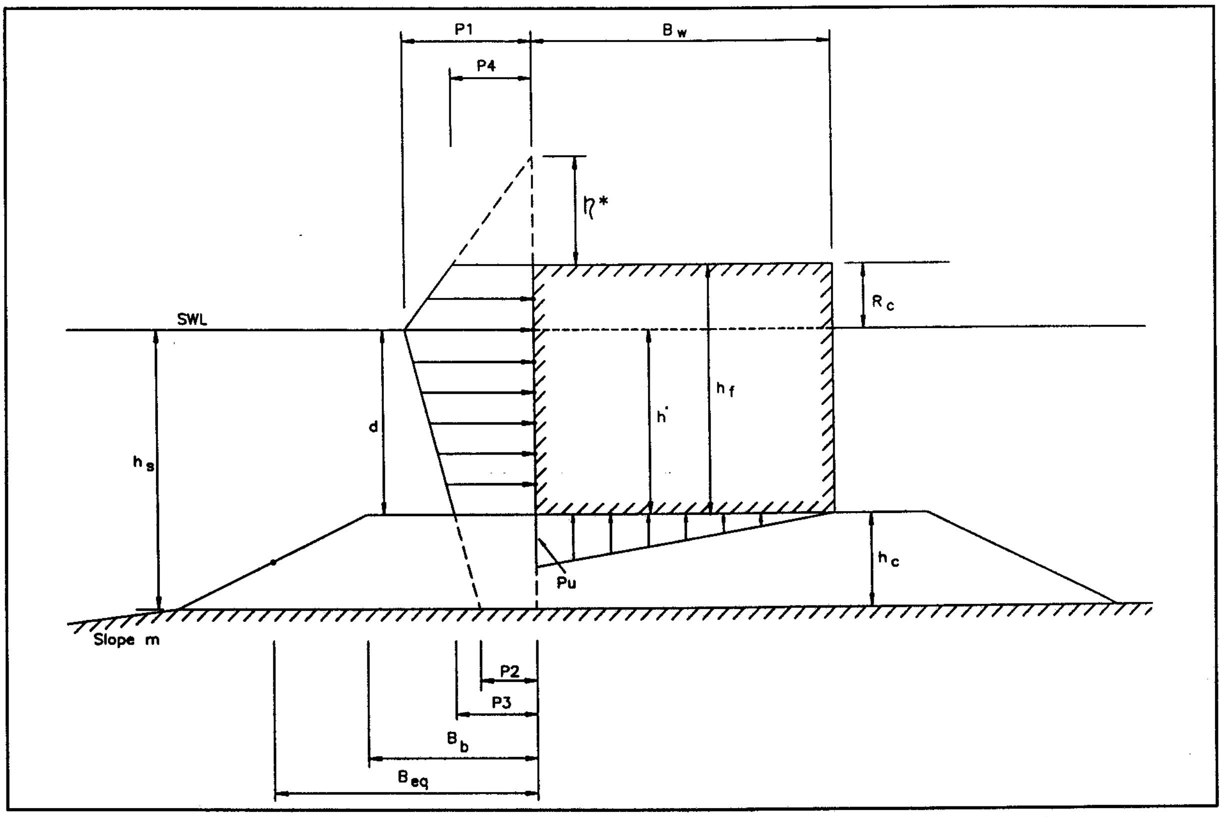

Figure 3.2 Pressure distribution and definitions for caissons, after Goda (1985)

Hiroi's formula gives a uniform wave pressure on the front face up to 1.25H above still water level:

$$p = 1.5\rho_w gH \tag{3.1}$$

where p = the average wave pressure, and H the wave height.

Sainflou's method derives a pressure distribution with maximum, p_1 at static water level, tapering off to zero at a clapotis height above s.w.l. of $H+\delta_0$, and reducing linearly with depth from p_1 to p_2 at the rubble base:

$$p_1 = (p_2 + \rho_w gh)(H + \delta_0) / (h + H + \delta_0) \tag{3.2a}$$
$$p_2 = \rho_w gH / (\cosh(2\pi h/L)) \tag{3.2b}$$
$$\delta_0 = (\pi H^2/L) \coth(2\pi h/L)) \tag{3.2c}$$

Shore Protection Manual (1984) suggests that Sainflou's method may over-estimate wave forces for shorter non-breaking waves, and uses the Miche - Rundgren formulae to derive the height of the clapotis from which an (assumed) linear hydrostatic pressure is calculated. The accompanying up-lift pressure is assumed to be triangular from the front face, with the pressure at the seaward corner consistent for front face or underside. For long waves of low steepness, SPM recommends Sainflou's method, showing design curves varying with H_i/gT^2.

Ito discusses the use of Hiroi's formula where the water depth over the mound, d, is less than $2H_{1/3}$, and Sainflou's methods when $d>2H_{1/3}$. It is interesting to note that Sainflou's method generally gives pressures of about $0.8\text{-}1.0\rho_w gH$, rather smaller than Hiroi's.

In use in Japan, there was some uncertainty whether Hiroi's method gave safe results, particularly when using $H=H_{1/3}$, and over the effects of waves breaking over the mound. A simple method by Ito, discussed by Goda (1985) gave a rectangular distribution of horizontal pressures acting on the front face of the caisson, calculated in terms of H_{max}. The value of H_{max} is $2H_s$, or H_b if waves are depth-limited. The pressure, p, is then determined for 2 different regions of relative water depth, H/h_s. Ito assumed a triangular up-lift pressure distribution, but uniform pressures on the vertical face. Bruining approximates Ito's method by:

$$p = 0.7\rho_w g H_{max} \quad \text{for } H<d \tag{3.3a}$$

$$p = \rho_w g H_{max}(0.15 + 0.55H/d) \quad \text{for } H>d \tag{3.3b}$$

The Shore Protection Manual (1984) distinguishes between breaking and non-breaking wave conditions, recommending that loads under non-breaking conditions be estimated by Miche-Rundgren with an assumed triangular distribution of up-lift pressures.

Minikin's and related methods

In Europe, Sainflou's (1928) simple hydro-dynamic method had been judged as giving too low pressures for waves breaking onto structures. Engineers had noted but not been able to measure very large forces on some walls, and it was well established that the momentum of the wave could be related to the pressure impulse. Unfortunately it was clear that some conditions led to very short impact durations, coupled with very large pressures, perhaps larger than could be accommodated by engineering of that era.

Bagnold (1939) postulated a conceptual model of air compressed by the piston of water, where momentum from the wave crest compresses the air pocket. The wave slows and stops as the pressure in the air pocket rises. At maximum pressure, the wave momentum has been converted to pressure over the impact rise time. Bagnold's approach however required the identification of the thickness of the air pocket, and of the virtual length of the water piston. Neither of these could be measured.

Minikin's (1963) method was developed in the early 1950s to estimate local wave impact pressures caused by waves breaking directly onto a vertical breakwater or seawall, and therefore addressed the problems of impact pressures. Minikin used Bagnold's piston model and calibrated a version of this model with Rouville et al's (1938) pressure measurements on a sea wall at Dieppe to give maximum peak pressures for typical wave impact events. The resulting expression for p_{max} may be written:

$$p_{max} = \tfrac{1}{2} C_{mk}\, \pi\, \rho_w\, g\, H_{max}\, (1+d/h)\, (d/L) \tag{3.4a}$$

where C_{mk} is a coefficient defined to allow fitting to Rouville's data, and accounting for the typical size of an air pocket. Minikin suggests a value of $C_{mk}=2$, which is then cancelled within eqn. 3.4a to give the simpler version used by BS6349 Pt1 (1984):

$$p_{max} = \pi \rho_w g H_{max}(1+d/h)\, (d/L) \tag{3.4b}$$

Unfortunately, this expression was then re-written by Minikin with $\pi\rho_w g$ replaced by 2.9! The resulting expression has units of tons (force) per square foot. This (mis-)use of dimensioned coefficients was later compounded by other authors, including the Shore Protection Manual, which re-writes Minikin's formula with πg replaced by 101, but adds confusions over the use of tons or tons force, or perhaps some other (un-stated) units.

The confusions over the use of Minikin's method is exaggerated by mis-calculations by Minikin himself in the quasi-hydrostatic element of the overall wave force, discussed in more detail by McKenna (1996). Minikin takes the vertical distribution of dynamic wave pressures to be parabolic about the static water level. The total force is given by approximating the impact force as $p_{max}H/3$, and then adding the contribution of hydrostatic pressures at the point of run-up to H/2. The final expression for the total horizontal force may be then be written in dimensionally correct terms:

$$F_{hmax} = ½C_{mk}\, \pi\, \rho_w\, g\, H_{max}\, d\, \{\ (1+d/h)\ H/(3L) + 1/(2\pi) + H/(8\pi d)\ \} \qquad (3.4c)$$

It appears that all later versions of Minikin's formula for total horizontal force, except that used in BS6349 Pt 1 (1984), included the factor of 101, but without the appropriate qualification on the units. These later interpretations were therefore dimensionally incorrect, and give rather larger forces than the original method, see discussion by McKenna (1996). This otherwise minor error becomes much more serious when later authors imply that the version using 101 can be used in other units than f.p.s, and have thus propagated the erroneous version of Minikin's formulae ever since!

As if this was not enough, another serious confusion is introduced in the use of the (quasi) hydro-static element in the total horizontal force in eqns 3.4c, and this confusion was compounded by errors by Minikin himself in applying the example calculations. The overall force prediction method described in the SPM includes a full triangular hydro-static pressure without explaining whether this is balanced by equivalent pressures on the other side of the structure, or by pore / ground water within the structure. The reader of the SPM may therefore be left uncertain as to whether the full triangular distribution should be applied, so may in many cases have done so. The resulting forces are often very large, but increase change markedly with increasing water depths.

The effect of these various methods can be contrasted by plotting the different vertical distributions of pressures for identical wave conditions. An example which matches one of the test conditions discussed later in Chapters 5 and 6 (test 10003) has been used to calculate the pressure distributions shown in Figure 3.3. Goda's method yields a simple trapezoidal distribution with the maximum pressure at still water level, and this method is discussed further below. Pressures calculated by two versions of Minikin's method discussed above are also plotted. The lowest pressures are given by the corrected version using eqns. (3.4b) and (3.4c). The largest pressures are given by the SPM version of Minikin, demonstrating the substantially greater peak pressure, and the triangular hydro-static element.

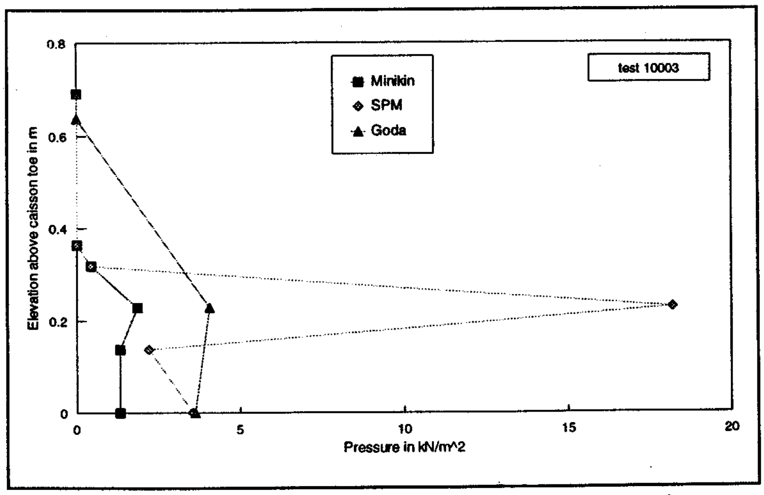

Figure 3.3 Vertical distributions of pressures using Goda, Minikin, and SPM methods

In practice it has been found by other reviewers, and perhaps by practising engineers, that the SPM version of Minikin's method gave substantially greater pressures than other formulae, and its use for calculations of wave forces for practical design has been very limited. This is epitomised by Goda writing on wave force formulae in Herbich (1990) who summarises the prevalent view on Minikin's formulae "can be considered to belong to a group of pressure formulae of historical interest".

<u>Other methods for impact pressures</u>
Much attention has been devoted to pursuing the goal of quantifying impact pressures. At small scale, very large (comparatively) pressures may be measured if small fast-responding transducers are sampled very rapidly. There has however been much doubt that this would be found at large scale.

Partenscky (1988) quoting Oumeraci uses results from the large wave channel at Hannover / Braunschweig (GWK) to suggest that impact pressures of very short durations (0.01 to 0.03s) may be calculated from:

$$p_{dyn} = K_L \rho_w g H_b \tag{3.5a}$$

where H_b is the breaking wave height, and the coefficient K_L is given in terms of the air content a_e of the breaking wave:

$$K_L = 5.4 \left((1/a_e) - 1 \right) \tag{3.5b}$$

Partenscky also derives formulae for the vertical distribution of wave impact pressures, but these formulae take no account of air content. Blackmore & Hewson (1984) conducted field measurements at four sea walls in the UK, from which they developed a model based on momentum exchange. Impact pressures p_i depend on the shallow water wave velocity, v_c; the wave period, T; and an aeration factor, λ, which depends on the roughness of the foreshore:

$$p_i = \lambda \rho T v_c^2 \tag{3.6a}$$

A value of λ = 0.3 is recommended for a rough and rocky seabed, and λ = 0.5 for a regular seabed. Breaking wave heights are indirectly considered by using shallow water wave velocities calculated from the breaking water depth, h_b, and breaking wave height, H_b:

$$v_c = [\, g\,(h_b + H_b)]^{0.5} \tag{3.6b}$$

This method was developed for vertical seawalls, and no up-lift pressures were discussed. Where these methods can be used to estimate up-lift pressures / forces, these are implicitly assumed to occur at the same time as the peak horizontal force.

Goda's method

Goda's method represents wave pressure characteristics by considering two components, the breaking wave (impacts) and the deflected wave (slowly-varying or pulsating pressures), represented in the method by coefficients α_1, α_2, and α_3. The influence of relative depth to wavelength on the slowly-varying component is represented by α_1; the effect of impulsive wave breaking due to the relative level of the mound is represented by α_2; and α_3 accounts for the relative crest level of the caisson and the relative water depth over the toe mound.

This method is one of the few to give estimates of the up-lift forces, and hence of the overturning moments for the caisson. Wave pressures on the front face are distributed trapezoidally, reducing from p_1 at s.w.l. to p_2 at the caisson base, see Figure 3.1. Above s.w.l. the pressure reduces to zero at the notional run-up point given by a height η^*. The up-lift pressure at the seaward edge is determined by a separate expression, and may therefore be less than the pressure calculated for the toe of the seaward face. Up-lift pressures are distributed triangularly from the seaward edge to zero at the rear heel. The main response parameters are determined from:

$$\eta^* = 0.75(1+\cos\beta)H_{max} \tag{3.7a}$$
$$p_1 = 0.5(1+\cos\beta)(\alpha_1+\alpha_2\cos^2\beta)\rho_w g H_{max} \tag{3.7b}$$
$$p_2 = p_1 / (\cosh(2\pi h/L)) \tag{3.7c}$$
$$p_3 = \alpha_3 p_1 \tag{3.7d}$$
$$p_u = 0.5(1+\cos\beta)(\alpha_1\alpha_3)\rho_w g H_{max} \tag{3.7e}$$

Where η^* is the maximum elevation above s.w.l. to which pressure could be exerted, taken by Goda as $\eta^* = 1.5H_{max}$, β is the angle of wave obliquity, in plan, and the design wave height, H_{max} is taken as $1.8H_s$ for all positions seaward of the surf zone. In conditions of broken waves, H_{max} should be taken as H_b.

The parameters α_1, α_2, and α_3 are determined from:

$$\alpha_1 = 0.6 + 0.5 \, [\, (4\pi h/L)/\sinh(4\pi h/L)\,]^2 \quad (3.8a)$$
$$\alpha_2 = \min \{\, ((h_b-d)/3h_b)(H_{max}/d)^2 \, , \, 2d/H_{max} \,\} \quad (3.8b)$$
$$\alpha_3 = 1 - (h'/h)\, [\, 1 - 1/\cosh(2\pi h/L)\,] \quad (3.8c)$$

The water depth h is taken at the toe of the mound, and d over the mound at the front face of the caisson, but h_b is taken $5H_s$ seaward of the structure.

The caissons on rubble foundations considered by Goda (1974) had natural periods around 0.1 to 0.3s. When subjected to loads of durations shorter than the natural period, the effective load will itself be smaller than the applied load. Thus for the very short peak pressures caused by breaking waves, the Goda formula does not give the actual peak pressure, but pressures which give the equivalent static load for the dynamic system of caisson, mound and foundation. This method was not intended to predict pressures of short duration, or of limited restricted spatial extent. Goda (1974) noted that impulsive pressures caused by waves which break in front of or onto the wall may rise to $10\rho_w gH$, but judged that vertical breakwaters would not be designed to be exposed to direct impulsive pressures.

Various researchers have found uncertainties with the Goda' method, and some have identified differences with measurements of forces / pressures. Bruining (1994) has discussed many of the inconsistencies in the derivation of the Goda method, and particularly of the parameters α_1, α_2, and α_3. Despite these limitations, the methods developed by Goda (1975, 1984) and others constitute the best methods available, and include many points of good advice.

Takahashi's extension

More recently, Takahashi (1994) developed an extension to the Goda method to include the effect of breaking wave impacts. This modification was obtained by re-analysing the results of comprehensive model tests of caissons sliding under wave impacts, together with analysis of the breakwater movements at Sakata Port, Japan 1973-74. The modification is applied to the Goda method by changing the formulation for the α_2 coefficient. Takahashi introduces a new coefficient which is the maximum of α_2 or a new impulsive coefficient α_I, itself given by two coefficients representing the effect of wave height on the mound, and mound shape. The modification is applied by changing the α_2 coefficient to be the maximum of α_2 or a new impulsive coefficient α_I, itself given by two coefficients representing the effect of wave height on the mound, and mound shape, α_{I0}, and α_{I1}:

$$\alpha_{I0} = H/d \qquad \text{for } H/d \le 2, \text{ or} \quad (3.9a)$$
$$\alpha_{I0} = 2 \qquad \text{for } H/d > 2 \quad (3.9b)$$

$$\alpha_{I1} = \cos\delta_2 / \cosh\delta_1 \qquad \text{for } \delta_2 \le 0, \text{ or} \quad (3.10a)$$
$$\alpha_{I1} = 1 / (\cosh \delta_1 (\cosh\delta_2)^{0.5} \qquad \text{for } \delta_2 > 0 \quad (3.10b)$$

$$\delta_1 = 20\, \delta_{11} \qquad \text{for } \delta_{11} \le 0 \quad (3.11a)$$
$$\delta_1 = 15\, \delta_{11} \qquad \text{for } \delta_{11} > 0 \quad (3.11b)$$
$$\delta_2 = 4.9\, \delta_{22} \qquad \text{for } \delta_{22} \le 0 \quad (3.11c)$$
$$\delta_2 = 3\, \delta_{22} \qquad \text{for } \delta_{22} > 0 \quad (3.11d)$$

$$\delta_{11} = 0.93\, (\, (B_b/L)-0.12) + 0.36\, (\, (h_s-d)/h_s) - 0.6\,) \quad (3.12a)$$
$$\delta_{22} = -\, 0.36\, (\, (B_b/L)-0.12) + 0.93\, (\, (h_s-d)/h_s) - 0.6\,) \quad (3.12b)$$

This modification only operates where the water depth over the toe mound, d, is relatively small, and the mound is therefore most likely to precipitate wave breaking onto the wall. Takahashi's method does not alter peak pressures near the water level relative to those above or below, but simply increases all pressures by the same factor. It does not change up-lift pressures calculated by Goda's method. It includes the effect of mound width, B_b, but not of the slope angle to the mound.

Crown walls

Wave forces on a crown wall section on rubble mound may be treated as an extension of forces on a composite wall with extremely high mound. The CIRIA Rock Manual, Simm (1991) recommends the empirical formulae derived from model tests by Jensen (1984) and Bradbury & Allsop (1988) for the evaluation of wave forces on crown walls, Figure 3.4:

$$F_{h99.9\%} = \rho_w\, g\, h_f\, L_p\, (a\,(H_{si}/A_c) - b) \qquad (3.20a)$$
$$F_{u99.9\%} = 0.5\, \rho_w\, g\, B_{cw}\, L_p\, (a\,(H_{si}/A_c) - b) \qquad (3.20b)$$

These formulae were derived from model tests by Jensen and Bradbury & Allsop on a number of rubble mound / crest configurations, leading to a range of values of the coefficients a and b derived from regression analyses on forces using simple force tables to measure the horizontal forces only. The maximum force in 1000 waves was divided by the height of the front face of the crown wall, h_f, to give an assumed rectangular pressure distribution on the front face.

On the underside of the crown wall, this pressure was assumed to be transferred with no losses to the forward edge, with the uplift pressure decreasing linearly over the element width, B_{cw}, to zero at the rear edge. These assumptions were used to calculate the uplift force acting on the structure.

These formulae give a simple empirical fit to the original data from which they were derived, but considerable scatter suggests that some parameters may have been omitted, or the governing processes have not been fully described. One example of potential over-simplification of the physical processes is that the horizontal pressure is assumed to act over the full height of the crown wall.

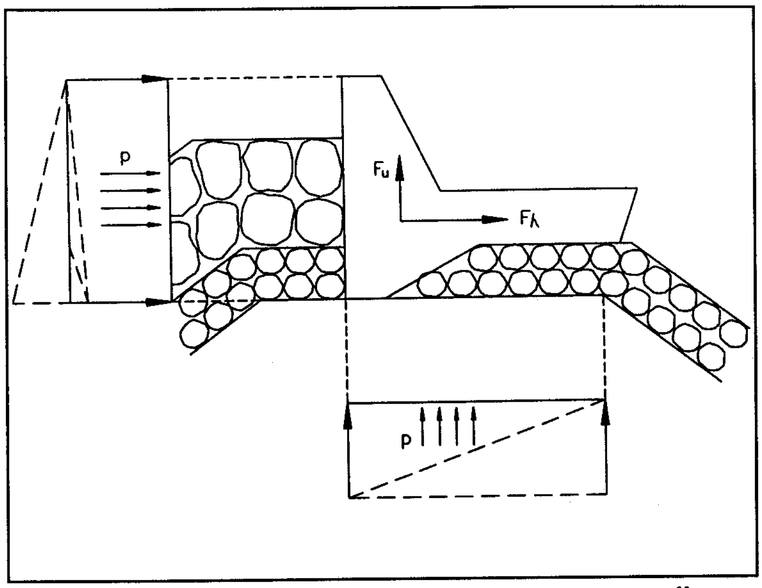

Figure 3.4 Horizontal / up-lift forces on crown wall, after Simm (1991)

Hamilton & Hall (1992) conducted an extensive study on crown wall stability, but did not propose any amendments or alterations to the above formulae. They described quantitatively the effects of changing a range of parameters in terms of the stability of the model structure, but did not provide any specific design guidance.

3.2.2 Up-lift forces

Relatively little information is available on up-lift forces acting on the underside of caissons or crown walls. Those design methods which give guidance on up-lift forces generally assume that the up-lift pressure at the seaward edge is equal to that acting at the base of the vertical wall. It is then usually assumed that up-lift pressures are distributed triangularly, reducing to zero at the rear of the caisson / crown wall. There are however few data to describe the shape of this pressure distribution, which may depend on parameters such as: the structure geometry; permeability of the rubble mound; siltation along the rear side of the structure; and the incident wave conditions.

Goda's method uses a further equation, see eqn (3.7e) in section 3.2.1, to determine the up-lift pressure at the seaward edge, potentially disconnecting it from that acting horizontally at the base of the caisson. The distribution of pressures under the caisson follows the assumed triangular distribution discussed above.

In few if any instances are methods to predict these pressures based on any measurements. Yet the overall loadings on the structure, and pore pressures acting in the foundation material and contributing to its strength, all depend upon reliable estimates of up-lift forces. Franco (1994) notes particularly that field measurements of pressures on a breakwater at Genoa had demonstrated that up-lift pressures could vary rectangularly if drainage of pressures at the rear side is inhibited by siltation in the harbour. This effect could increase the total up-lift force above that assumed by a factor of 2.

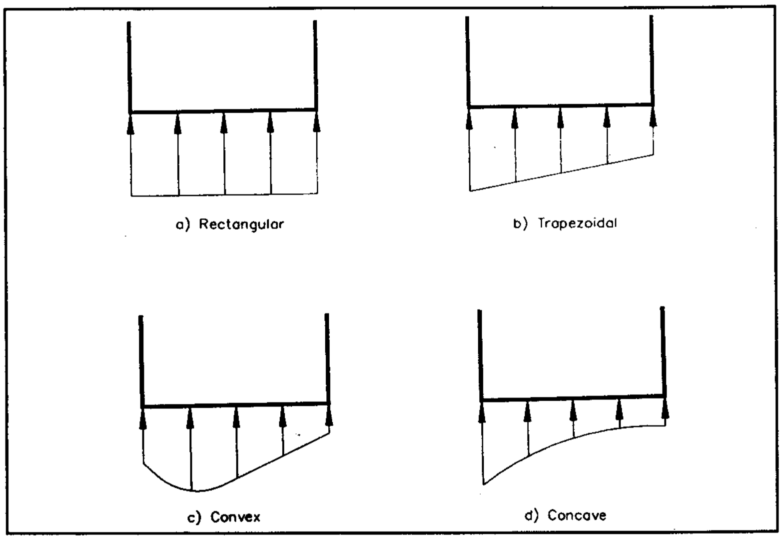

Figure 3.5 Forms of up-lift distributions, after McKenna (1996)

Oumeraci (1991) described caisson model tests where up-lift pressure distributions differed from the simple assumptions, and noted that the effective point of application of the up-lift force is of particular importance when overturning stability of a structure is considered. An exponential decay of up-lift pressure could move the point of application forward, thus increasing the overturning moment. McKenna (1996) describes four different forms of up-lift pressure distribution that have been seen in the results of these tests, summarised here in Figure 3.5. The simplest two are the rectangular and trapezoidal forms a) and b) in Figure 3.5 discussed earlier, but two other forms have been seen in measurements. The convex form shown in c) probably occurs at a short time after b) and often coincides with the maximum up-lift force rather than with the maximum horizontal force. The concave form in Figure 3.5d) generally occurs at the time of maximum horizontal force, but therefore does not necessarily indicate maximum up-lift force, nor the lowest overall stability.

3.2.3 Seaward or suction forces

A substantial proportion of failures of vertical walls are by overturning or sliding forward, that is in the opposite direction to the horizontal forces discussed above. Further, most blockwork breakwaters or seawalls fail by progressive movement seaward of individual blocks.

Despite the occurrence of these two effects, there few generally established methods to estimate seaward forces or suction on a vertical wall. A simple graphical method to estimate the quasi-static pressure difference across a caisson breakwater at the point of maximum wave draw-down is suggested by Goda (1985).

Goda writing in Herbich (1990) gives a very simple method to estimate the pressure under a wave trough at a vertical wall:

$$p = \rho_w g \qquad \text{for } -0.5H_{max} \le z < 0 \qquad (3.21a)$$

and

$$p = -0.5\rho_w gH_{max} \qquad \text{for } z < -0.5H_{max} \qquad (3.21b)$$

3.3 Hydraulic model tests

The evidence of damage / failure of structures identified in Chapter 2 suggests that design methods in use internationally do not always give reliable estimates of loadings or responses for these types of structures. The discussions in section 3.1 - 3.2 on prediction methods have identified different design / analysis methods which give varying estimates of the different loadings or responses, and whose regions of application differ widely. Both the evidence of damage / failures, and the variabilities in prediction methods, lead to significant uncertainties in the analysis / design of these types of structures, and demonstrate that more reliable methods are needed to give engineers improved predictions of wave loadings and of structure responses.

The most reliable methods to predict wave loadings have been for many years, and still remain, hydraulic model tests at scale ratios that allows the correct reproduction of wave forces and / or structure responses. The main purpose of such tests, outside of those conducted for research studies on particular responses, has been to determine whole body forces or, less often, wave pressures, thus allowing the designer to set the main caisson dimensions / weight. Hydraulic responses of wave transmission, wave overtopping, and/or reflections may also be measured. These measurements commonly use hydraulic models of scales between 1:20 and 1:70.

Typical model studies of the hydraulic performance / stability of a caisson breakwater would be conducted in a 2-dimensional wave flume (2-d), and/or in a 3-dimensional wave basin (3-d). In each instance, a range of different wave conditions would be used to quantify the performance over a range of return periods / risk levels. Random wave tests might typically cover 1000 to 5000 waves. Measurements that made during such tests might include:

a) Wave forces and moments acting on a section of caisson using a force table, dynamometer, or other force measuring devices;
b) Wave pressures at points on the front face, and/or on the underside;
c) Wave overtopping, mean discharges and/or wave by wave;
d) Number / proportion of waves overtopping;
e) Transmitted wave energy / heights;
f) Reflected wave energy / heights;
g) Movement / displacement of toe armour elements;
h) Scour changes to bed levels in front of the structure.

It is unlikely that any particular study would include all of these measurements, but would certainly include a) or b), and probably c) and/or d). Examples of such studies using force measurements have been discussed by van der Meer et al (1994), and using pressure transducers by Franco (1994) and Noli et al (1995). Franco et al (1994) discuss wave overtopping measurements in such studies.

3.3.1 Selection of model scale

The size of the model will be set to avoid any unnecessary scale effects, and to fit the test facilities available. It is worth noting that the scale ratio itself is of little relevance in the avoidance of scale effects. Most scale effects in breakwater models may be minimised by ensuring that flow conditions are in the same regime in model and prototype. Owen & Allsop (1983) and Owen & Briggs (1985) reviewed studies of armour stability in laboratories in the USA, Denmark, and UK, and concluded that scale effects in the flow in the primary armour on rubble breakwaters are insignificant provided that the Reynolds number, defined by the nominal armour diameter, is kept above Re = $3x10^4$. For rubble breakwaters, this is achieved by ensuring that model wave conditions do not fall below H_s=0.15m.

A similar argument may be pursued for flow in / around perforated wave screens, where the Reynolds number may be defined in terms of the screen thickness, t_s. In studies of wave reflections from vertical and perforated walls, by Allsop et al (1994b) assessed data from a perforated screen in a wave disturbance model to determine the lowest (model) wave height below which levels of energy dissipation start to change significantly. Allsop et al (1994b) plotted the sum of relative reflected and transmitted wave energies ($C_t^2 + C_r^2$) against model wave height. The energy dissipation response is generally flat, but rises for Re < $4x10^3$, as flow resistance of the screen increases giving greater reflections and less relative dissipation within the screen.

The remaining responses which may suffer from scale effects, even in models that meet the requirements outlined above, are wave impact pressures. Such pressures are likely to be greater in magnitude in small scale hydraulic model tests, but shorter in duration than their equivalents at full scale in (invariably aerated) sea water. Peak pressures measured in hydraulic model tests therefore represent over-estimates of those likely to occur at full scale, thus providing some (as yet un-quantified) safety factor.

The argument on scaling these peak pressures requires information not presently available on the relationships between the statistics of the pressure time gradients and the magnitude of the pressure impulses. Major research programmes have been underway at University of Plymouth with support from EPSRC, and at Hannover / Braunschweig under the MAST II-MCS project, but these studies had not at the time of these studies resulted in any significant guidance on the scaling of wave impacts. New research by HR Wallingford and Bristol University on concrete armour units on breakwaters, see Howarth (1996), has however been used here to address this problem in Chapter 7 of this report

It should be noted that the use of a force table or dynamometer to measure horizontal loads, a) above, generally precludes the reliable determination of up-lift forces, and hence of total overturning moments. A force table must usually be mounted close to the base of the (model) structure on which loads are to be measured, thus placing the device within the (model) mound or foundation. Conversely, a dynamometer may be mounted above the measurement caisson, removing any sensing elements from below the caisson. Unfortunately, these devices still require that the measurement caisson be free to move, if only slightly, without restraint from the under-lying mound / foundation material. This inevitably leads to a preferential flow path, substantially distorting any up-lift forces on the caisson.

These particular problems can be overcome by using pressure transducers mounted in the front face and underside of the caisson. The pressures may then be summed to give horizontal and up-lift forces, and moments about a chosen point, usually the rear heel point of the caisson. Correct reproduction of flow / pressure conditions beneath the caisson can be ensured by scaling (model) mound / foundation materials to reproduce the correct permeabilities, and construction the model carefully to avoid unrealistic flow conditions along the lower face of the caisson. The up-lift transducers must be mounted and protected to avoid any possible damage by stones protruding from the mound / foundation.

4 Design of research studies

It is apparent from previous work in the laboratory and in the field that there remain considerable uncertainties in determining wave forces on composite walls; in predicting conditions that lead to wave impacts; and in estimating the loadings themselves. Analysis of recent laboratory and field data suggests that impact loadings are considerably more important than had previously been presumed, and have probably been implicated in damage or movement of a number of structures. It was therefore clear that new research studies were needed to provide a consistent and comprehensive source of data on wave loads on vertical and composite walls / breakwaters.

Model studies alone will not complete the gaps in information, but resources available in this two year project did not permit field measurements, nor the extended laboratory studies needed to resolve uncertainties in model / prototype scaling effects. It was expected, however, that these issues were already being addressed by other researchers in the MCS and PROVERBS projects under the EU's MAST II and III research programmes.

In the event, an (informal) extension of the reporting of this project has allowed the inclusion of new information on scale effects on wave impact pressures measured in hydraulic model tests, thus yielding guidance on scale corrections for the measurements in this study.

4.1 Overall plan of studies

Hydraulic model tests were therefore conducted to measure wave loads on a range of simple vertical and composite breakwater configurations. In designing these tests, it was noted that many previous model studies, particularly those used to derive Goda's and Takahashi's prediction methods, had been based primarily on studies of the sliding distance of model caissons. No force measurements had been made. In other studies, the overall force on the front face had been determined by a force plate or dynamometer, but the need to ensure clearance for (slight) displacement of the sensing element precluded reliable measurement of up-lift forces. It was determined therefore that the only way to avoid these limitations was to measure wave pressures on both the front and underside of model caisson sections.

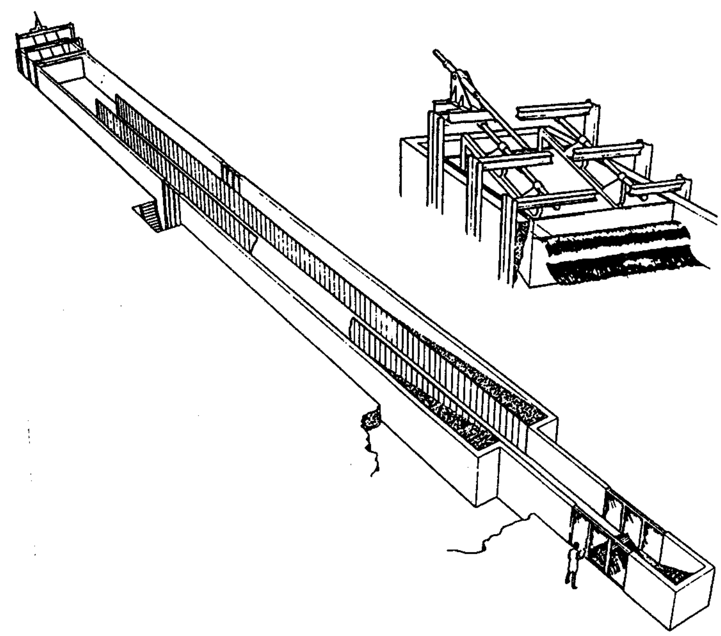

Figure 4.1 Deep wave flume

The model tests were conducted in the Deep Random Wave Flume at Wallingford, Figure 4.1, which is 52m long and operates with water depths between 0.8m and 1.75m. The flume is configured to reduce any reflection of wave energy from the test section in its absorbing side channels. The bed level at the position of the structure was +1.00m relative to the flume floor, and the bathymetry approaching the test section was formed to a uniform slope with a gradient of 1:50. The main caisson was formed as a hollow box in marine plywood with pressure transducers mounted flush with the front face and the underside, Figures 4.2 and 4.3. The design and construction of the model caissons, and of the measurement systems, were discussed with the MCS project by McKenna et al (1994) and Vicinanza et al (1995).

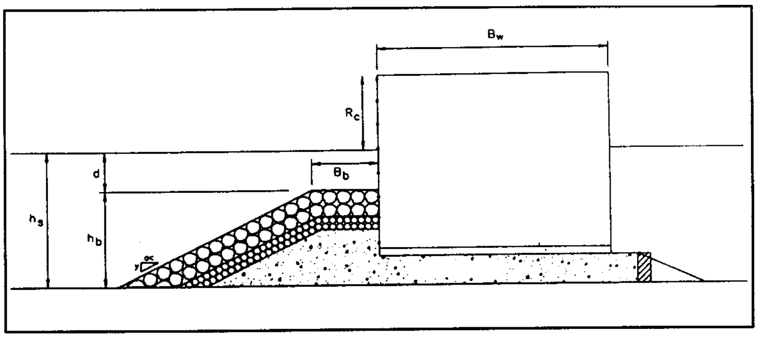

Figure 4.2 Caisson/mound geometrical parameters

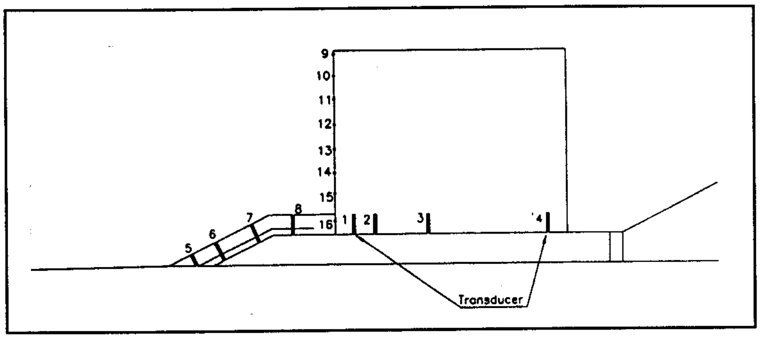

Figure 4.3 Pressure transducer positions

The geometric and wave parameters that influence wave forces include:

a) significant offshore or inshore wave heights, H_{so} and H_{si};
b) water depth in front of structure, h_s; and crest freeboard, R_c
c) wave steepness, s_{mo}, and wave length at structure toe, L_s;
d) water depth over mound in front of wall, d; and berm height, h_b;
e) berm width, B_b, and front slope of mound, α;
f) depth of embedment of caisson into mound, h_b-h_c

Studies to vary each of these systematically would have required up to 1500 tests, equivalent to some 55-65 weeks testing. The contract period for the DOE supported work was however limited to 2 years including: study design; construction and installation of all test sections and instrumentation; and analysis of the results; so drastic reductions of the programme were required. These were achieved by concentrating on those dimensionless parameters believed to be most important to the processes, particularly the relative wave height, H_{si}/d, the relative berm length, B_b/L, and the relative berm height, h_b/h_s. The main geometric parameters are defined in Figure 4.2.

These tests were not intended to reproduce any particular structure, nor was any particular model scale implied in the study design. Most of the design and analysis was intended to be conducted in dimensionless terms, in which case no scale is needed. It is however often convenient to bear in mind a scale or range of scales, both to check for any potential scale effects, and to calculate the significance in prototype terms of particular measurements. These studies generally relate to prototype situations at model scales between 1:10 and 1:50, giving incident wave conditions up to H_s=2m or 10m, so many practical situations may be covered by a scale of say 1:30. After completion of these tests, it was noted that related tests conducted by Politecnico di Milano and Delft Hydraulics were also assigned a nominal scale of 1:30, see Franco (1996).

Storm waves around the coastlines of UK and Europe generally give wave steepnesses of about s_{mo}= 0.04 to 0.06. It is known that some response functions are strongly geared to wave steepness, so tests were also run for a lower wave steepness, s_{mo}= 0.02, corresponding approximately to diffracted waves within a harbour, to reduced wave heights / growth of wave length following a storm, or in some areas preceding the arrival of a storm. Tests were limited to three nominal wave steepnesses, s_{mo}= 0.02, 0.04 and 0.06.

Water depth is important for its effects on incident waves, in the position of action on the wall, and in determining the effects of any approach slope or mound. The model was designed to be tested at up to 5 water levels (each 0.09m apart in the model). All 5 water levels were used during these tests, but not for all structures.

The wave heights used in the test facility were limited in magnitude by the capacity of the wave generator, but were varied to give intermediate and shallow water conditions. For the simple vertical wall, values of relative wave height H_{si}/h_s varied between 0.1 to 0.6, but this range was restricted to 0.15 to 0.4 for some other structures.

For the simple wall, the parameters varied were limited to the wave conditions and the local water depth. The crest level of the wall was not changed, although its freeboard R_c varied as a consequence of the changes to the water level. For the composite walls, the main change was to the relative height / depth of the rock mound in front of the wall, both by varying the absolute height of the mound, and by varying the water level. The other changes were to the width of the berm, 3 widths were tested, and to front slope angle of the mound, varied between 1:1.5 and 1:3 with most tests using 1:2.

The level of the caisson base was varied to study the influence of relative embedment on up-lift forces acting on the underside of the caisson. The caisson base was set at 3 different levels, equivalent to 3 depths of embedment, but giving 7 different values of the submerged depth, h', used in Goda's prediction method.

4.2 Design of model tests

4.2.1 Test structures

Eleven structures were tested in this study. Structure 0 was a simple vertical wall, tested to describe the horizontal loadings on the simplest configuration. The main composite walls were Structure 1 with a small mound, Figure 4.4; Structures 2 or 3 with intermediate mounds, Figures 4.5 and 4.6; and Structures 9 and 10 with large mounds, Figure 4.7. The remaining structures were variations from these intended to yield a coherent data set from which the influence of each parameter could be identified. The combinations to investigate certain parameter influences may be summarised:

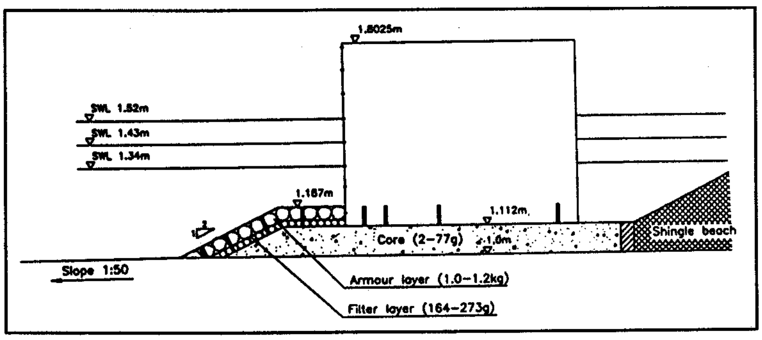

Figure 4.4 Structure 1

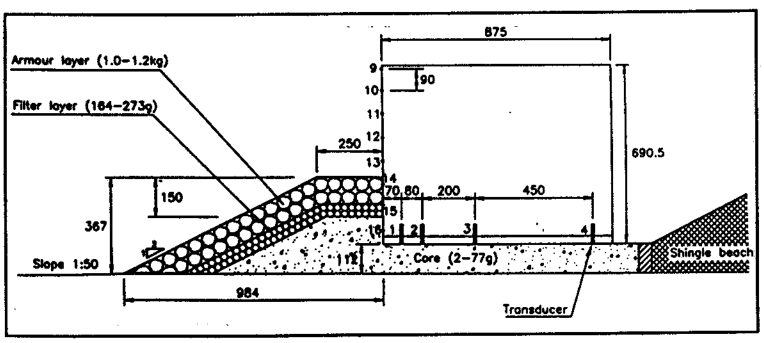

Figure 4.5 Structure 2

berm width, B_b	-	structures 3, 6, 7, and indirectly 4 and 5
front slope, $\cot\alpha$	-	structures 3, 4, 5
core depth, h_c	-	structures 2, 3, 9, (8, 10)
mound depth, h_b	-	structures 3, 8 (1, 2) (9, 10)

Structure 0, the simple vertical wall was placed with the toe of the caisson at +1.000m, the measurement caisson was itself elevated by 0.112m to give a crest level at +1.802m, 0.802m above the toe level. The main geometric features of the test structures are summarised in Table 4.1.

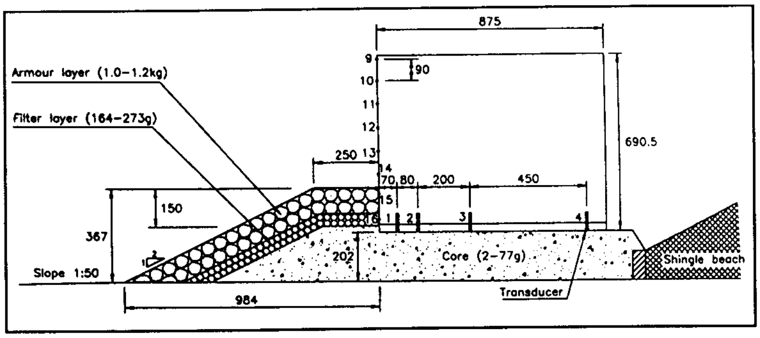

Figure 4.6 Structure 3

When considering the influence of the berm width B_b, and the front slope angle cot α, it was found that a single parameter could be defined to include the influence of both parameters. The equivalent berm width, B_{eq}, is defined halfway up the berm, rather than at its crest:

$$B_{eq} = B_b + (h_b/2\tan\alpha) \qquad (4.1)$$

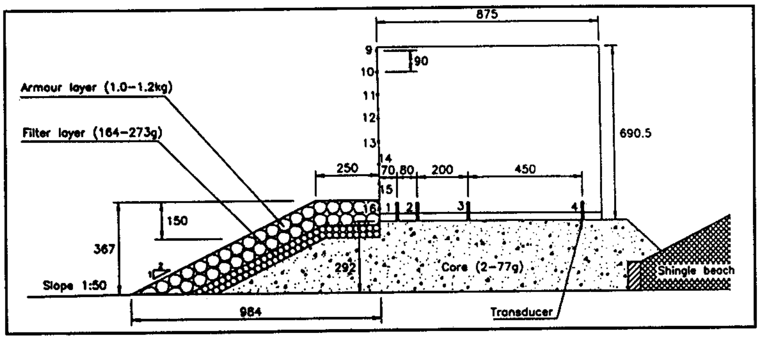

Figure 4.7 Structure 9

The model caisson was formed as a hollow box in marine plywood, and was secured to the seabed by 8 screw rods. The front face and the underside of the model were stiffened with stainless steel plates. For each of these structures, the caisson box was mounted onto two longitudinal timber beams which gave the desired mound height beneath the caisson and ensured that the caisson could be restrained rigidly. For Structure 0 where there was no mound, the void between the narrow beams beneath the caisson was blocked by a plate flush with the front face. For the composite structures, this space was filled by the rubble mound.

Table 4.1 Main geometrical parameters for walls and mounds

Structure	cot α	h_b	h_c	B_b	Crest level
		(m)	(m)	(m)	(m above bed at toe)
0	vertical	-	-	-	0.802
1	2.0	0.187	0.112	0.25	0.802
2	2.0	0.367	0.112	0.25	0.892
3	2.0	0.367	0.202	0.25	0.892
4	3.0	0.367	0.202	0.25	0.892
5	1.5	0.367	0.202	0.25	0.892
6	2.0	0.367	0.202	0.375	0.892
7	2.0	0.367	0.202	0.50	0.892
8	2.0	0.457	0.202	0.25	0.892
9	2.0	0.367	0.292	0.25	0.982
10	2.0	0.457	0.292	0.25	0.982

Pressure transducers were installed at 8 positions on the front face of the caisson, 4 on the underside and 4 just below the surface of the rubble mound. The use of a hollow box enabled overtopping collection and measurement equipment to be installed inside the box, reducing the need for external collection or measurement devices.

The rubble mound consisted of three rock gradings: the core (2-77g); the filter layer (164-273g); and the armour layer (1.0-1.2kg). During construction of each model configuration, the model caisson was lowered onto a bed of core at the appropriate level, and any gaps at the caisson / mound interface were filled by careful addition of core material. The berm and front slope were then formed in core material, to which filter and armour layers were added.

4.2.2 Test facility

The test flume is 52m long, and operates with water depths at the paddle between 0.8m and 1.75m. The flume is configured to reduce re-reflection of unwanted wave energy from the test section by the use of absorbing side channels on either side of, and separated from, the central channel by perforated dividing walls. The two outer (absorbing) channels are each 0.9m wide and 42m long; and the central (test) channel is 1.2m wide and 52m long.

The bathymetry in the flume was formed by moulding cement mortar over fill in the central channel to the required shape. From deep water near the paddle, the seabed sloped initially at 1:10 with a gradual transition to a more gentle slope of 1:50, and terminated in a 5m horizontal section where the model was placed. The bed level at the test structure was +1.00m relative to the flume floor at the wave paddle.

Waves were generated by a sliding wedge paddle, driven by a double acting hydraulic ram. The paddle movements are computer controlled using software developed at HR Wallingford (HR WAVEGEN), enabling regular or random waves to be produced. The random wave signals are generated using a white noise filter technique with a single shift register, to match any wave spectrum that can be specified at 16 equal frequency ordinates. JONSWAP spectra were generated for all of the tests. The nominal wave heights in Table 1 were generated and measured in the deep water section of the flume. The wave conditions in the central section of the flume approaching the test section were measured during the calibration tests described in section 4.4.

4.2.3 Test conditions

A range of wave conditions at five water levels were used to investigate the performance of the different structure types under different relative wave conditions. These were chosen so that the influences of significant wave height and mean sea steepness could be investigated separately, and direct comparisons could be made between different water levels. Wave conditions and water levels are summarised in Table 4.2. At each point marked with a water level (eg +1.43) waves were run the nominal wave heights indicated

Table 4.2 Test conditions, wave steepness, wave height, and water levels

s_{mo}	H_{so}=0.10m	H_{so}=0.20m	H_{so}=0.25m	H_{so}=0.30m
0.02	-	+1.43	-	-
0.02	-	+1.52	-	-
0.02	-	+1.61	-	-
0.02	-	+1.70	-	-
0.04	-	+1.34	+1.34	+1.34
0.04	+1.43	+1.43	+1.43	+1.43
0.04	+1.52	+1.52	+1.52	+1.52
0.04	+1.61	+1.61	+1.61	+1.61
0.04	+1.70	+1.70	+1.70	+1.70
0.06	-	+1.34	+1.34	+1.34
0.06	-	+1.43	-	-
0.06	-	+1.52	-	-
0.06	-	+1.61	-	-
0.06	-	+1.70	-	-

4.3 Instrumentation and test measurements

The main measurements made during these tests may be summarised:

a) Instantaneous water levels used to determine wave height / period, using standard HR twin wire wave probes and logging modules;
b) Volumes of water collected in the overtopping tanks, using a continuously recorded load cell under the collection tank, and/or volumetric measurement of total volume collected over (usually) 500 waves;
c) Number of overtopping waves detected by short wave probes mounted on the structure crest;
d) Wave reflections derived by analysis of the output from an array or 3 wave probes in front of the test structure;
e) Wave pressures on the front face (8) and underside of the caisson (4);
f) Wave pressures at (4) positions in the seaward face of the mound;
g) Video record of wave profiles observed through a side window of the wave flume.

Three computers were used during testing. On the first of these, data were acquired from all 16 pressure transducers at 400 Hz using the DATS package. The second computer collected data from the wave gauges (one offshore, three for reflections and one at the toe of the structure), and from the overtopping cell, using HR WAVES. The third computer was used for random wave generation using HR WAVEGEN.

The pressure transducers installed on the front face of the caisson were supplied by Control Transducers and were Model AB with a rated capacity of 0 - 6 psi and up to 2x over-load, but with 4x over-load before permanent damage to the devices. These transducers gave an upper limit for high resolution measurements equivalent to about 8m (fresh) water head, and a maximum pressure before damage on the transducers equivalent to 15m. The transducers on the underside of the caisson were Druck PDCR 810 with a range of 0 - 2.5 psi.

Before testing started, each set of transducers were checked and calibrated. The AB pressure transducers on the front face were set up so that 1m of (fresh) water head was equivalent to about 1 volt. With a range of 0-10v on the analogue to digital computer board (A/D card), this ensured that all pressure signals that could be measured at high resolution would be recorded in 0-8volts, the remaining range being available for any further over-load conditions. The up-lift and mound transducers were set up so that 1m of (fresh) water head was equivalent to about 5 volts.

The principal recording parameters used here necessarily represented compromises between the need to measure fast-acting events; the need to collect statistical information over a realistic number of waves; and restrictions on data volumes which could be recorded, stored, and processed.

It is generally agreed that faster sampling rates will yield greater wave pressures / forces, provided that the transducers are able to respond quickly enough. Some researchers interested in impacts have used sampling rates up to 5,000 or 10,000Hz, see particularly Müller (1993) and Kirkgöz (1995), but such rates have been restricted to very short test durations, often limited to regular waves or pre-determined wave packets. In contrast, most engineering studies have used force plates, tables, or frames, with sampling rates limited to no more than 25Hz, see particularly van der Meer et al (1994). Oumeraci et al (1994a) provide a graph based on experiments at Hannover which suggests reduction factors for impact pressures, impact forces, and impulses, as functions of the sampling frequency. This graph suggests that sampling at 400Hz may give under-estimates of maximum pressures by up to 50%, but that the equivalent reduction for horizontal force would be limited to 20%. At these rates, the total impulses are not significantly affected.

The statistics of wave pressures / forces are improved with longer test durations, and increased numbers of events sampled will tend to increase the maximum pressures / forces recorded. The original test design had specified 1000 waves, although previous tests described by Meer et al (1994) used 1000 - 3000 waves. During early tests, it was found however that 1000 waves at 400Hz generated files that were too large for the recording computer / software. The test length was therefore restricted to 500 waves.

4.4 Test procedures

4.4.1 Wave measurements

Before the model breakwater was installed in the flume, wave conditions at the position of the structure were measured during calibration tests. Short sequences of waves were generated during calibration and were determined using spectral analysis. Measurements of water surface elevations were made using 8 twin wire wave probes, located along the approach to the caisson.

Once the nominal wave condition had been achieved, more comprehensive measurements were then made using longer sequence lengths, analysed using statistical methods. This ensured that extreme waves were reproduced correctly, and that the statistical distribution of wave heights was recorded. Statistical analysis allowed the significant, 0.1%, and other extreme values of the wave height distribution to be determined at each wave probe position, together with the mean wave periods.

These long wave sequences were used during testing to ensure that extreme waves were correctly represented. Incident and reflected wave conditions were measured using 3 wave probes, located approximately 2 wave lengths seaward of the structure. The overall reflection coefficient, C_r, was determined by summing energies for each test condition.

4.4.2 Wave overtopping

During most of these tests, the number of waves overtopping the structure, the wave by wave overtopping volumes, and the mean overtopping discharges, were each determined. The numbers of waves overtopping the structure were counted using four overtopping probes spaced across the width of the flume. The mean overtopping discharge was calculated from overtopping volumes measured using a weighing mechanism located inside the caisson which formed the vertical wall. A 100mm wide chute directed overtopping water into the tank. The sensitivity of the weighing mechanism allowed the measurement of wave by wave overtopping discharges. The mean overtopping discharge was calculated at the end of each test. When a high mean overtopping discharge was expected during a test, the weighing cell was removed and a large reservoir was used to collect the water. The water was then pumped into calibrated volumetric cylinders. These results have been analysed by Madurini & Allsop (1995), and have already been discussed further by McBride et al (1995), so are not included in this report.

4.4.3 Pressures

Pressure data from the 16 transducers were acquired at a rates up to 400Hz. Wave impacts recorded by the 8 front face transducers were recorded at 400Hz. Pressures measured by 4 slower transducers on the underside, and the further 4 in the seaward face of the rubble mound were filtered at 20Hz, yet still sampled at 400Hz to avoid excessive complication in the logging and computation procedures. Data were acquired continuously for all channels through each test for about 500 waves to prevent the data loss which occurs with selective acquisition systems. The files generated were very large even in multiplexed binary format, and had to be expanded by de-multiplexing before analysis. Once de-multiplexed, these files were then put through a preliminary analysis process, in which interesting data were selected for further analysis.

Within the analysis program, pressure measurements in volts were notionally converted to metres head of fresh water, and these values were then converted to pressures in kN/m^2 by multiplying the pressure head values by $\rho_w g$.

5 Results of test measurements

The principal responses of interest here are the individual wave pressures acting on the front face and underside of the caisson. As individual pressure records, these data are very difficult to handle and to assimilate, so values of the horizontal and up-lift forces, F_h and F_u, are calculated by integrating these pressures over the front face and underside of the test caisson.

Pressure data were collected at 400 Hz from 16 channels for 500 waves, giving about 30 Mbytes of results per test. With over 200 tests, the initial analysis task was therefore to extract key information for each test. This need to reduce data volumes had however to be balanced by the need to avoid imposing any particular prejudice on the information likely to be of most interest and/or utility. The analysis approach therefore tried to balance these conflicting needs to maintain as much information as possible, whilst compressing data sufficiently to allow judgements to be made on the occurrence and magnitude of particular responses. Later analysis therefore operated at various levels of detail.

The analysis program described in report IT430 by Centurioni et al (1995) was used to identify "wave force events", about 500 per test. After all such events had been defined in a particular test, the program read each pressure channel to detect peak pressures and rise times (Δt) for each event on each transducer. Pressures on the front face, and on the underside, were also summed to give total horizontal and up-lift forces, and overturning moments using the approach derived by McKenna et al (1994) and modified by Centurioni et al (1995). Results are given, with a summary of test conditions, in the Appendix to this report.

This chapter describes the form of the pressure measurements, how the data were handled; the derivation of 'force events'; and aspects of data quality, handling and archiving.

5.1 Example pressure measurements

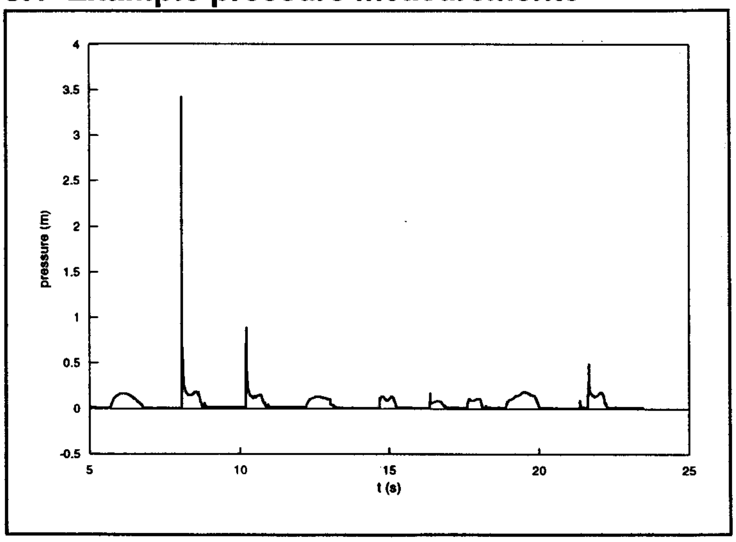

Figure 5.1 Typical pressure events from test 10003 on Structure 1

Before discussing the detailed analysis of parameters derived from the pressure signals in Chapter 6, it is helpful to consider a few examples selected from the (in excess of 1 million) waves sampled. Pressures measured by a transducer mounted at the static water level are shown in Figure 5.1 for about 9 waves. This example from tests 10003 on Structure 1 with a low rubble mound in front of the wall, shows some waves with sudden pressure rises and high peaks termed, impact events; and others with substantially smaller pressures with much longer rise times, termed pulsating events.

The forms of these wave pressure traces vary widely, depending most strongly on the type of wave breaking, and the position of the pressure transducer. The shape of the pressure / time records may be broadly classified in four types shown in Figures 5.2 - 5.5, and described below:

Type 1 Impact pressure on the vertical wall characterised by a short rise time, $\Delta t < 0.01 T_p$, and high pressure peak, followed by a much lower, but longer pressure peak, Figure 5.2;

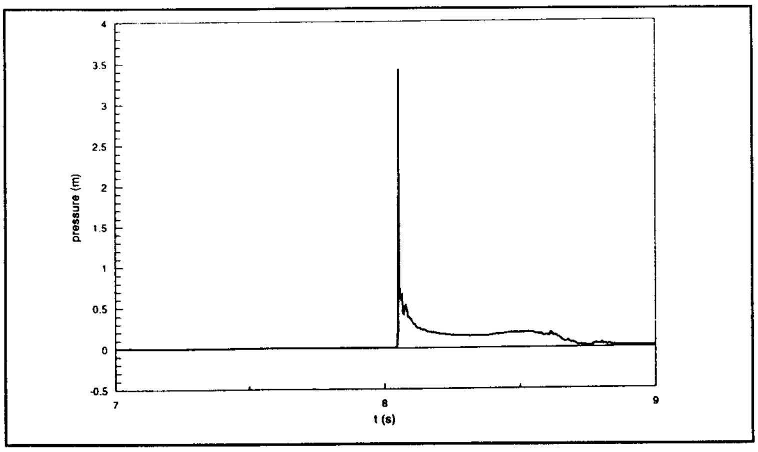

Figure 5.2 Impact event from test 10003 on Structure 1

Type 2 Less severe impact pressure, or up-lift / mound pressure at the time of impact, with similar characteristics as Type 1, but with smaller peak pressures and longer rise times, $\Delta t < 0.1 T_p$, Figure 5.3;

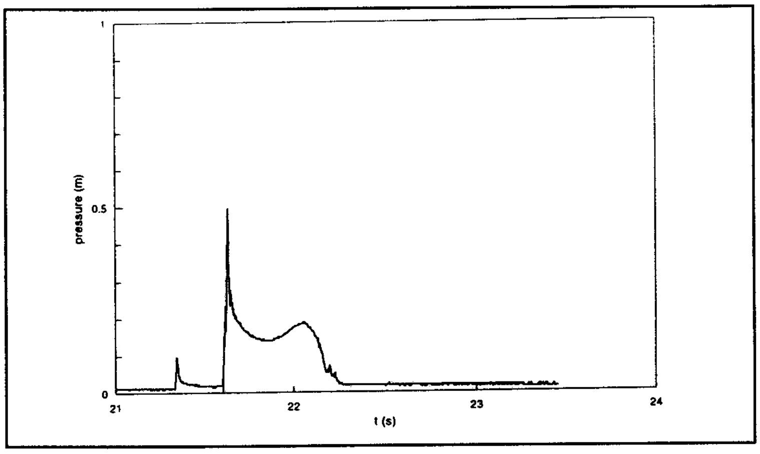

Figure 5.3 Small impact event from test 10003 on Structure 1

Type 3 Double peaked pressures from steep near-breaking waves with both pressure peaks of similar magnitude, and with long rise times, $\Delta t \approx 0.2 T_p$, Figure 5.4;

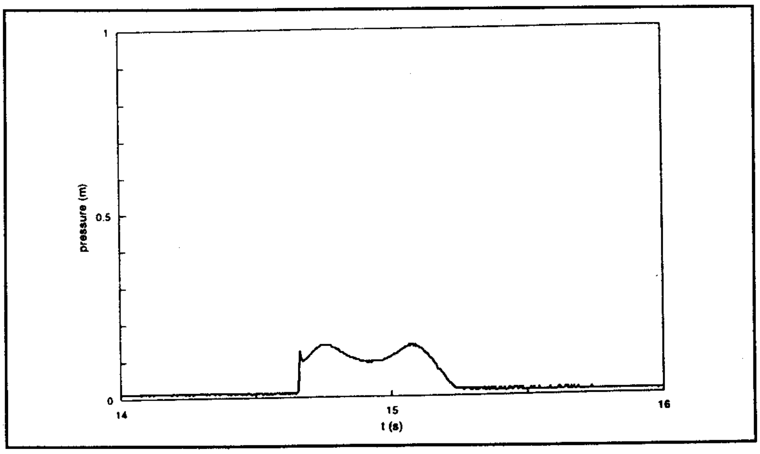

Figure 5.4 Double-peaked event from test 10003 on Structure 1

Type 4 Non-breaking or pulsating wave pressures with single peaks, and with long rise times, $\Delta t \approx 0.2T_p$, Figure 5.5.

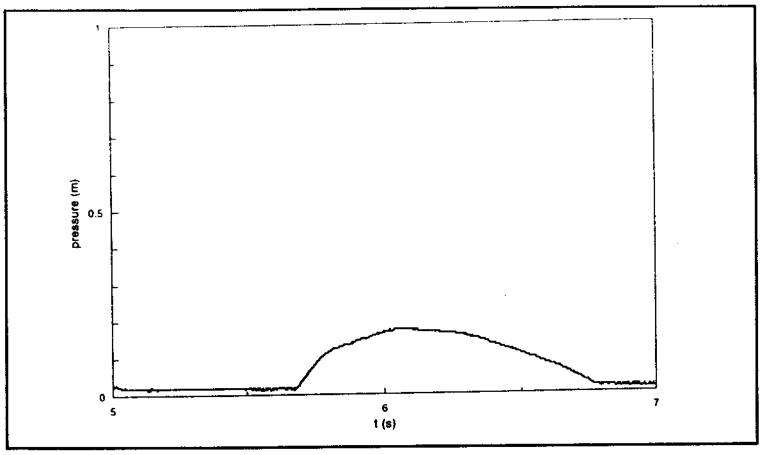

Figure 5.5 Pulsating event from test 10003 on Structure 1

[The requirement to describe as fully as possible the pressure peaks in Types 1 and 2 as shown in Figures 5.2 and 5.3, as well as giving a full description of the longer events in Types 3 and 4 motivated the requirement for rapid sampling, chosen here at 400Hz.]

Individual pressure events are of little practical application without information on the overall level of forces acting on the wall, and information on the distributions of pressures on the structure. The examples shown in Figure 5.6 illustrate how pressures vary in time, and between the different pressure transducers, with transducers 12 and 13 above the water level, 14 at s.w.l. and 15 and 16 below. Inspection of these impacts show how the peak pressures tended to propagate away from the point of maximum pressure, moving both spatially (up and down the wall) and thus temporally. This illustrates the potential for phase lags between different peak pressures, or forces.

Initial stages of the main analysis of these results concentrated on the total horizontal and up-lift forces acting on the caisson, F_h and F_u. These forces were determined by summing pressures over the height or width of the caisson as appropriate, see section 5.2 for more details. Each test gave approximately 500 force events, which were then ranked by magnitude to give probability or exceedance distributions of force for each test. These exceedance distributions of horizontal and up-lift forces were plotted on Weibull axes to identify the form of the force statistics; to check for any inconsistencies; and to identify if / where changes of wave breaking altered the type / distribution of loads. These are discussed more fully in section 6.1.

At an early stage in the analysis, there was some discussion as to the statistical level at which the main responses should be analysed. It was noted during testing, and during the statistical analysis, that all four types of wave pressure event shown in Figure 5.1 could occur in any single test. The use of the Weibull presentation of the force statistics however reduced the data to much simpler form, but did not resolve which statistical level would be representative of the complete distribution. Inspection of the statistics revealed that no single value would give the full distribution, and that at least 4 parameters would be needed to give the full description. It was therefore decided to concentrate on the statistical level used by Goda, and therefore inherently accepted in the British Standard, CIRIA / CUR manual, and by other researchers comparing with Goda's prediction. Most later analysis has therefore used the mean of the highest 1/250 values, so for tests with 500 values this corresponds to the average of the highest 2 values, or here to the average of 99.6 and 99.8% non-exceedance levels.

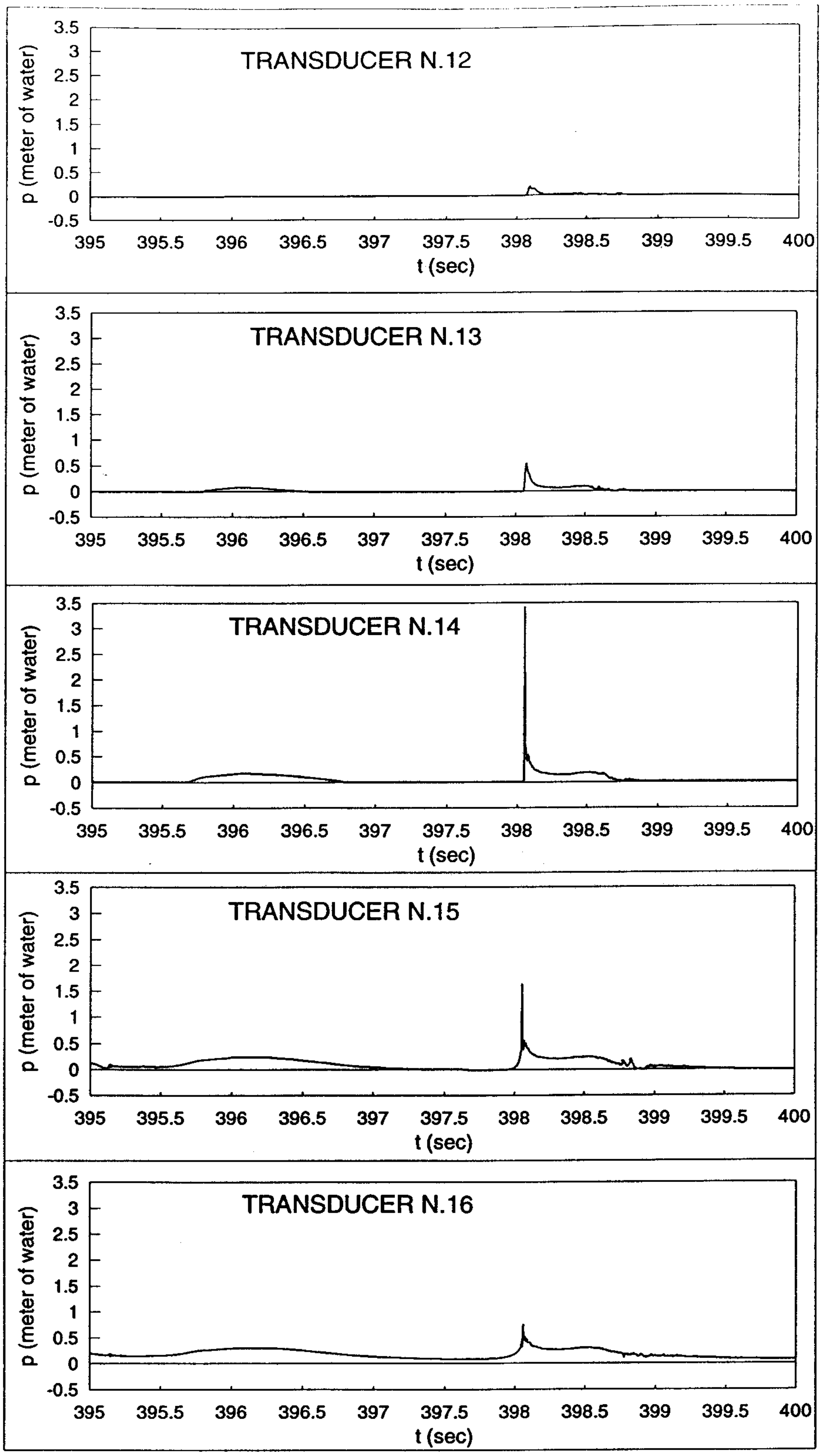

Figure 5.6 **Example pressure / time series over height of caisson**

5.2 Definition of pressure / force events

The first problem in the analysis of the data was to reduce the files to a manageable volume, particularly with over 200 tests each with data files of 1.5-2.0Mbyte x 16 transducers = about 30Mbytes. The first part of the analysis identified those parameters to be recorded for each impact "event", and thus reduce the volume of data to be processed.

Measurements of wave pressure were processed using a new program by Centurioni et al (1995) to define each "event", so that every time there is a wave impact, the analysis program found a rapid pressure rise to mark the beginning of the event. This involved a series of steps to threshold the signal, then to search for a rise past the threshold that large enough to exclude noise on the pressure signal. Once the start of the event had been identified, another section of the program checked if the signal is decreasing and falls below an appropriate threshold which is a function of the zero level. When this double condition is verified, the program starts again to look for a new event so that, if a signal has two peaks or is stepped, the program will only record a single start of event. The event definition is checked only for the record from the still water level pressure transducer. The very first event is always discarded because the measurements might begin somewhere inside it.

The level ánd sign of the noise level (value and sign) needs to be identified to define a threshold for event processing. A somewhat complex procedure has been developed, but tests have shown that a careful definition of this threshold is needed to avoid errors, particularly if the set-up of the transducer is at all uncertain. A parameter proportional to the noise level is also added to the signal so that the maxima are always positive.

The algorithm used for event definition calculates 2 running averages, and their ratio. When this ratio is greater then 1.1 for $(T_m/6)*400$ consecutive times, the program recognizes an event and transfers control to another section. The program later seeks an "end of event", after which the program searches for the next event.

After all events have been identified, the program reads through all the channels and the pressure peaks are detected for all transducers. For each event and for each transducer, the routine finds the time interval between the pressure peak and when the signal is 20% of the peak (Δt). Before moving to the next event, the program derives the main output parameters: the horizontal and up-lift forces, and the overturning moments. Pressures on front face and under side are summed using the trapezium rule, and example force results are shown in Figure 5.7. The program also records the maximum pressure for each event, and for each channel.

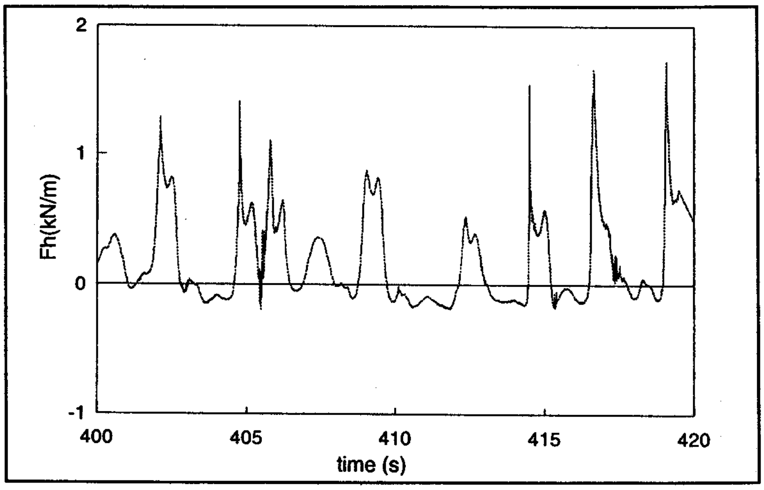

Figure 5.7 Example force - time series

The forces and moments acting on the (model) caisson at each timestep were calculated from the pressure measurements using an approximate integration method. The positions of the transducers do not cover the full height or width of the caisson, and are not spaced at even intervals. Some interpolation and indeed extrapolation is therefore necessary. The trapezium rule was chosen in preference to the staircase method or Simpson's rule since it permits flexibility in the spacing of the intervals, yet gives results which are in good agreement with analytical integration methods. Integration by the staircase method tends to over-estimate forces and moments where there is a high local pressure since it assumes that pressure acts over the whole area between the measurement points. Simpson's rule might have improved accuracy in integration, but the parabolic distribution over three adjacent points might also have given erroneous results in some cases, so the simpler method was preferred.

5.3 Data quality and repeatability

One of the major concerns in research is always to establish the quality / reliability of the data produced. In this work, this procedure was of particular importance due to:

a) The direct link between these measurements and the development of new / revised design methods for wave loadings, and hence impact on the safety of structures designed using them, as in BS 6349.
b) The highly variable nature of many previous measurements of wave loadings, particularly those laboratory tests using repeated regular waves from which conclusions have been based on pressures / forces at extreme exceedance levels, see Müller (1993) or Kirkgoz (1995).

During the model testing programme, a number of checks were made to evaluate data reliability, falling into four main areas.

At the end of data acquisition, measurements were de-multiplexed and a module within the DATS software package was used to view pressure - time traces. This procedure gave an instant confirmation that there were no major problems with the data, and that the pressure traces were of the type and level to be expected from the observations made during the test.

The same procedure was used to inspect pressure traces for signs of 'clipping', and to check that the sample rate was sufficient to cope with the very fast rise times. Analysis at this stage also included the propagation effect of the wave pressures, where the maximum pressure first occurred at one point on the front wall, then (say) one timestep later had moved to the neighbouring transducers. Times at which large impacts had been observed in tests had been noted in the model diary, and these times could be compared with the pressure traces to check that these times coincided with impact pressure signals.

During tests on Structure 1, a number of particularly severe impacts were noted, giving pressures up to at least $p=40\rho_w gH_s$. These excited significant interest, particularly as previous research studies by Müller (1993) and Kirkgoz (1995) had suggested that such severe impacts might be very variable. Demonstration tests (without pressure measurements) were performed on a number of occasions for visitors to the tests. As the times of the first few big impacts had been recorded in the test diary, impacts observed in subsequent runs of the test chosen for these demonstrations could be compared with that in the original test. These comparisons confirmed that severe impacts always occurred at the same point in the test.

Tests were later repeated using more sensitive transducers and a faster scan rate for some of the tests which had given high pressures in the original test series. A comparison of pressure - time histories again showed that peak pressures occurred at the same point in the corresponding tests and the general form of the pressure traces from corresponding tests in each series were very similar. There were some differences in the peak pressures where the second series of tests recorded lower values than in the first. This was not fully explained, but was ascribed to changes in the acquisition system and signal conditioning electronics.

Within the original test series, the only differences between some tests were in the core depth (ie the caisson base was raised, but all other dimensions remained the same). The pressure - time traces for specific transducer locations relative to water level (as opposed to specific transducers) were compared for the same incident wave conditions, and were found to agree very well. Again, these comparisons confirmed that measurements of wave pressures at specific locations under tests with the same wave conditions were repeatable.

5.4 Data handling / storage / archiving

During each of the tests in this study, measurements were recorded at rates up to 400Hz using a data recording and analysis software package DATS. These data values, from up to 16 channels were multiplexed to give a data acquisition file of up to about 20-30 Mbytes per test. With over 200 tests being conducted, and a computer limited to about 200-300 Mbytes storage, it was clear that there would be several problems associated with holding and analysing these data.

The problem was compounded as each multiplexed file had to be de-multiplexed into 16 individual binary files containing the time series data for each pressure transducer before any analysis could be completed. The de-multiplexed data files then occupied twice the disk space volume of the acquisition files. Initially data were to be recorded for 1000 waves, but this was soon reduced to 500 waves to reduce storage requirements.

The acquisition computer was equipped with a relatively small hard disk, so it was only possible to store one or two data acquisitions on the computer before down-loading them to another device. This was particularly important as the sampling / writing speeds used here approached practical constraints on disk access speed, particularly when such a small disk was more than about half-full. Testing, therefore, had to be interrupted regularly in order to transfer the data files. The files were transferred from the logging computer to the HR network for short term storage, de-multiplexing and analysis. Both the multiplexed and de-multiplexed files were then written to the HR magnetic tape archive system for longer term storage. The capacity of each magnetic tape was 100 Megabytes. For security reasons it was necessary to make duplicate copies of each archive tape. Over 200 tests were completed during this study resulting in some 50+ archive tapes being written. During late 1995 and early 1996, the majority of this data was also transferred to compact disks (with each of 650 Megabyte capacity).

6 Analysis of wave force / pressure results

The general form of the wave force / pressure data collected in these studies has been discussed in Chapter 5. Here the results are analysed in more detail to:

a) Describe the form of the statistical distributions of forces;
b) Identify the occurrence of wave impacts;
c) Identify parameter regions of significantly different wave behaviour at the wall.

Later sections then discuss:

d) Prediction of horizontal and up-lift forces at a given exceedance level;
e) Comparisons of measured forces with those predicted by methods described in Chapter 3;
f) Examples of vertical pressure distributions;
g) Wave impulses and impact rise times.

This chapter also discusses an approach to the calculation of overall stability of monolithic caissons on rubble mounds.

The early analyses by Vicinanza et al (1995) and Allsop et al (1995b) of results from these tests tried to describe the response of F_h, F_u, and later the total overturning moment M_t, to the main wave and geometry parameters using simple formulae, each intended to apply across the full range tested. That initial analysis developed simple equations to predict horizontal and up-lift forces, and overturning moments at the 99.6% non-exceedance level, $F_{h99.6\%}$, $F_{u99.6\%}$ and $M_{t99.6\%}$. Those equations appeared to give reasonable predictions for the initial set of structures considered by Vicinanza et al (1995), but the reliability of the prediction methods reduced when tested against the full data-set. The methods suggested by Allsop et al (1995b) extended this initial approach, but scatter in some regions of the parameter space covered factors of up to 2-3 times, and it became clear that these simplistic approaches were concealing important aspects of the wave / structure interaction.

It was then concluded that such simple methods are unlikely to give reliable predictions, and the approach of Allsop et al (1995b) was abandoned. Careful consideration of the initial data analysis showed that the simplifications had disguised significantly different hydro-dynamic processes. Two major improvements were therefore developed in the analysis described here: distinguishing the relative structure configurations; and then the types of wave breaking / loading conditions.

In the first change, the relative structure configurations tested in the study were divided into three ranges, as illustrated in Figure 6.1:

$0 < H_{si}/d < 2$ and $d > 0$,	when the mound is relatively small, and is always submerged;
$2 < H_{si}/d < 3$, and $d > 0$,	when the mound is relatively large, but is still submerged;
$-7 < H_{si}/d < -1$, and $d < 0$,	when the top of the mound is emergent.

Most of the analysis described in this chapter concentrates on the first of these configurations (163 tests out of 217). Analysis of tests covering the third range has been conducted under crown walls, section 6.3.3.

In the second change to the analysis method, the measured wave forces within each of the above datasets were further divided into 'impact' or 'pulsating' conditions, in many ways analogous to the 'breaking' and 'non-

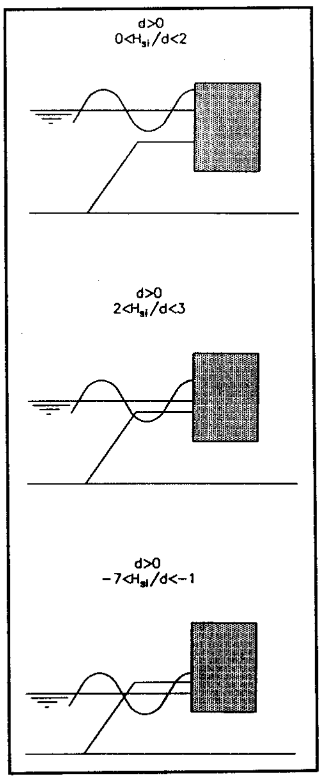

Fig. 6.1 Main parameter regions

breaking' conditions used by the Shore Protection Manual, CERC (1984). This revised analysis therefore proceeded in 3 steps:

a) Identify parameter ranges over which wave action at the structure leads to 'pulsating' or 'impact' conditions;
b) For conditions identified hers as pulsating, compare wave loads with predictions by Sainflou, Hiroi, Goda, or perhaps Goda modified by Takahashi;
c) For impact conditions, compare wave loads with predictions by Goda modified by Takahashi, or suggest new methods.

6.1 Statistical distribution of forces

Wave impact forces acting upon any coastal structure are highly variable, sometimes more so than the waves that cause them, so wave forces may best be described by their statistics rather than by single values. Most design methods in common use are however deterministic, so single values are required for design calculations. An appropriate probability level must therefore be derived at which to calculate the important parameters. In doing so, it is important to establish the extent to which any single probability level is indicative of the full distribution.

For each test, the analysis program gave a peak horizontal force for each event. These values of F_h were ranked, allowing the exceedance distribution to be plotted on Weibull probability axes to examine the statistical distribution. These axes, given by plotting ln(-ln(1-P)) against ln(F_h) where P is the probability level, were selected to give a good description of forces at low levels of exceedance (high levels of non-exceedance). The Weibull distribution may also be used to examine any link with the statistics of wave heights within a random sea, as wave heights generally fit a Rayleigh distribution, itself a special case of the Weibull.

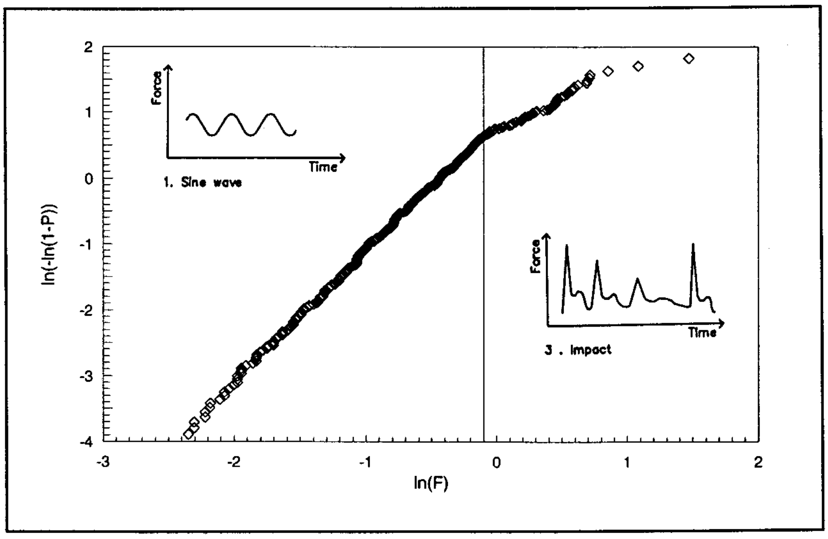

Figure 6.2 **Example Weibull distribution of horizontal forces for pulsating and impact conditions**

These exceedance distributions allowed wave forces to be divided into the two zones: 'pulsating' or 'impact' illustrated in Figure 6.2. Pulsating forces were defined as those varying linearly with exceedance probability on a Weibull distribution. These forces generally lie in ranges calculated by Hiroi or Sainflou's methods. Impact forces however increase much more rapidly over the upper part of the distribution, corresponding approximately with those waves that break directly against the wall.

In any general analysis, the factors that influence the force or pressure responses must be non-dimensionalised in a way that identifies the different form of wave breaking at the wall. Before doing so below, it is helpful to review example measurements, here plotted at model scale. The measurements considered here were limited to cases with moderate mound heights, $0 \leq H_s/d \leq 2$, as discussed above. Each of the distributions shown in Figure 6.3a-e is derived from a test of 500 waves at a single sea state and water level, and all those shown have s_{mo}=0.04.

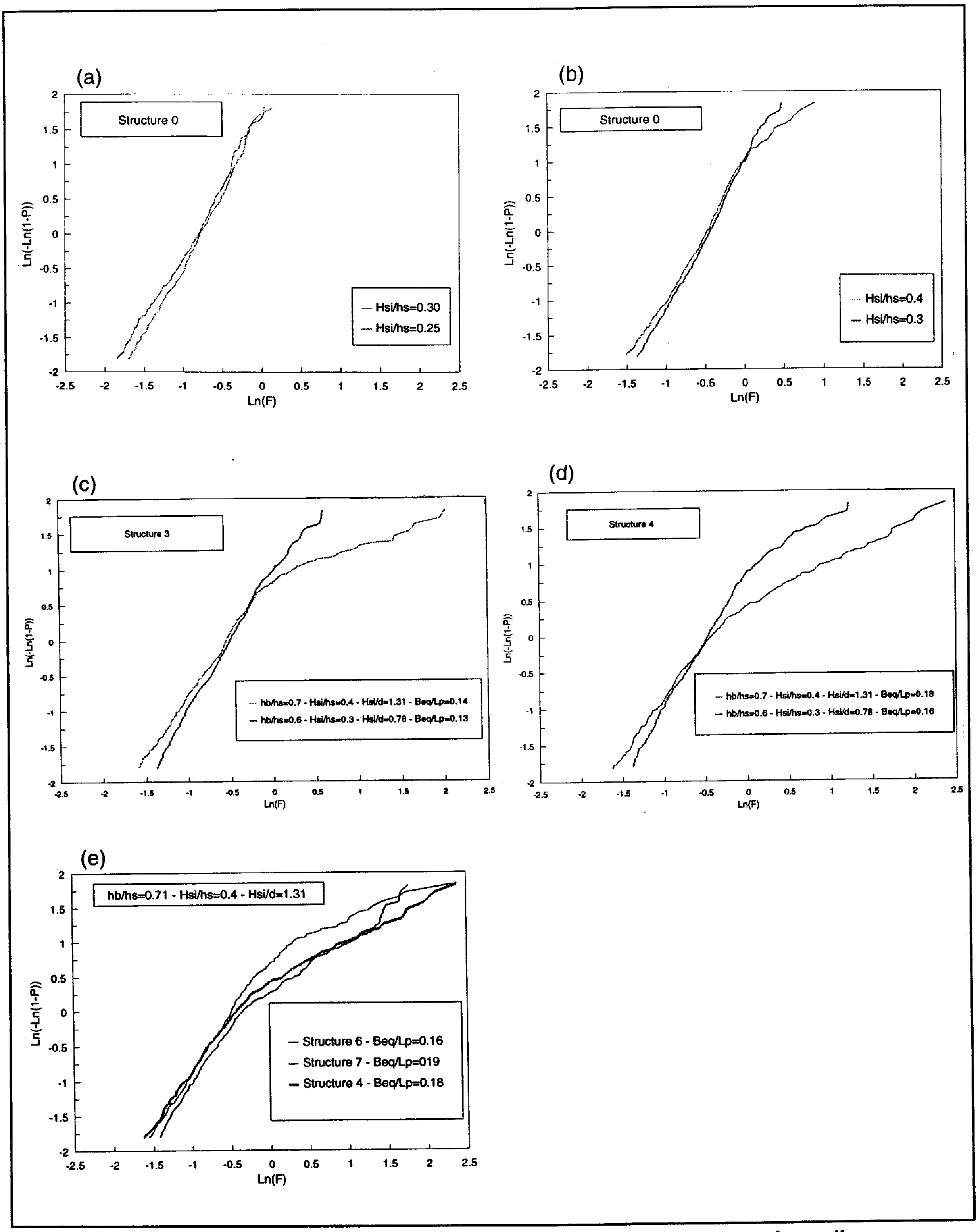

Figure 6.3 Weibull distribution of horizontal forces, vertical and composite walls

Distributions of wave forces on vertical walls

Wave forces at the plain vertical wall (Structure 0) shown in Figure 6.3a are generally pulsating. Forces from two comparative tests which differ only in water level giving relative wave heights of $H_{si}/d=0.25$ and $H_{si}/d=0.29$ show close agreement with a Weibull distribution.

Increasing the relative wave height from $H_{si}/d=0.3$ to $H_{si}/d=0.4$ in Figure 6.3b shows that a few of the forces (about 2%) depart from the main Weibull distribution for $H_{si}/d=0.4$, as larger waves break onto the wall. The overall level of wave forces are not greatly increased by this number / severity of impacts, but extreme loads at non-exceedance levels of 99.6% and 1/250 are increased significantly. The overall level of forces increases further as the wave condition approaches the breaking limit for shallow bed slopes around H_{si}/h_s = 0.55 to 0.6. For simple vertical walls with no mound, $d=h_s$, so depth-limited breaking is approached at $H_{si}/h_s = H_{si}/d = 0.55$.

It is then probable that further increases in offshore wave heights would lead to more significant proportions of broken waves. These broken waves would probably not further increase the proportion of impacts, as aerated broken waves generally give lower wave forces.

Distributions of forces on composite walls

It has been noted previously that a mound in front of a wall may significantly increase the proportion of impacts, and this effect is well illustrated in Figures 6.3c-e for composite walls with rubble mounds. In these discussions, the effect of the rubble berm is related chiefly to its level below the water surface, d, and its effective width given by B_{eq}. Each of these parameters is non-dimensionalised by the wave height, H_{si}, or the wave length, L_p, hence the use of the relative wave height H_{si}/d and berm length B_{eq}/L_p.

The test on Structure 3 with a small mound in front of the wall, and with a high water level where $H_{si}/d=0.8$ and $B_{eq}/L_p \approx 0.13$ gives pulsating forces in Figure 6.3c which fit the Weibull distribution. Reducing the water level to give a relative wave height over the mound of $H_{si}/d=1.31$ significantly increases the proportion of impacts to about 15%, and thus increases the magnitude of the extreme forces.

Somewhat similar increases in forces are seen in Figure 6.3d for Structure 4 where the mound slope angle has been slackened to 1:3, giving an increased mound volume. The test at $H_{si}/d=0.8$ and $B_{eq}/L_p \approx 0.16$ gives about 4% impacts, but the lower water level at $H_{si}/d=1.3$ significantly increases impacts to about 25%.

This effect is illustrated by comparing results for three structures with different mounds. Tests with the same wave height, period and water level on Structures 4, 6 and 7 compare the effect of relative berm width, B_{eq}/L_p, thus including the effect of mound slope angle. Forces plotted in Figure 6.3e show relatively close agreement for Structures 4 ($B_{eq}/L_p \approx 0.18$) and 7 ($B_{eq}/L_p \approx 0.19$) where the outer toe positions of the mounds are very close. The proportion of impacts are very similar, and other than at the most extreme level, the wave forces are much the same.

The other mound, Structure 6, with a slightly smaller relative berm width, $B_{eq}/L_p \approx 0.16$, shows similar behaviour in Figure 6.3e, but the proportion of impacts is a little less and most of the wave forces on this structure are smaller.

A similar approach in Figures 6.4a-c compares responses to different structures under the same wave condition and relative water level, H_{si}=0.2m, s_{mo}=0.04, and H_{si}/d=1.3. The effect of the relatively short mound (B_{eq}/L_p=0.14) in Structure 3 is compared with that of the simple wall in Figure 6.4a. Wave impacts on Structure 3 reach about P_i=9%, and wave forces at the higher non-exceedance levels are significantly increased.

Increasing the relative berm width to B_{eq}/L_p=0.19 in Structure 7 further increases the extreme forces in Figure 6.4b, and impacts increase to P_i=35%. A similar effect is shown in Figure 6.4c for Structure 4, where the berm width is increased but the seaward slope angle is significantly shallower at 1:3. This similar effective berm width, B_{eq}/L_p=0.18 gives impacts at about P_i=20% for Structure 4.

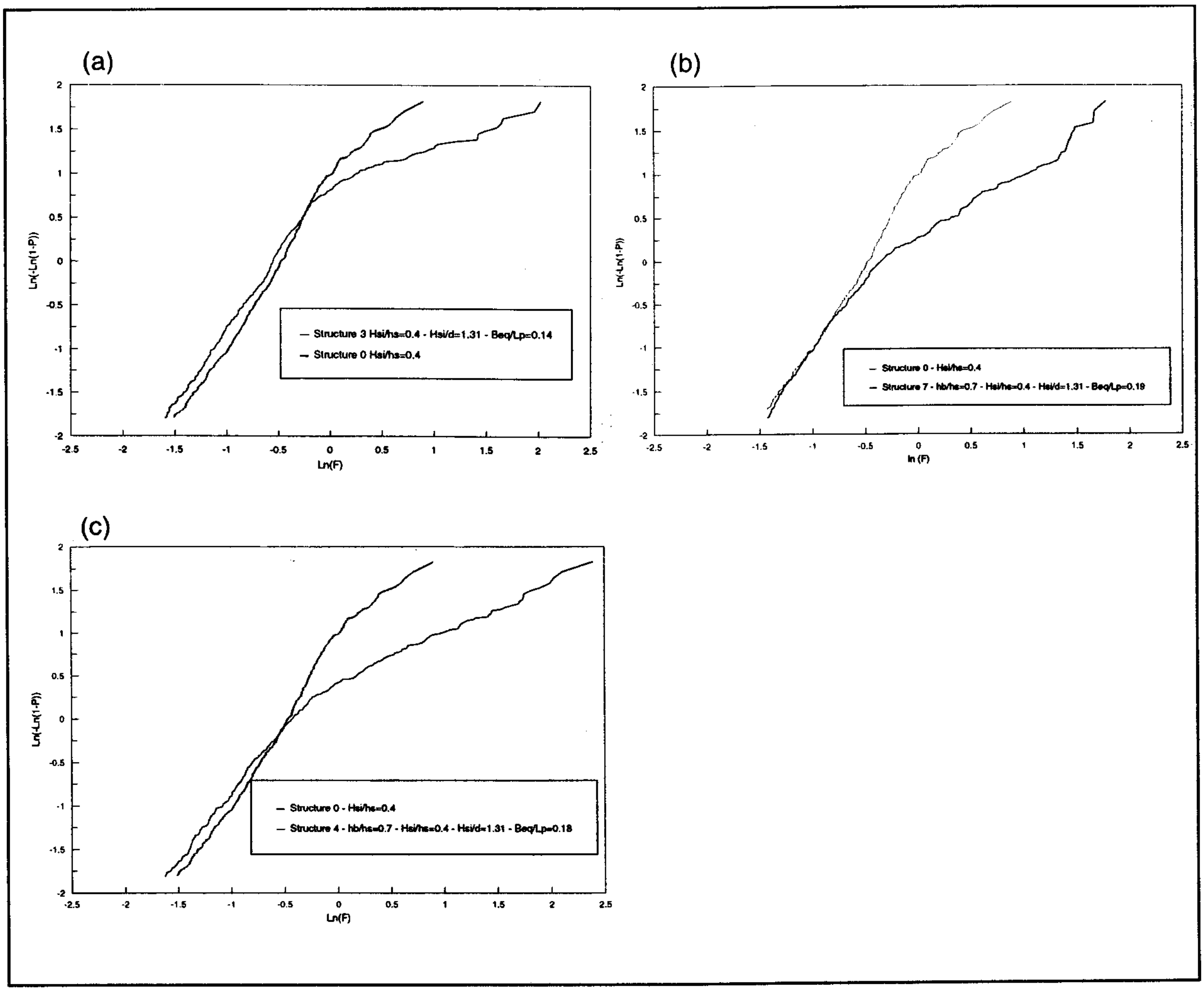

Figure 6.4 **Weibull distribution of horizontal forces, effect of berm width**

These statistical distributions of forces are useful in identifying the form of the wave loads, but are much less convenient to use in practice than a single representative force. Most of the remaining discussion on wave forces will therefore concentrate on single values of F_h derived for each test, allowing more direct comparisons of the effects of structure geometry, and relative wave conditions. In previous analysis of these measurements, forces were represented by the 99.6% exceedance level. Forces predicted by Goda's method are based on the average of the highest 1/250 waves, and if based on a standard sample size, $F_{h1/250}$ may be more stable than $F_{h99.6\%}$. Values of $F_{h99.6\%}$ are statistically more meaningful, but comparisons with Goda's and Takahashi's methods will use values of $F_{h1/250}$. This exceedance level was chosen for consistency with previous work, particularly design methods based on work by Goda and analysis by van der Meer et al (1994). The proportion or % of impacts P_i will continue to be used to distinguish impact from pulsating conditions.

6.2 Analysis of impacts and forces

The combined influences of wave conditions and structure geometry on wave forces are particularly complicated. Initial simplifications in analysis of this dataset by Vicinanza et al (1995) and Allsop et al (1995b) did not reflect fully the complex nature of the hydro-dynamic process of wave interaction at these structure, and the initial prediction methods did not therefore give wholly reliable predictions. The analysis presented here has therefore concentrated on dividing the tests into those for which pulsating or impact conditions have most influence on the more extreme forces in the distributions. The cases analysed are further divided between the simple vertical wall with no toe mound, Structure 0, and composite walls, Structures 1-10. This analysis was started in a paper in Italian to the Ravenna conference by Allsop et al (1995c), and is developed further in this report.

6.2.1 Simple vertical walls

Horizontal pressures only were measured on the simple vertical wall, so this analysis considers the occurrence of impacts, and the total horizontal force. The proportions (%) of impacts P_i are illustrated in Figure 6.5, where P_i is plotted against H_{si}/d (equivalent to H_{si}/h_s because $d=h_s$ for simple vertical walls). This shows a very clear onset of impacts for $H_{si}/d > 0.35$, suggesting that this may give a simple limit for the onset of impact conditions.

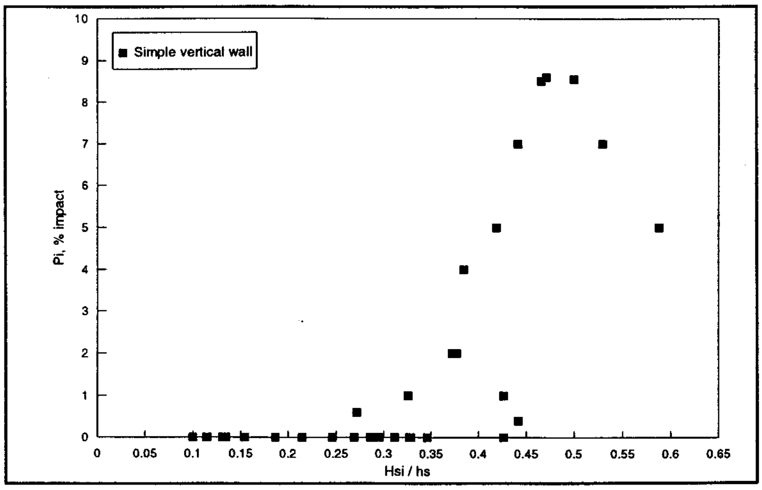

Figure 6.5 Influence of H_{si}/d on % impacts, P_j, vertical wall

This value of $H_{si}/h_s=0.35$ is rather lower than the relative wave height given by the simple rule of thumb for wave breaking over shallow bed, $H_{si}/h_s=0.55$. It is however reasonable to expect that a few waves will break at wave conditions below $H_{si}/h_s=0.55$. It may be noted that the upper few waves in the distribution may be approximately 1.8 to 2 times greater than H_s, and that the limiting conditions for single waves over shallow slopes is $H/h_s=0.78$. These suggest that a limit for the onset of breaking might well be given by $H_{si}/h_s=0.35$.

An alternative approach has been explored in which the largest wave heights from the statistical distributions measured in the calibration tests (represented here by $H_{99.6\%}$) are expressed as a proportion of the limiting breaking wave height (calculated here as $H_{b(Goda)}$). Results of this comparison are illustrated in Figure 6.6, and suggest that an alternative limit for the onset of impacts might be given by $H_{99.6\%}/H_{b(Goda)}>0.8$, but this approach is not as clear, nor as simple as the limit of $H_{si}/h_s=0.35$ given above, and is not pursued further in this report.

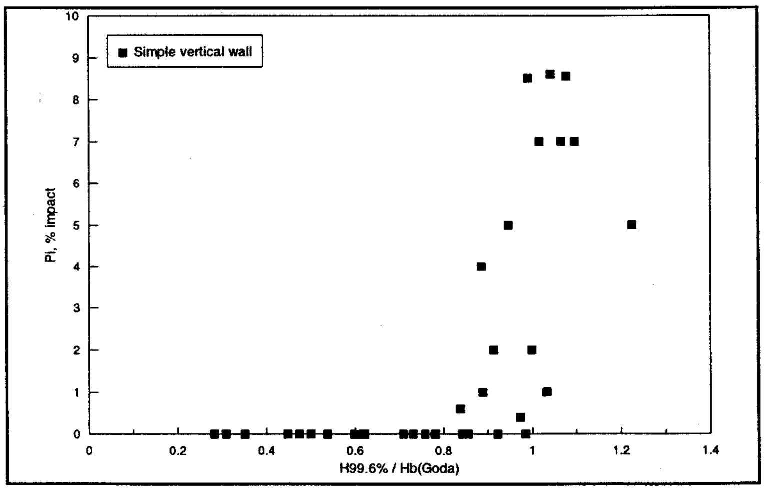

Figure 6.6 Influence of $H_{99.6\%}/H_b$ on % impacts, P_j, vertical wall

These limits are potentially useful in identifying different types of wave / structure interaction, but do not of themselves permit predictions of forces. Values of the measured horizontal force non-dimensionalised as $F_{h1/250}/\rho_w g d^2$ have therefore been plotted against H_{si}/d in Figure 6.7. Values of the horizontal force predicted by Goda's method are also shown, illustrating relatively good agreement for relatively small waves in the region $H_{si}/d \leq 0.35$, but significant errors for larger waves, $H_{si}/d>0.35$.

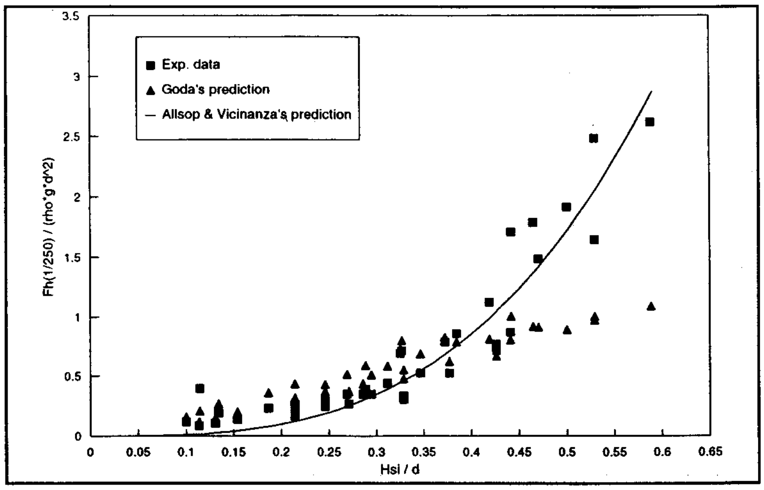

Figure 6.7 **Dimensionless horizontal forces against H_{si}/d, vertical wall**

For the simple wall with no mound, Goda and Takahashi's predictions are equal and for $H_{si}/d<0.35$, generally fall above the measurements in Figure 6.7. Goda's method may therefore be taken as giving a safe estimate of wave loads on simple walls for $H_{si}/d<0.35$.

For waves closer to breaking given by $0.35<H_{si}/d<0.6$, the prediction methods under-estimate measured forces. The differences are greatest where the incident wave conditions approach the breaking limit, approximated for shallow slopes by $H_{si}/h_s \approx 0.55$. This uncertainty can be partially overcome by a simple prediction curve of the form discussed by Vicinanza et al (1995) fitted here to results covering the range $0.35<H_{si}/d<0.6$:

$$F_{h1/250}/(\rho_w g d^2) = 15\,(H_{si}/d)^{3.134} \qquad \text{for } 0.35<H_{si}/d<0.6 \tag{6.1}$$

6.2.2 Composite structures, horizontal forces

The responses of composite structures are significantly more complex than for simple vertical walls, being influenced by the height, width and seaward slope of the rubble mound berm, as well as by the relative water depth and wave conditions. Some of these complexities were discussed earlier in section 6.1 where example responses to H_{si}/d, and B_{eq} were illustrated for particular wave conditions. The overall analysis here uses a similar approach to that in section 6.2.1, but is substantially extended to reflect the further geometric parameters, and hence the greater complexities of the processes.

The first distinction used in the analysis was to separate data by the relative berm height, h_b/h_s into "low" and "high" mounds. The lower mounds studied here were described by $0.3<h_b/h_s<0.6$, and higher mounds by $0.6 \le h_b/h_s<0.9$. These limits are not themselves of great significance, but give convenient divisions between regions of somewhat different response characteristics.

<u>Low mounds, $0.3<h_b/h_s<0.6$</u>

For low mounds, the onset of wave breaking and hence the change from pulsating to impact conditions appears to be maintained at $H_{si}/h_s= 0.35$, see Figure 6.8. This impression is however not well supported by data, as there are no measurements for Structure 1 below $H_{si}/h_s= 0.35$. It will also be shown later that increased mound levels move the onset of impacts to lower values of H_{si}/h_s. It is however useful to note from Figure 6.8 that the combined influence of near-breaking waves and the mound together give a significantly higher proportion of impacts than for a simple vertical wall. An alternative

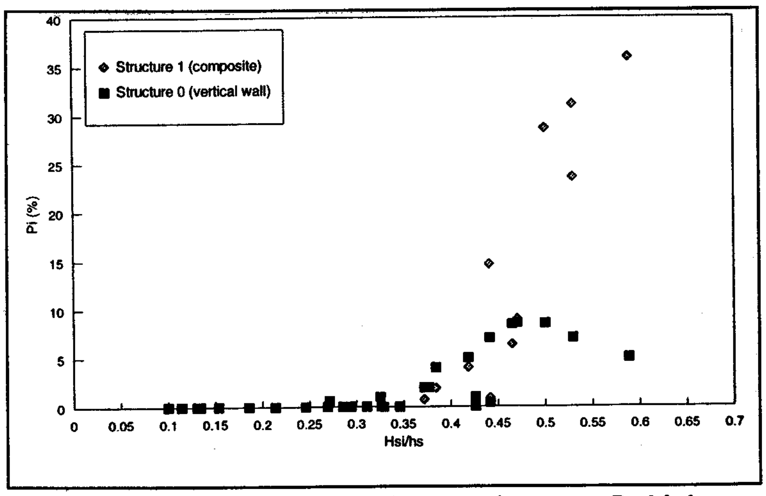

Figure 6.8 **Influence of H_{si}/h_s on % impacts, P_i, high mound**

approach is shown in Figure 6.9, where P_i is plotted against H_{si}/d, thus including more directly the effect of the relative berm level. This figure suggests that the onset of impacts is shifted by the presence of the mound to $H_{si}/d=0.65$, rather than $H_{si}/d=0.35$ noted for the simple wall.
Within the range $0.3<H_{si}/d<0.6$, with the data examined covering $0.11<H_{si}/h_s<0.33$ and $0.07<B_{eq}/L_p<0.23$, wave loads are pulsating, and the Goda equations generally give slightly conservative predictions of the overall horizontal forces, see Figure 6.10.

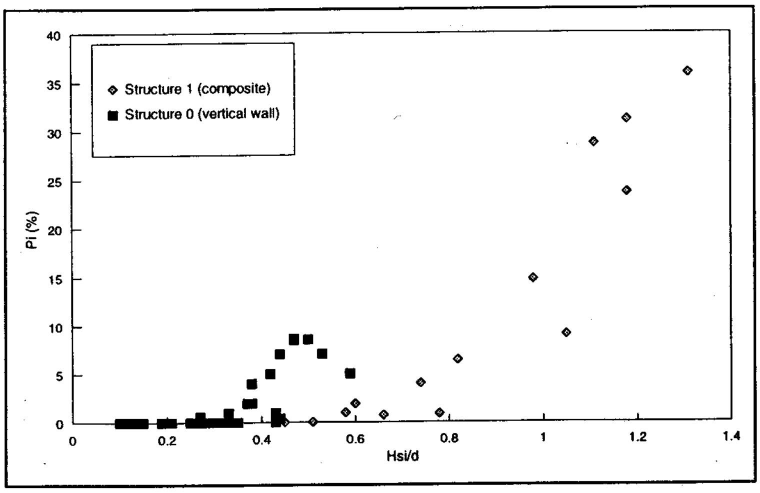

Figure 6.9 Influence of H_{si}/h_s on % impacts, P_i, low mound

For higher relative wave conditions, $0.6<H_{si}/d\leq1.3$, the influence of seabed and mound combine to increase the proportion of impacts, as shown in Figures 6.8 and 6.9. The forces have been plotted in Figure 6.10 in the same form as Figure 6.7 for the simple vertical wall. Also shown is the simple prediction method of eqn (6.1), developed for the simple wall and $H_{si}/d>0.35$. Surprisingly, this equation seems also to give a good description of the horizontal forces for low mounds given by $0.3<h_b/h_s<0.6$, and higher relative wave heights given by $0.6<H_{si}/d\leq1.3$.

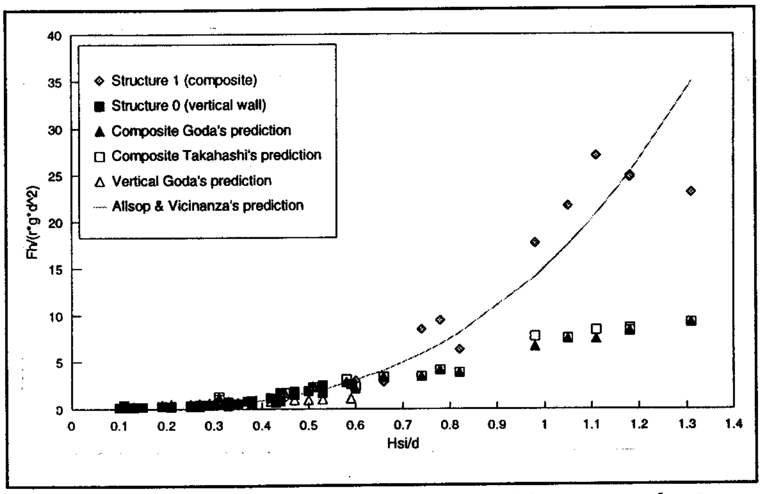

Figure 6.10 Dimensionless horizontal forces against H_{si}/d, low mound

<u>High mounds, $0.6\leq h_b/h_s<0.9$.</u>
Wave loads are again pulsating for high mounds with relative wave heights in the range $0.3<H_{si}/d<0.6$, for data covering relatively deep water $0.11<H_{si}/h_s<0.16$ and moderate berm widths $0.2<B_{eq}/L_p<0.34$. Over these regions, Goda's equations give conservative predictions for horizontal wave forces.

As relative wave heights H_{si}/h_s or H_{si}/d increase, more waves are likely to break on the structure, and the situation becomes more complex. The test results suggest that there is a transition zone around $0.55<H_{si}/d<0.65$, but few data are available to describe the processes reliably, so it is recommended that this zone is treated as the more conservative of the two adjoining zones.

Within the last zone examined here, covered by the largest waves tested given here by $0.65<H_{si}/d<1.3$, the influence of berm width expressed as B_{eq}/L_p is substantially more important. For short berms, given by $0.08< B_{eq}/L_p<0.14$, the waves are still pulsating with few if any impacts, and again Goda's method can be used to estimate wave forces. At the opposite end with long berms given by $B_{eq}/L_p>0.4$, wave breaking occurs over the berm before the wall, and wave loads on the wall are due to broken waves. Again the use of Goda's method gives a safe estimation of forces.

The remaining region of moderate berm widths covered by $0.14<B_{eq}/L_p<0.4$ shows significant levels of impacts, and wave forces are much larger. If P_i is presented against H_{si}/h_s using the form of Figure 6.8, it can be seen in Figure 6.11 that impacts start to occur at very low values of H_{si}/h_s. These results may alternatively be presented in Figure 6.12 in relation to H_{si}/d, as in Figure 6.9, covering the region $0.65<H_{si}/d<1.3$.

An alternative way to present the effects of B_{eq}/L_p is to plot P_i against B_{eq}/L_p for constant values of H_{si}/h_s, as in Figure 6.13. The proportion of impacts, P_i, increases as the relative berm width increases. It may be expected that this will reach a limit for very wide berms where the waves are broken before they reach the vertical wall, and the proportion of impacts, and the overall level of peak wave pressures would then decrease. This limit was not reached in these experiments, although there are some suggestions that $B_{eq}/L_p > 0.4$ or 0.5 would give lower impacts.

The overall picture of the different wave loading conditions over these regions is summarised in a type of flow chart in Figure 6.14. The parameter regions are divided by the type of wave breaking onto the structure, chiefly influenced by the relative berm height h_b/h_s, the relative wave height H_{si}/d, and the relative berm length B_{eq}/L_p. This chart represents a considerable simplification of the overall processes, but renders decisions on the type of wave loading substantially more tractable.

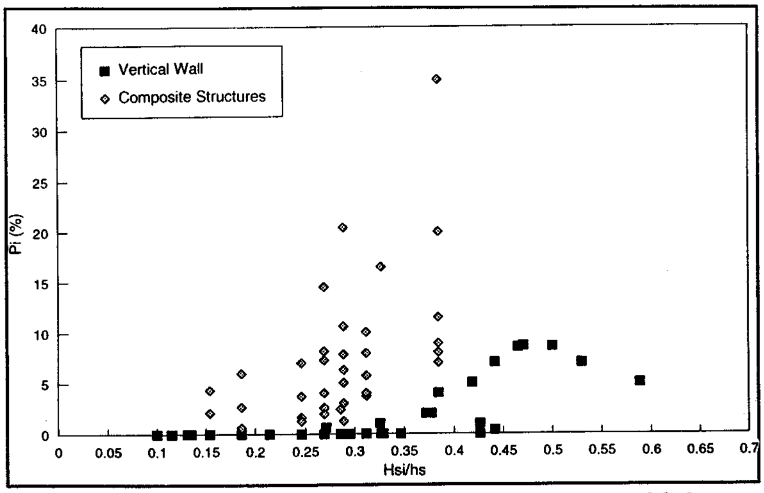

Figure 6.11 Influence of H_{si}/h_s on % impacts, P_i, high mound

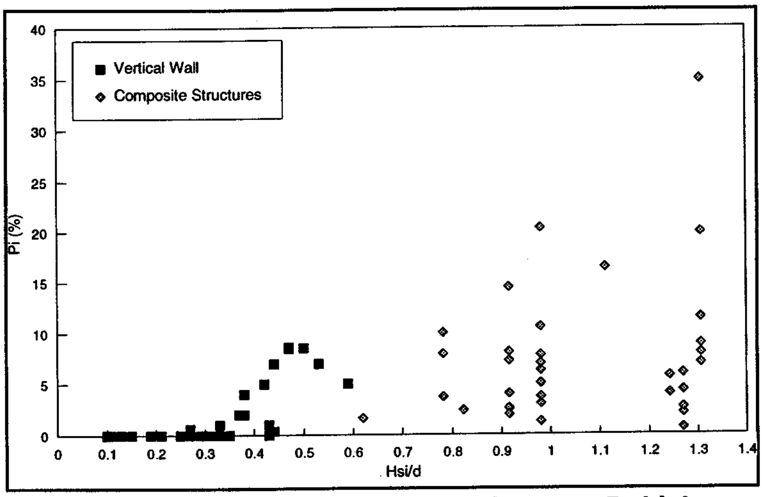

Figure 6.12 Influence of H_{su}/d on % impacts, P_i, high mound

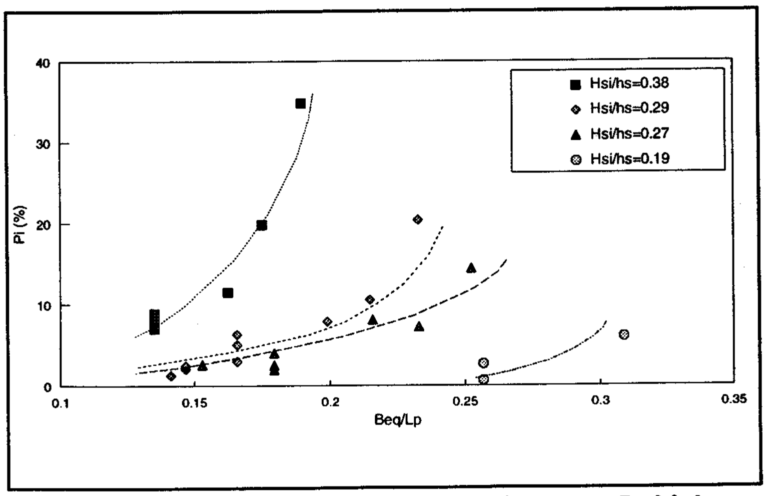

Figure 6.13 Influence of B_{eq}/L_p on % impacts, P_i, high mound

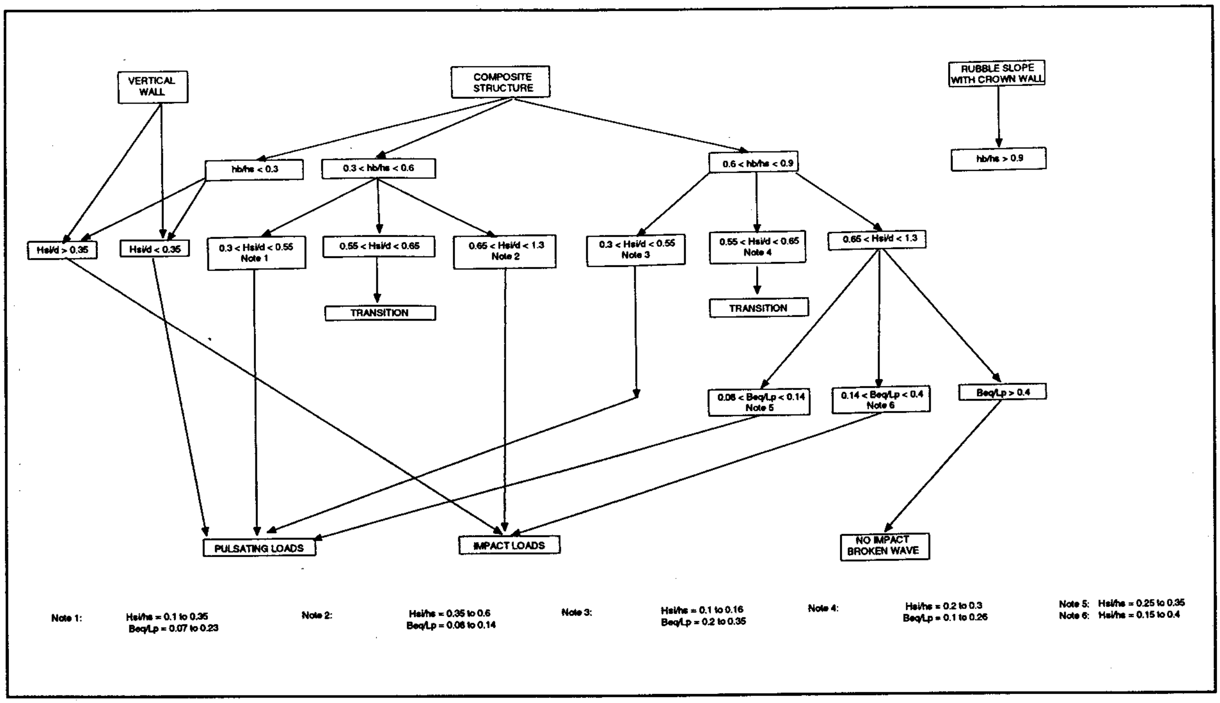

Figure 6.14 Flow chart of parameter regions for wave impacts

6.2.3 Composite walls, up-lift forces

Up-lift forces were analysed in two ways. In the first instance, the influence of the depth of the core, h_c, was explored to investigate the influence of these parameters on the overall level of up-lift forces. The overall level of up-lift forces, generally expressed as $F_{u1/250}$, were then considered using similar approaches as used for horizontal forces in 6.2.2 above.

The influence of core depth, h_c, was explored by inspecting the up-lift forces for three structures, identical except for the level of the caisson base: Structure 2, $h_c = 0.112$m, Structure 3, $h_c = 0.202$m, and for Structure 9, $h_c = 0.292$m. Up-lift forces were plotted for each test on Weibull axes, as for the horizontal forces earlier. Example sets are shown in Figures 6.15 - 6.18 for the same (offshore) wave height and wave steepness, but decreasing water depths, and hence increasing H_{si}/d.

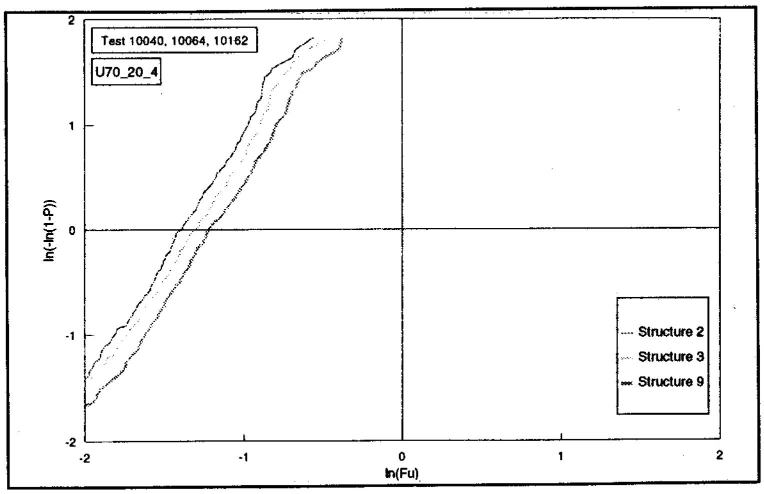

Figure 6.15 Weibull distribution of up-lift forces, s_m=0.04, H_{si}/d=0.45

At H_{si}/d=0.45 and H_{si}/d=0.62, up-lift forces are generally low, with Structure 2 with the lowest caisson base giving the lowest values of $F_{u1/250}$, Figures 6.15 - 6.16. At H_{si}/d=0.98 and H_{si}/d=2.54, up-lift forces have increased significantly, by 2 to 4 times at 1/250 level, Figures 6.17 - 6.18. Structure 2 with the lowest caisson base still generally gives lower forces than Structures 3 or 9, although the form of the distribution over the higher non-exceedance levels is often complex.

Inspection of similar graphs for other configurations and wave conditions suggests that up-lift forces are generally greater for increasing core depth, where the caisson base is higher, but that this trend is only clear for pulsating conditions. Under impact conditions, both horizontal and up-lift are more variable, and no clear influence of core depth was discerned.

Taking the analysis more generally, the results were split into three areas of H_{si}/d. For $H_{si}/d<0$, the configurations tested most closely relate to crown walls on rubble mounds, and forces on these structures are discussed in section 6.3.2 below. The other two regions considered here were defined as low mound, $0.3<h_b/h_s<0.6$; or high mound, $0.6\leq h_b/h_s<0.9$; as used in section 6.2.2 above. Where appropriate, regions are further divided into pulsating or impact conditions.

In general, F_u increases with greater incident wave height H_{si}, but decreases with lower mounds, ie greater d, Figure 6.19. The up-lift forces appear to cover two regions, given approximately by $0<H_{si}/d<0.8$ or perhaps 1.5, and $2<H_{si}/d<4$, and these are discussed further below. It is interesting to note the significant variation of F_u for the same values of H_{si}/d, suggesting influence of other parameters, perhaps including wave steepness and/or relative core depth.

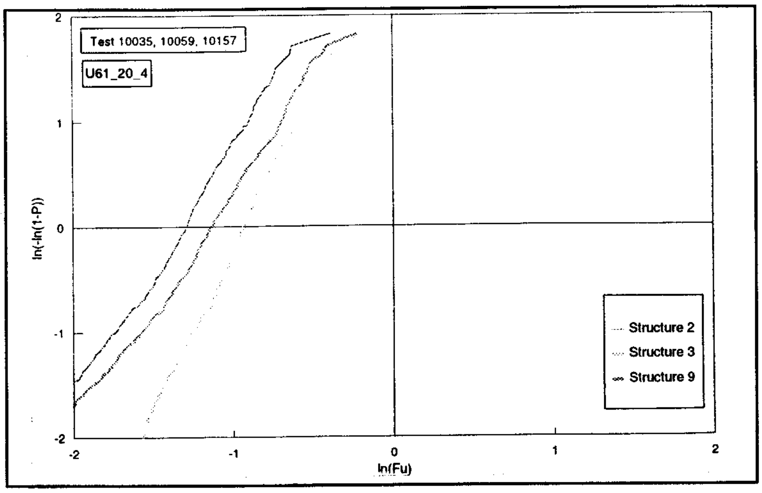

Figure 6.16 **Weibull distribution of up-lift forces, s_m=0.04, H_{si}/d=0.62**

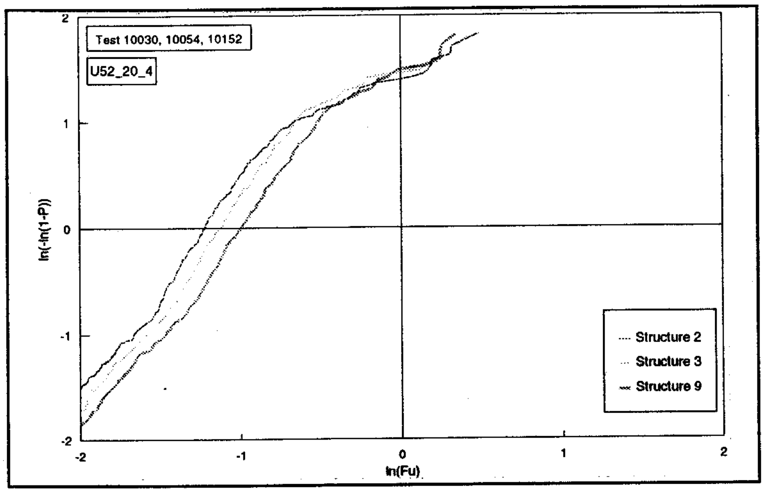

Figure 6.17 **Weibull distribution of up-lift forces, s_m=0.04, H_{si}/d=0.98**

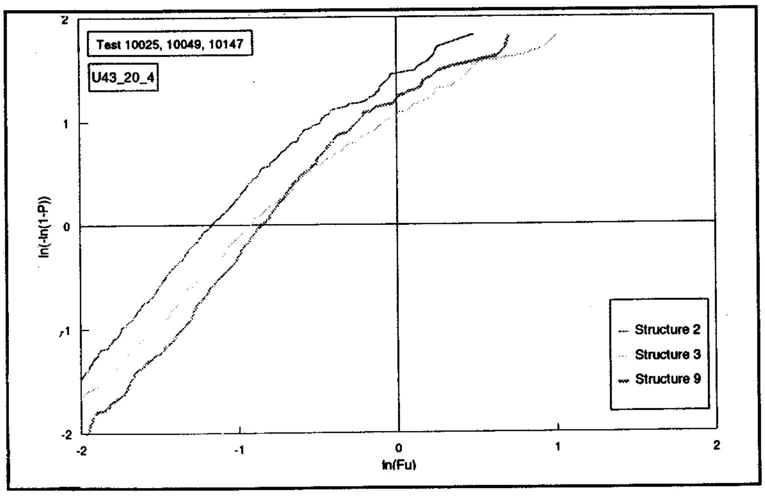

Figure 6.18 **Weibull distribution of up-lift forces, s_m=0.04, H_{si}/d=2.54**

The scatter of results can be much reduced by non-dimensionalising up-lift forces as $F_u/\rho_w g d^2$, and a generally increasing trend of increasing $F_u/\rho_w g d^2$ with increasing H_{si}/d. The results still appear to cover two different regions, so have been split into $0<H_{si}/d<1.5$, and $2<H_{si}/d<3.5$ in Figures 6.20 and 6.21.

It has been shown earlier that horizontal force are more likely to be increased by impacts for $H_{si}/d>0.6$ as the effect of the berm on the form of the wave breaking is increased, Figure 6.14. For up-lift forces, a slightly higher limit of $H_{si}/d=0.8$ in Figure 6.20 appears to better describe the transition from pulsating to impact conditions. This increase in the limit of pulsating behaviour for up-lift forces can be explained by damping of wave pressure propagation in the rubble mound for small proportions of impacting waves. As the waves increase and thus change from pulsating to impact conditions, horizontal forces respond immediately, but a small percentage of wave breaking is not sufficient to significantly increase up-lift forces. When the percentage of breaking waves increases (say to $H_{si}/d = 0.8$) up-lift forces begin to respond to the change of regime.

For the larger relative wave heights in Figure 6.21, variations of F_u at the same values of H_{si}/d are reduced, particularly at higher relative wave heights.

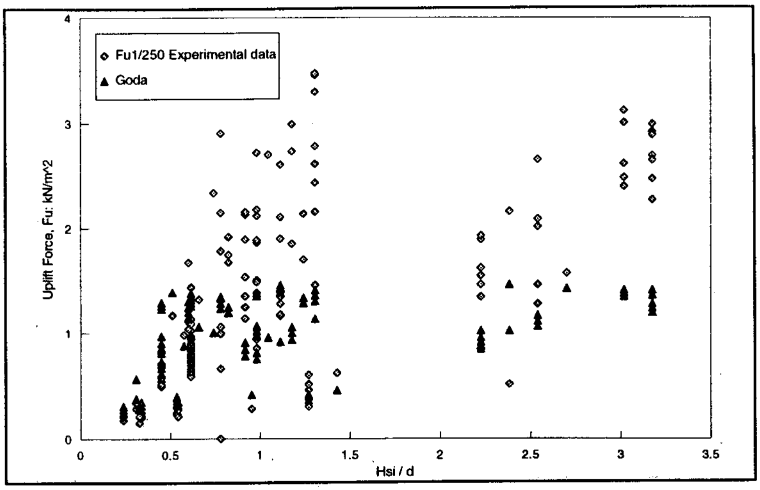

Figure 6.19 Up-lift forces for $0<H_{si}/d<3.5$

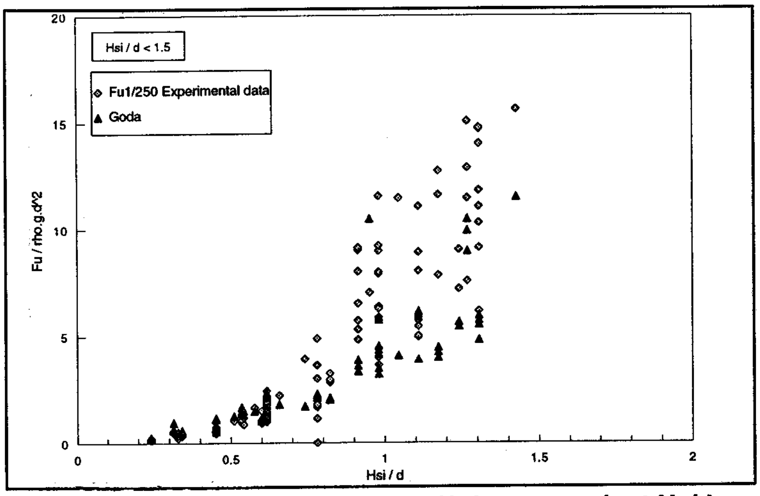

Figure 6.20 Dimensionless up-lift forces against H_{si}/d, $0<H_{si}/d<1.5$

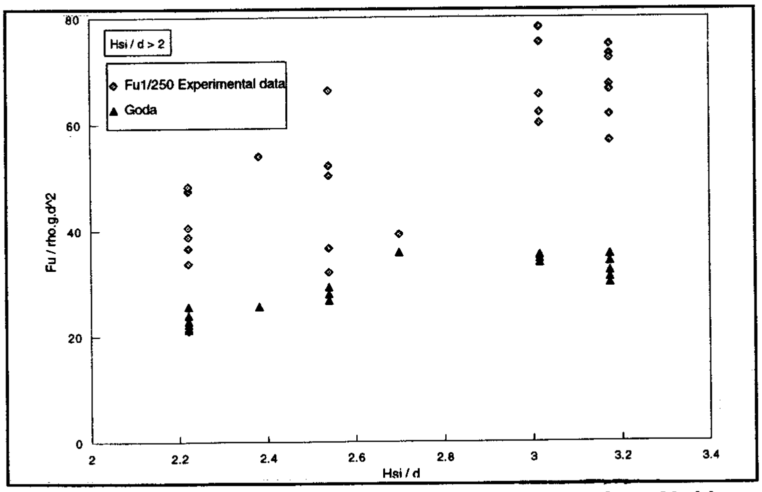

Figure 6.21 Dimensionless up-lift forces against H_{si}/d, $2<H_{si}/d<3.5$

6.3 Comparison with design methods

6.3.1 Simple vertical walls

Horizontal forces on simple walls with no mounds were discussed briefly in section 6.2.1 above. The responses were divided into two regions, $h_{si}/d < 0.35$ or $h_{si}/d > 0.35$. For the lower relative wave heights, $h_{si}/d < 0.35$, Goda's method generally over-estimates the horizontal force, but not very severely, so this prediction method may be taken as giving a safe approach. The degree of agreement is illustrated in Figure 6.22, showing an average bias or over-estimate of about 40%. It is interesting to note that the use of a factor of safety of 1.5 with Goda's prediction method for the horizontal forces would give a mean safety factor of 2 relative to the experimental results.

For higher relative wave heights, $H_{si}/d > 0.35$, Allsop & Vicinanza (1996) suggested a simple equation to estimate wave forces, given in section 6.2.1 above as eqn (6.1). The region of application, and experimental data are summarised in Figure 6.23. A direct comparison between measurements and predictions in the form of Figure 6.22 is then given in Figure 6.24. This shows wider scatter than for the smaller forces covered by Figure 6.22, but that any over- or under-estimate (bias) is small. It is also interesting to compare the experimental results with predictions from Goda's method in this region. Here the scatter is still large, but the average under-estimate or bias is about 30%.

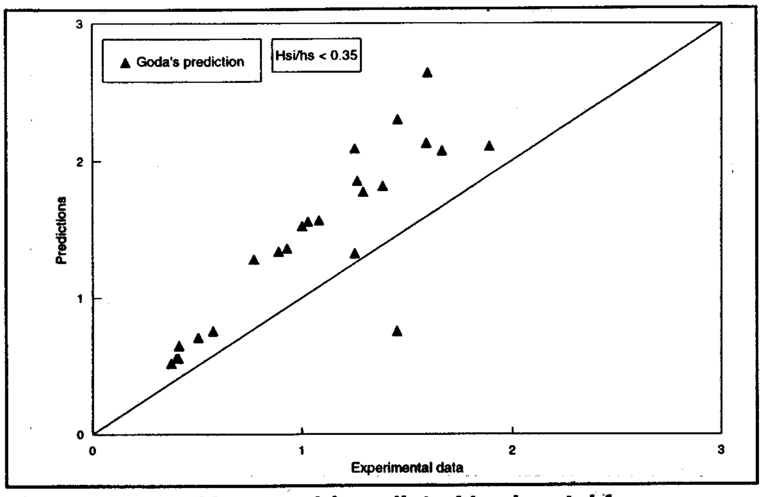

Figure 6.22 **Measured / predicted horizontal forces, Goda, vertical walls, $H_{si}/d<0.35$**

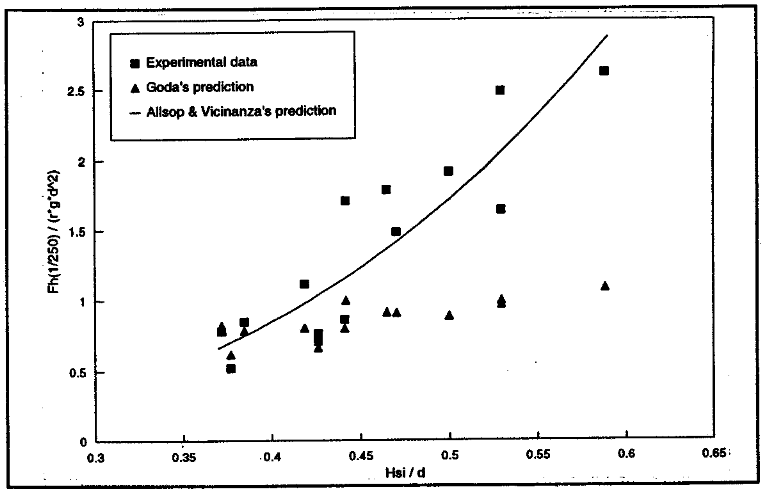

Figure 6.23 **Dimensionless horizontal forces against H_{si}/d, vertical walls, A & V's prediction $H_{si}/d>0.35$**

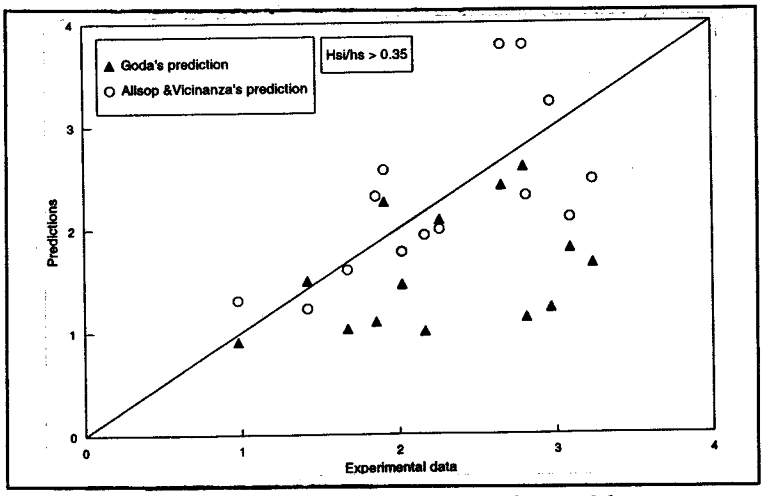

Figure 6.24 **Measured / predicted horizontal forces, Goda and A & V, vertical walls, $H_{si}/d<0.35$**

6.3.2 *Composite walls, horizontal forces*

The comparison of measured and predicted forces using Goda / Takahashi on composite structures follows the general form used in section 6.2.2 above, and the results are therefore treated in the regions summarised in Figure 6.14.

<u>Low mounds, $0.3<h_b/h_s<0.6$</u>

For low mounds, the onset of impact conditions is shifted to $H_{si}/d=0.65$, rather than $H_{si}/d=0.35$ noted for the simple wall. Over the region of pulsating loads, $H_{si}/d<0.65$, the measured wave forces are safely predicted by Goda's method, see comparison in Figure 6.25. Takahashi's method makes very little difference for the conditions considered here. The single outlying point falls in the transition zone identified in Figure 6.14, $0.55 < H_{si}/d < 0.65$.

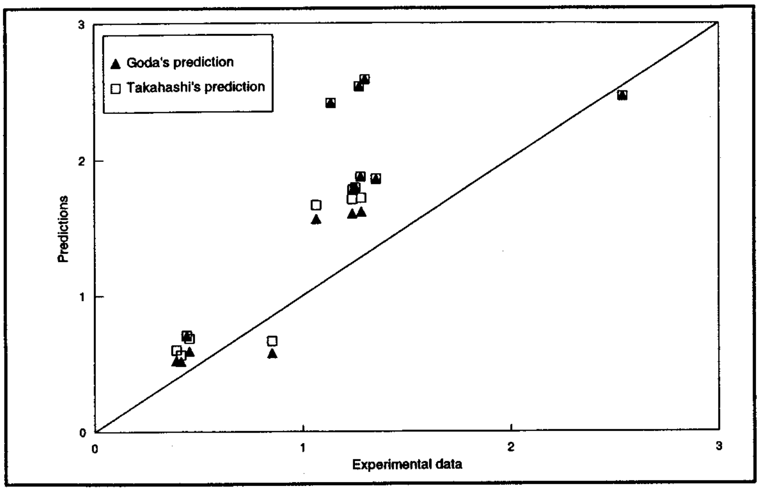

Figure 6.25 Measured / predicted horizontal forces, Goda & Takahashi, low mounds, $H_{si}/d<0.65$

Wave loads increase substantially with the onset of impacts for greater relative wave heights, $H_{si}/d > 0.65$, as was shown previously in Figure 6.10. Here the simple prediction equation for wave impact forces, eqn (6.1) gives reasonable estimates in the range of $0.65 < H_{si}/d < 1.2$, although there is some indication that this simple method may over-estimate forces at higher values of H_{si}/d.

The comparison between measurements and prediction using this simple equation shown in Figure 6.26 shows very little bias, but quite wide scatter. The comparison between measured loads and Goda / Takahashi predictions also in Figure 6.26, shows much greater bias, equivalent to an under-estimate with respect to the measurements of about 60%.

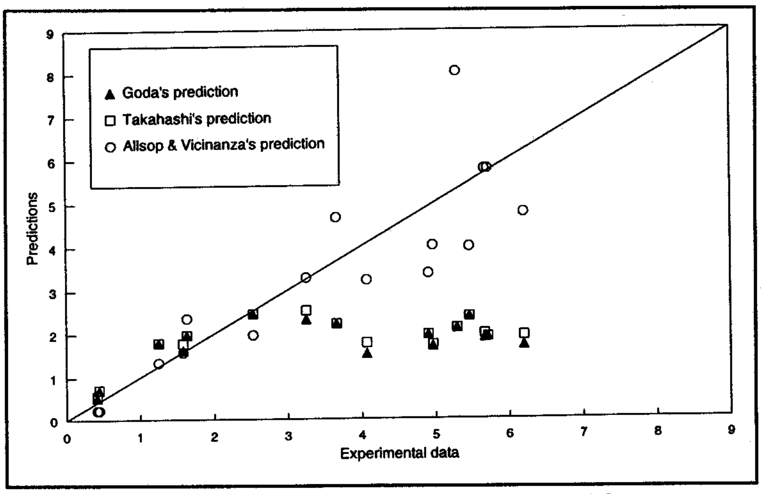

Figure 6.26 Measured / predicted horizontal forces, Goda & Takahashi, low mounds, $0.65<H_{si}/d<1.2$

Further comparisons between the measurements and predictions based on Minikin's method are given by McKenna (1996). Three alternative versions of Minikin / Shore Protection Manual methods were tested by McKenna, but none of these approaches gave any improvement over the methods reviewed above. The use of Minikin's method as correctly (dimensionally) phrased, and as used in BS6349, always gave very low forces, well below those measured. Conversely, the SPM version with triangular hydro-static pressure always gave much greater forces for pulsating conditions, yet failed to match forces under impact conditions.

high mounds, $0.6 \le h_b/h_s < 0.9$.
Relative wave heights in the range $0.3 < H_{si}/d < 0.55$ generally give pulsating loads, and Goda's equations give conservative predictions, Figure 6.27. Over this region, Takahashi's modification has much more effect, but this gives substantial over-estimates of loads. Again the outlying points in Figure 6.28 fall in the transition region identified in Figure 6.14, $0.55<H_{si}/d<0.65$.

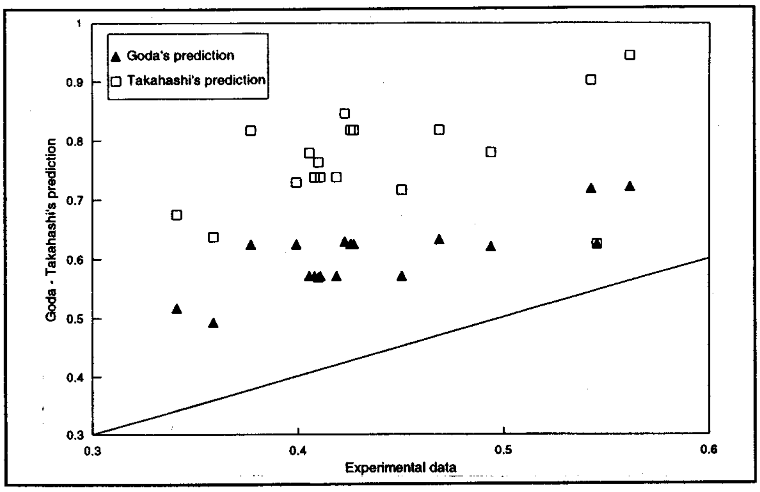

Figure 6.27 Measured / predicted hirizontal forces, Goda & Takahashi, high mounds, $_{.3}0<H_{si}/d<0.55$

The higher relative wave height give greater possibility of wave impacts, but here the response is more influenced by the relative berm width, B_{eq}/L_p. For the smaller relative berm widths tested here, $0.08 < B_{eq}/L_p < 0.14$, Goda's method again over-estimates the loads, but significantly less so than Takahshi's method, Figure 6.28, so Goda's method should be preferred. For both methods, the higher forces measured in these experiments are less severely over-estimated.

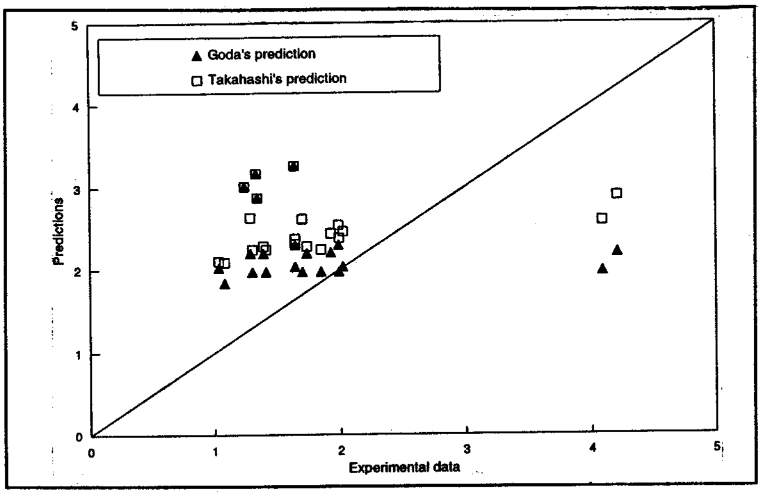

Figure 6.28 Measured / predicted horizontal forces, Goda & Takahashi, high mounds, $_{.65}0<H_{si}/d<1.3$, short berm

For the longest relative berm lengths considered here, $B_{eq}/L_p > 0.4$, waves are more likely to break on the mound, reaching the wall as broken waves. In these studies, only one test falls in this region, and the wave force is quite close to the value predicted by Goda's method.

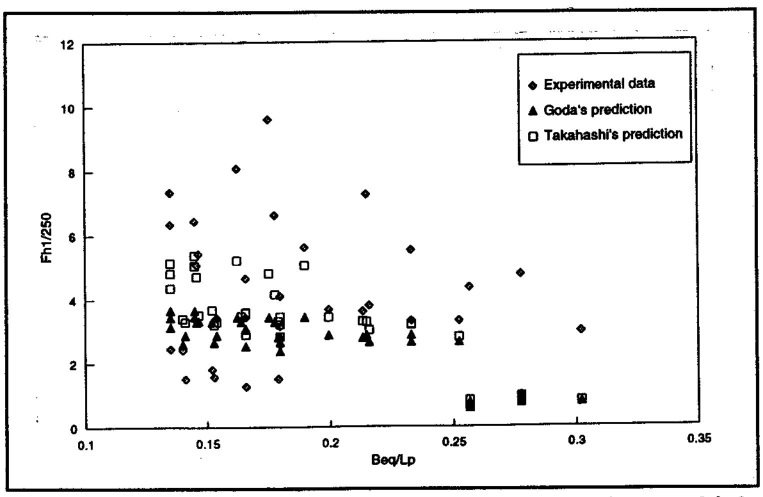

Figure 6.29 Influence of B_{eq}/L_p on horizontal forces, high mounds, intermediate berm widths

In the intermediate region, the combination of greater mound height and width is sufficient to initiate wave breaking against the wall, the increase in wave impacts giving substantially greater forces. The resultant forces depend upon B_{eq}/L_p, see Figure 6.29, and on H_{si}/d, see Figures 6.30 and 6.31, but the relationships are complicated, and no reliable and simple method can be devised. An upper limit estimate appears to be given by a simple equation in H_{si}/d:

$$F_h/(\rho_w g d^2) = 22\,(H_{si}/d)^{4.5} \qquad (6.2)$$

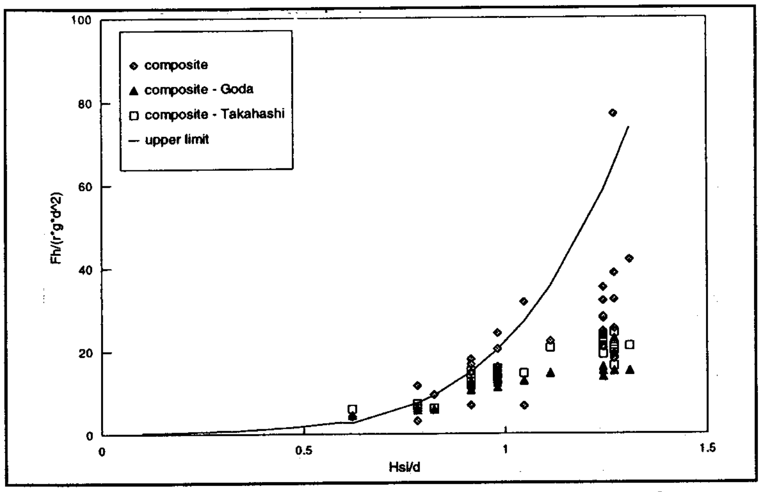

Figure 6.30 **Dimensionless horizontal forces against H_{si}/d, high mounds, G & T's predictions, $0.65<H_{si}/d<1.3$**

Closer inspection of the comparison between measurement and prediction in Figure 6.32, suggests however that this upper limit is much too conservative, but it is also clear that neither Goda nor Takahshi's methods give safe predictions. An extremely crude, and safe approach for wave forces in this region is to use the Takahashi prediction multiplied by 2. This gives a generally safe result for the combinations of conditions tested here, but has little other merit except its relative simplicity!

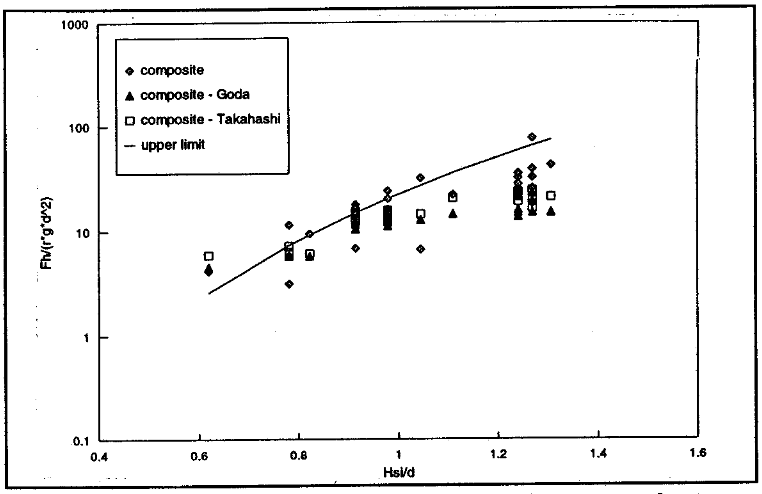

Figure 6.31 **Dimensionless horizontal forces against H_{si}/d, high mounds, G & T's predictions, $0.65<H_{si}/d<1.3$**

Again, McKenna (1996) makes comparison's between the measurements and predictions based on the alternative versions of Minikin / Shore Protection Manual methods. The use of Minikin's method as used in BS6349 again gave forces well below those measured. Conversely, the SPM version with triangular hydro-static pressure always gave much greater forces for pulsating conditions, yet failed to match forces under impact conditions.

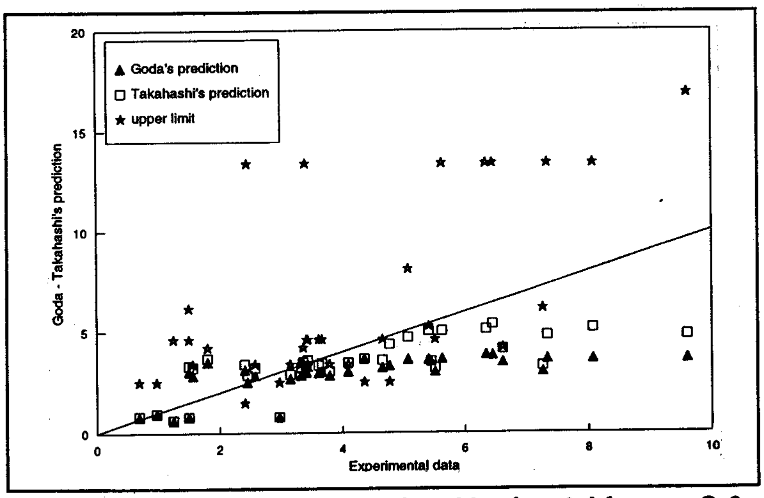

Figure 6.32 **Measured / predicted horizontal forces, G & T and V's upper limit, high mounds, wide berms**

6.3.3 Composite walls, up-lift forces

Low mounds, $0.3<h_b/h_s<0.6$

For composite walls with low mounds, Goda's method gives generally safe predictions of up-lift force for pulsating and transition conditions $H_{si}/d \leq 0.65$, Figure 6.33. Above that however, the non-dimensional up-lift force $F_u/(\rho_w g d^2)$ increases rapidly to 2-3 times that predicted by Goda's method.

For the region of Hsi/d > 0.65, where the measurements give greater up-lift forces than predicted by Goda, a simple regression line was fitted to the results:

$$F_u/(\rho_w g d^2) = 23.2 (H_{si}/d) - 15.2 \quad (6.3a)$$

This line is however strongly biased towards a set of data points with very low up-lift forces, which were judged not to be representative of the overall data set. An alternative prediction line was therefore fitted to give a more appropriate estimate of the upper bound to the results in Figure 6.33 over the range $0.65 \leq$ Hsi/d ≤ 1.3:

$$F_u/(\rho_w g d^2) = 19.7 (H_{si}/d) - 11.1 \quad (6.3b)$$

High mounds, $0.6 \leq h_b/h_s < 0.9$

As was seen for horizontal forces, and discussed in 6.2.3, the influence of high mounds is more complicated. For pulsating and transition regions covered by $H_{si}/d \leq 0.65$ and perhaps up to 0.8, the non-dimensional up-lift force $F_u/(\rho_w g d^2)$ remains relatively low, and agrees well with that predicted by Goda's method, Figure 6.34.

Again for $H_{si}/d>0.8$, the non-dimensional up-lift force $F_u/(\rho_w g d^2)$ increases rapidly, and here the region is most usefully split using values of B_{eq}/L_p to divide into pulsating or impact regions, Figures 6.35 and 6.36.

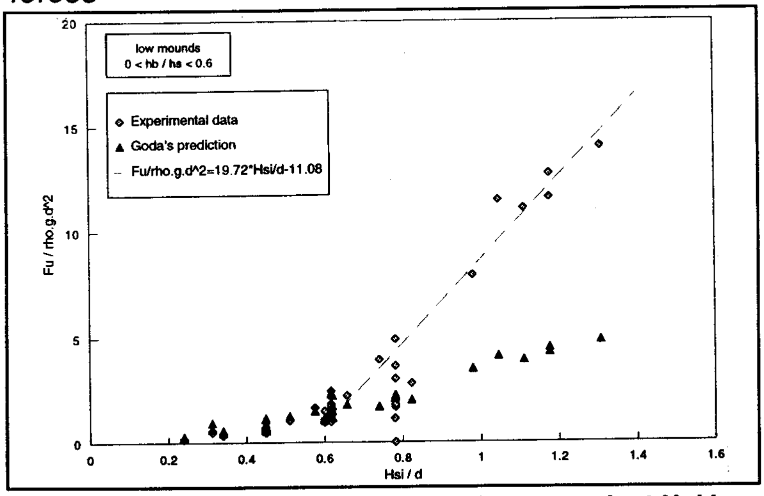

Figure 6.33 **Dimensionless up-lift forces against H_{si}/d, low mounds, Goda's predictions, $0.65<H_{si}/d<1.4$**

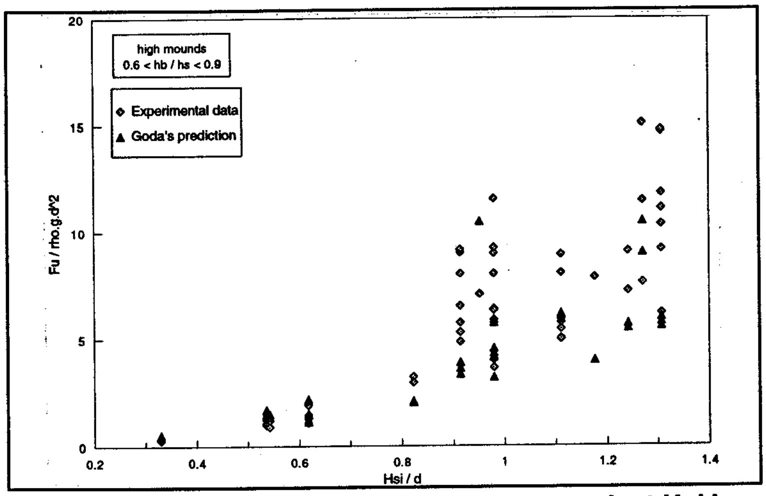

Figure 6.34 **Dimensionless up-lift forces against H_{si}/d, high mounds, Goda's predictions, $0.65<H_{si}/d<1.4$**

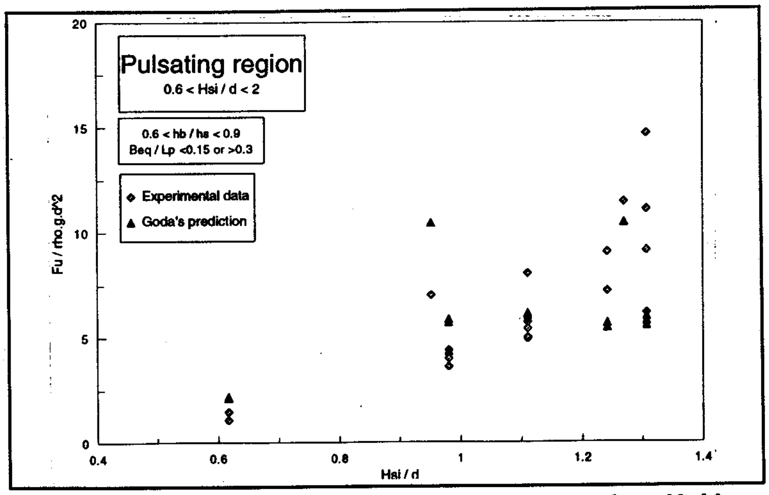

Figure 6.35 **Dimensionless up-lift forces against H_{si}/d, high mounds, Goda's predictions, $0.65<H_{si}/d<2$, pulsating conditions**

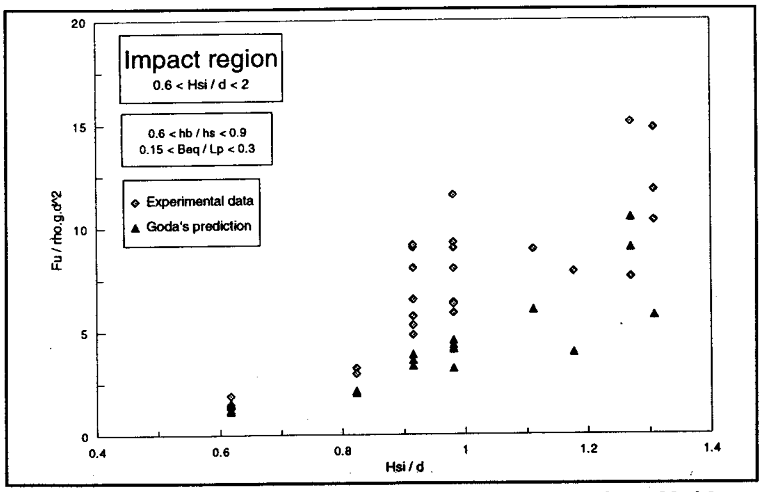

Figure 6.36 Dimensionless up-lift forces against H_{si}/d, high mounds, Goda's predictions, $0.65<H_{si}/d<2$, impact conditions

6.3.4 Crown walls

Prediction methods for wave forces on crown walls developed by Jensen, Bradbury & Allsop have been included in the CIRIA rock manual, Simm (1991), and these were summarised in Chapter 3. Horizontal forces were non dimensionalised as $F_{h1/250} / \rho_w g h_f L_p$, and were related to dimensionless mound depth given as H_s/A_c, where A_c=-d. Up-lift forces were expressed as $F_{u1/250} / 0.5\rho_w g B_c L_p$, which was based on assumptions that up-lift pressures at the front edge are equal to horizontal pressures at that corner, and that the distribution is triangular from the front edge. Simple empirical equations, given earlier as eqns (3.20a) and (3.20b), used coefficients derived for different configurations of rubble mound and crown wall to relate the dimensionless forces to H_s/A_c.

Whilst not a main objective of these studies, the expansion of the tests by McKenna (1996) allowed the configurations to be extended to include tests on structures which closely resembled a crown wall on a rubble mound. The results from these tests were divided from those representing standard caissons on rubble foundations and were analysed separately. This analysis therefore considered configurations where the depth of water on top of the rubble mound (d) was small, or where the water level was below the top of the berm (d is negative).

Horizontal forces from these configurations did not agree well with predictions by Goda or Takahashi, but the method of Bradbury & Allsop (1988) for crown walls as used in the CIRIA manual was used here to compare measured and predicted forces at 1/250 level.

$$F_{h1/250} = \rho_w g h_f L_p (a (H_{si}/A_c) - b) \tag{6.4a}$$

$$F_{u1/250} = 0.5 \rho_w g B_c L (a (H_{si}/A_c) - b) \tag{6.4b}$$

Sections A and C in the CIRIA manual were selected as most representative of the crown wall configurations tested here, for which coefficients a and b had been derived previously for the 99.9% exceedance level:

Section	a	b
A	0.054	0.032
C	0.043	0.038

The initial comparisons of predicted and experimental forces were confined to the parameter range studied by Bradbury & Allsop ie 0 < H_{si}/A_c < 2.5. Only four tests fell into this narrow range, all for Structure 10 with the lowest water level, so the region of interest was extended to cover the wider range of -4 < H_{si}/A_c < 8. Horizontal forces are compared with predictions for Bradbury & Allsop's Sections A and C in Figure 6.37, and up-lift forces are compared in Figure 6.38. Surprisingly, the simple predictions given by Bradbury & Allsop's equations with a=0.054 and b=0.032 gave reasonable estimations for the horizontal forces, although this method over-estimates $F_{h1/250}$ at higher values of H_{si}/A_c.

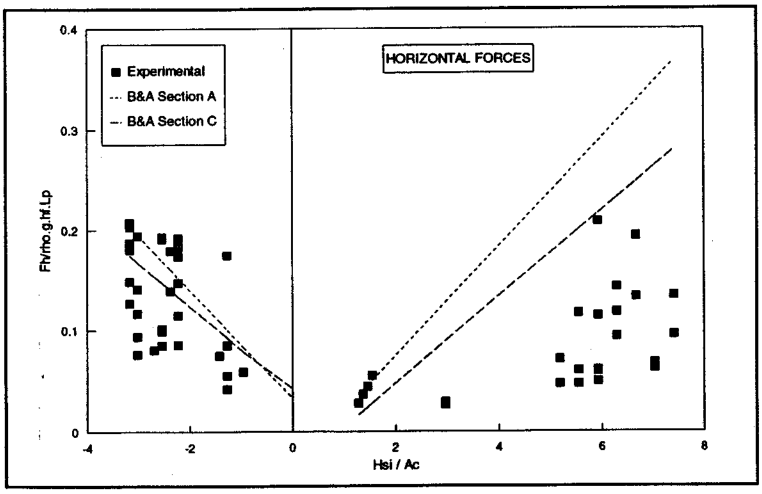

Figure 6.37 Dimensionless horizontal forces on crown walls, $-4<H_{si}/A_c<8$

At negative values of H_{si}/A_c, the measurements are scattered, but the simple prediction method gives a reasonable upper limit for most of the results. These configurations where the mound is just below the water level represent fairly unusual cases, and it is not surprising that no standard prediction method applies here.

Up-lift forces in Figure 6.38 were well predicted by Bradbury & Allsop's method at lower values of H_{si}/A_c, but significantly over-estimated at high values of H_{si}/A_c. At negative values of H_{si}/A_c, up-lift forces are again scattered, but the simple prediction method again gives an upper limit.

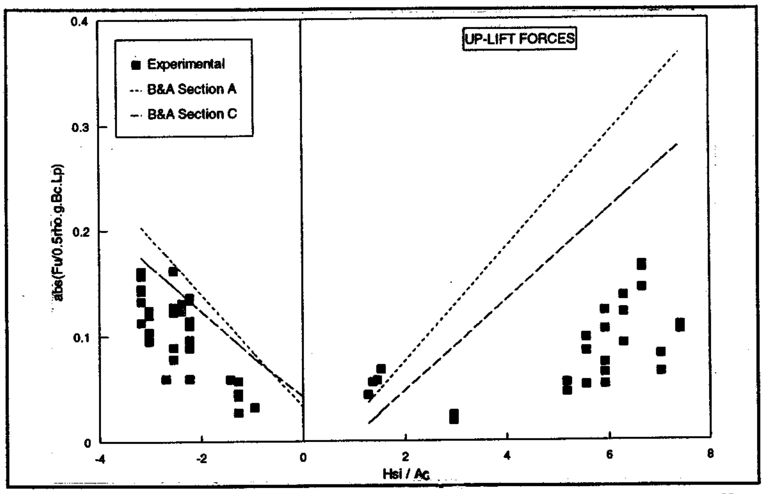

Figure 6.38 Dimensionless up-lift forces on crown walls, $-4<H_{si}/A_c<8$

Bradbury & Allsop's coefficients a & b are the same for horizontal and up-lift forces, thus assuming that the pressure at the bottom of the front face of the crown wall equals that at the front edge of the underside. The absolute magnitudes of the forces then depend on the height or breadth of the wall over which the pressures act and on the assumed shape of the pressure distribution. Goda's method suggests that a reduction factor be applied to the pressure at the bottom of the wall to give the corresponding up-lift pressure. The results considered here, however indicate that up-lift forces may be higher than these simplifying assumptions suggest. Initial inspections of up-lift distributions from tests here and at the large wave flume at Hannover / Braunschweig suggest that this may be because the up-lift pressures do not reduce linearly from front to rear. It is also clear that pressures at the rear heel may not always reduce to zero. The most conservative approach might therefore require the assumption of a rectangular distribution of up-lift pressures, although this would probably be excessive in those cases where the crown wall or caisson is placed on relatively free-draining materials.

6.3.5 Overall stability of caissons on rubble mounds

Previous sections treated horizontal and up-lift forces independently. The use of these forces in any stability analysis therefore assumes that peak horizontal and up-lift forces occur simultaneously. In practice, there will always be a lag between peak horizontal and peak up-lift forces, so it is possible that the structure would then be more stable than indicated by this simple approach. This analysis therefore uses a simple analysis of the stability of a monolithic caisson against sliding. Factors of Safety F_S against sliding are calculated using measured forces, and are contrasted against those predicted using Goda's formulae with Takahashi's modification.

The sliding stability analysis was carried out in three stages to investigate the most appropriate values of the horizontal and uplift forces to use, and to determine the consequences of simplifying the horizontal and uplift forces to single values. The first, and simplest, stage consisted of calculations of a single Factor of Safety per test, using the 1/250 values of the horizontal and up-lift forces together. These values do not occur at the same time, and do not even necessarily occur for the same wave, since the statistics of the horizontal and up-lift forces were treated separately in this study. The second stage was therefore to calculate a single Factor of Safety per test using the 1/250 value of the horizontal force with the concurrent value of the up-lift force. This was done to evaluate the effect of simplifying the forces to their 1/250 values in the first analysis. The third stage of the analysis was the calculation for selected tests of the Factor of Safety at each timestep using time series. The purpose of this analysis was to determine the effect of using averaged single values as input rather than the actual values of the forces over each wave event.

These simplifying approaches did not consider failures by overturning, or by local or gross foundation failure which would require significant modelling of the geotechnical response of the mound. Enhancement of stability by embedment of the caisson into the rubble has also been neglected.

In the model tests, the test structure was not free to move, so the Factor of Safety against sliding F_S was calculated for a caisson of the same size and shape as that used in the model tests, assuming that the mean density of concrete and fill was 2000kg/m^3, and that the coefficient of friction between rubble and the base of the caisson could be represented by $\mu = 0.5$ in accordance with the minimum recommended by BS 6349 (1991).

These simplifications allow the use of data discussed earlier in this chapter. Transient phenomena were not modelled in this analysis as this would require a dynamic stability model, with force - time series as inputs, and inertia and damping of the system (including the soil behaviour) being correctly modelled. Models of this type are under development, but are not yet validated. Recent work by Kortenhaus (1994), Ibsen (1994), and the MCS Geotechnical Group edited by De Groot (1994) has indicated the way in which such models may be developed, and it is probable that such models may be validated during the later stages of the PROVERBS project (1996-1999). Until such sophisticated models are available, determination of stability of caisson breakwaters will continue to require use of static loadings, with appropriate factors of safety to compensate for simplifications in the processes and uncertainty in estimation of input parameters.

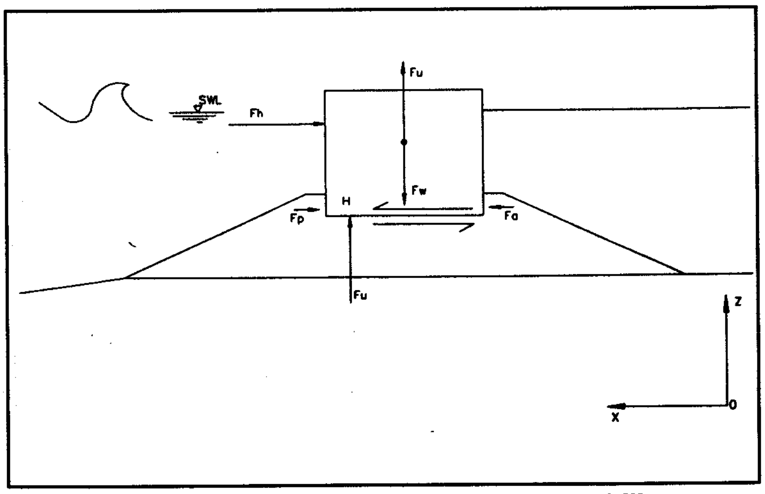

Figure 6.39 Forces / reactions for overall stability analysis

Static Sliding Model

The forces acting on a composite breakwater section, where the super-structure is embedded a small amount into the rubble mound, are as shown in Figure 6.39, and may be summarised as follows:

F_h, horizontal wave force, and F_u, up-lift force underneath the caisson,
Mg, dry weight of the caisson,
F_B, buoyant up-thrust on the caisson,
S_F, the shear force at the rubble / caisson boundary,
F_F, earth pressure force on the caisson from the seaward part of the mound,
F_R, earth pressure force on the caisson from the harbour side of the mound,

The simple sliding stability model considered these forces for the caisson tested in this study. The stability model employs a simplified cross section (as shown in Figure 6.40) where the caisson is not embedded in the rubble mound. Contributions of the earth pressure forces, F_F and F_R to the overall stability of the structure are generally small, and were omitted in this analysis. At the point of sliding, the stability of the caisson is expressed in terms of the Factor of Safety F_S against sliding, defined as the ratio of resistance forces to disturbing forces, with $F_S = 1$ denoting the point of failure:

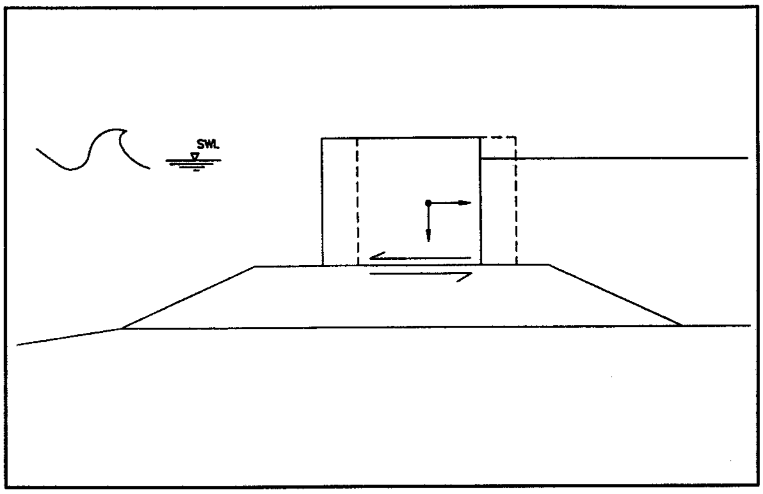

Figure 6.40 Simplified model for overall stability analysis

$$F_S = \mu \ (Mg - F_u - F_B) / F_h \qquad (6.5)$$

Results of Sliding Stability Analysis
The first stability analysis with $F_{h1/250}$ and $F_{u1/250}$ used $F_S \leq 1$ to identify that 28% of the structure / wave conditions would have failed. In practice, the factor of safety would be required to exceed at least 1.2, and BS6349 suggests the use of F_S= 1.5 to 2.0 in design to account for the uncertainties in estimating the wave loads and structure response. The percentage of failures for various levels of F_S were therefore determined from the measured loads, and are summarised below:

Limiting F_S	% failures
1.0	28
1.2	38
1.5	42
2.0	53

The sensitivity of this analysis to the assumed parameters was explored and the % failures are summarised below for different densities of the caisson / fill, and different coefficients of friction. These results confirm that the response of the analysis to the values selected is reasonably gentle, so the overall conclusions drawn from this analysis will not be significantly influenced by the particular values selected.

Friction factor	Caisson / fill bulk density	
	1700kg/m^3	2000kg/m^3
$\mu = 0.5$	38%	28%
$\mu = 0.6$	31%	20%

It has been noted previously that this analysis does not take into consideration any extra resistance provided by embedment of the caisson into the rubble mound, nor take account of the dynamic response characteristics. Initial inspection of example force - time series for horizontal and up-lift loads appear to demonstrate that peak (1/250) horizontal and up-lift forces do not generally occur simultaneously as assumed in this simple analysis. Up-lift at the time of peak horizontal force is generally less than the peak up-lift force. This is however complicated by a phase lag introduced by the 20Hz filter applied to the up-lift pressures, and it may be unsafe to assume that the actual phase lags between peak horizontal and up-lift forces will be the same as those measured in these pressure records

Comparisons of F_S used forces measured in these tests, and those predicted using Goda's method with Takahashi's extension for horizontal forces and Goda's method for up-lift forces. The comparisons addressed each branch of the overall impact response diagram given in Figure 6.14. In each branch, measured and predicted Factors of Safety were compared to indicate the degree of under- or over-estimate that might be given. The results of these comparisons may be summarised:

> For composite structures with low mounds, Goda & Takahashi's method will give safe predictions for $0.3 < h_b/h_s < 0.6$ except for those larger mounds and/or wave heights which lead to impacts.
>
> For composite structures with high mounds, Goda & Takahashi's method give safe predictions for $0.6 < h_b/h_s < 0.9$, except for $0.65 < H_{si}/d < 1.3$ when the mound again causes wave impacts.

<u>Stability analysis with $F_{h1/250}$ and concurrent F_u</u>

It is very likely that maximum values of horizontal and up-lift forces will not occur simultaneously due to the damping effect of the rubble mound on the up-lift pressures. The actual Factors of Safety for a structure subjected to specific loading conditions might therefore be higher than those given by the simple analysis described above. The implication of this in design would be the rejection of structures which would in fact be safe.

The second stage of the analysis explored the consequences of the assumption in the first stage that peak horizontal and up-lift forces occur simultaneously, comparing the factors of safety obtained from the first analysis with those calculated using values of $F_{h1/250}$ and F_u at the same timestep. This analysis showed that, although the Factors of Safety changed by about 10-20% if the concurrent values of force were used, the percentage of structures which failed did not change appreciably. In general, structures which failed using the simplest analysis ($F_{h1/250}$ and $F_{u1/250}$) also failed using the more accurate method ($F_{h1/250}$ and F_u at the same time), so there is no benefit to be derived from this refinement of the force inputs.

<u>Stability analysis with F_h and F_u for time series</u>

Both analyses described previously used averaged values of the maximum forces over more than one event. The combination of the actual values of the forces in an event may result in a greater instability than would be indicated by average values.

The third and most rigorous stage of this analysis calculated Factors of Safety F_S at each timestep in selected tests. This required a number of tests to be re-processed to produce force-time series (each about 30Mbytes) so this analysis was restricted to a few which fall within parameter ranges defined in Figure 6.14. Tests with large or negative H_{si}/d were excluded. The selection procedure aimed to investigate the following hypotheses:

1. Conditions which the second analysis indicated were 'just safe' (F_S just > 1) might actually become 'unsafe' at some time during the wave event. This corresponds to cases where the use of the simple analysis would give a marginally safe result. It would be normal for an engineer to reject a design with a factor of safety so close to 1.0, and this part of the analysis seeks to determine whether this is justified.

2. Conditions which the second analysis indicated were 'safe', $F_S > 1$, but for which the Goda and / or Takahashi predictions gave substantially greater factors of safety, might become 'unsafe' at some time during the wave event. This situation arises due to the significant uncertainty in the prediction of the forces in certain parameter regions. It investigates the importance of selecting an appropriate method for determining the input forces for the stability model.

3. Conditions which the second analysis indicated were 'just safe', $F_S > 1$, but for which the calculations with the Goda and / or Takahashi predictions gave 'unsafe' results, might become 'unsafe' at some time during the wave event. This is important for determining the extent (if any) to which the Goda and / or Takahashi predictions are over-conservative in certain parameter ranges. If the calculations using Goda and / or Takahashi predictions were consistently 'unsafe' when in fact the structure was 'safe' then some reduction in the factor of safety might be justified.

4. The duration of the 'unsafe' period for cases for which the second analysis showed would just fail (Fs < 1) might be close to the natural period of the caisson. This hypothesis was investigated only for marginal cases, where the static stability analysis was indicating that the structure would be 'unsafe'. The possibility exists of a short period of low stability not causing failure, as the dynamic response of the structure would reduce the effective force applied. If however the duration of the unstable phase approaches the natural period of the caisson, no allowances of this nature can be made.

The time-series stability analysis was carried out using a simple FORTRAN program to calculate the Factors of Safety against sliding for every timestep in the force-time histories. The program output listed those times during the tests when F_S had fallen below and then come back above 1.0, thus allowing the duration of the unsafe period to be calculated. The results of this were compared with those from the second stability analysis (using $F_{h1/250}$ and F_u at the same time) to investigate the issues listed above.

1. Structures which the second analysis indicated were just safe (F_S just > 1) might actually become unsafe at some time during the wave event.

   Here 8 tests were analysed, of which 5 failed, that is gave $F_S<1$ using the time series analysis. Failure durations were between 0.0025s to 0.0075s (model), which would scale (by Froude) at 1:30 to 0.014s - 0.04s. These results suggest that the hypothesis was correct and if F_S calculated from $Fh_{1/250}$ and Fu at the same time was just safe, the structure might actually fail. It is however likely that a structure with values of F_S this low would be rejected as well below the safety margins recommended in BS6349.

2. Structures which the second analysis indicated were safe, and for which the Goda & Takahashi predictions indicated that the structure was very safe, might become unsafe at some time during the wave event.

   A single test was analysed, and it failed for 0.0025s (model), equivalent to 0.014s by direct scaling. This suggested the hypothesis to be true. If Goda and Takahashi had been used F_S would have indicated a very safe structure ($F_S>2$), whereas in fact the structure might have failed. The second analysis had shown F_S from the measurements to be lower, and if these forces had been used, the design would have been rejected as F_S was then less than 1.2. The simple approach would therefore have been sufficient if appropriate force values had been used as input parameters.

3. Structures which the Goda & Takahashi predictions indicated were unsafe, but measurements indicated were safe, might become unsafe at some time during the wave event;

   Of 12 tests, only 2 failed, with durations of 0.0025s to 0.005s (model) equivalent to 0.014s to 0.03s. The use of Goda and Takahashi's methods would generally be conservative. Values of F_S

calculated from measurements were close to unity, and so would have failed the 'Factor of Safety' test. Again therefore the use of the simple approach can be justified.

4. The duration of the unsafe period for structures which the second analysis showed would fail might be close to the natural period of the caisson.

   Of four tests considered here, all failed, and 2 tests failed twice. Failure durations were short at 0.0025s to 0.0050s (model) equivalent to 0.014s to 0.027s at prototype if scaled directly. Again these calculations suggest that the hypothesis was untrue. The analysis however concentrated on those structures where F_S was close to 1.0, and did not consider those structures where there was an obvious failure. In those cases the duration of the unsafe period would be expected to be rather longer.

<u>Conclusions from sliding analysis</u>
This analysis has shown that a simple sliding stability analysis based on the values of the horizontal and uplift force maxima at an appropriate probability level (eg 1/250) is a useful and valid method. The approach however requires the use of force prediction methods which are suitable for the parameter range describing the conditions, and the implementation of a safety margin. There is no significant increase in reliability to be gained by the use of time-series information or more sophisticated descriptions of the forces than the maxima.

The only reliable alternative involves a full dynamic analysis with elastic-plastic characterisation of the mound / foundation, such as is discussed by Kortenhaus et al (1994). Such approaches will improve the accuracy with which the caisson response can be determined, and may thus permit the reduction of safety factors and therefore lead to more cost-effective design. Until reliable dynamic models are readily available, there would appear to be no particular benefit in pursuing marginal improvements of the simplest analysis approach described here.

6.4 Pressure gradients and local pressures

The major emphasis in any study of wave forces / pressures is on the overall or average level of pressures needed to determine the overall stability of the structure. Data on local pressures and pressure gradients are also needed in any analysis of conditions leading to local damage or instability of blockwork. Very little information is available from conventional methods on the spatial variability of pressures, or on local pressure gradients.

6.4.1 Vertical distributions of pressures

Goda's method assumes that wave pressures are distributed trapezoidally. For pulsating conditions this assumption is reasonably well-supported, as is illustrated by the example pressures at $p_{1/250}$ level plotted in Figure 6.41 for a simple vertical wall at H_{si}/d=0.3. For this case, the waves are pulsating, and the vertical distribution of pressures follows the general form assumed by Goda. Pressure magnitudes are relatively close to those predicted by Goda's method.

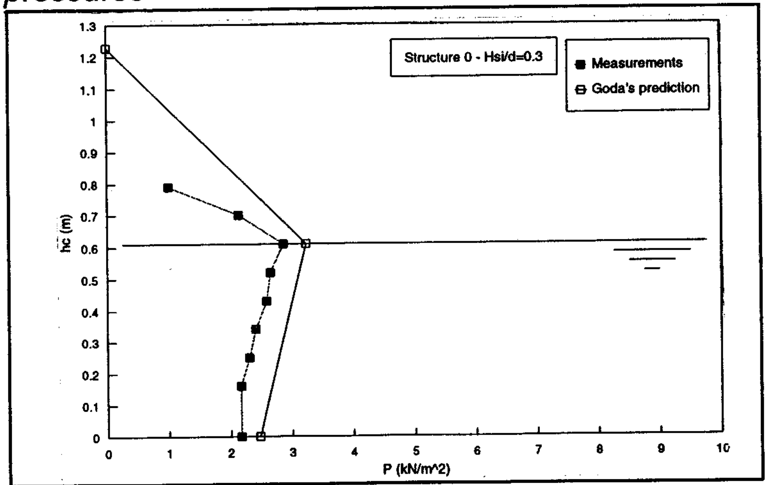

Figure 6.41 Vertical distributions of pressures, vertical wall, H_{si}/d<0.35

Agreement with this simplification is much less good for impact conditions. The distribution of pressures in Figure 6.42 is derived for the same simple vertical wall, but at greater relative wave height, H_{si}/d=0.4. Here the peak pressure is substantially greater than predicted, and for this case is slightly above the static water level.

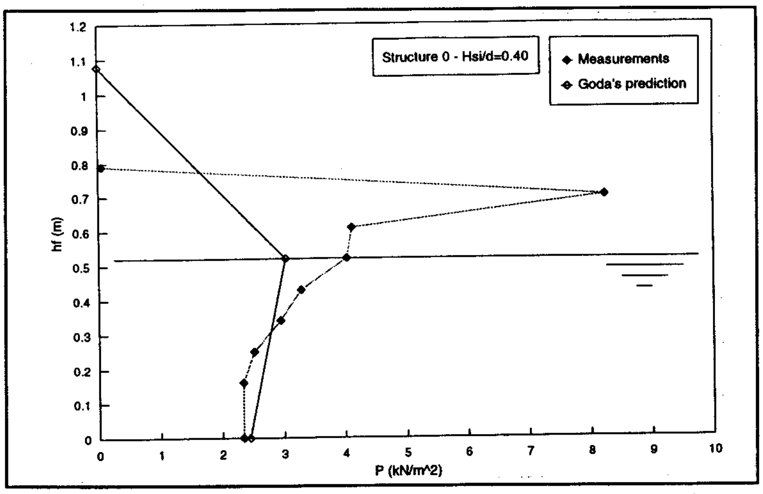

Figure 6.42 **Vertical distributions of pressures, vertical wall, H_{si}/d>0.35**

The onset of impacts therefore not only increases the overall force as discussed in earlier sections of this chapter, but also substantially increases local pressures and hence pressure gradients. This effect is illustrated dramatically in Figure 6.43 where the only physical difference between the tests was the effective berm width, B_{eq}. As seen earlier, even quite small changes in the structure may significantly alter the proportion of impacts, and the overall force on the wall. The lowest and most uniformly distributed pressures in Figure 6.43 occur for the simple vertical wall, Structure 0, and for the composite structure with moderate berm, 3. Structures 4 and 7 have only slightly larger berms, yet the local pressures and pressure gradients increase significantly. Here increasing the berm width has initiated the breaking process, giving greater impact forces for greater relative berm width, and dramatically greater peak pressures.

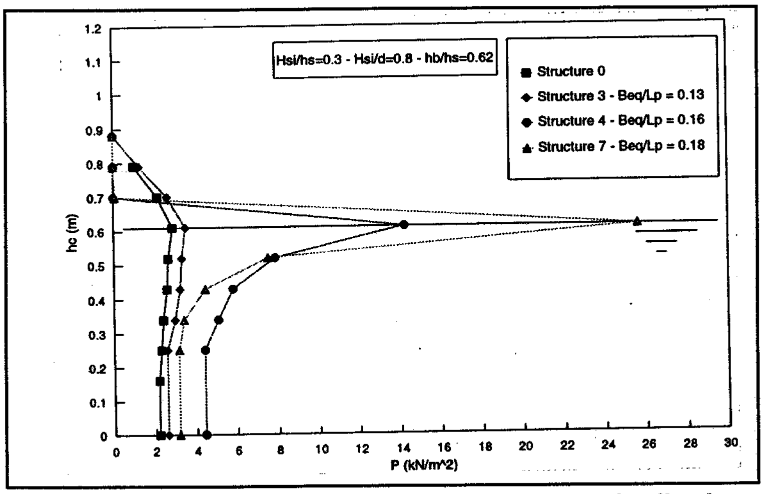

Figure 6.43 **Effect of berm width on vertical distributions of pressures, composite walls**

These effects are compared with predictions by Goda and Takahashis in Figures 6.44 - 6.45 where the difference between the structures compared is again of berm width. The structure with a high mound, Structure 3, gives pulsating conditions, and pressures below Goda's prediction in Figure 6.46 for B_{eq}/L_p = 0.13. A small increase of relative berm width to B_{eq}/L_p = 0.16 is however sufficient to initiate impact conditions, with substantially greater wave pressures at the static water level, Figure 6.45.

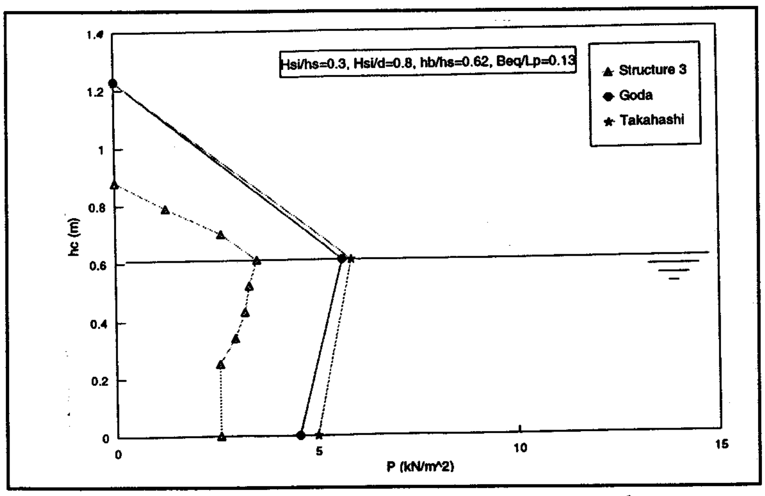

Figure 6.44 **Measured distributions and goda / Takahashi predictions for pulsating conditions (Structure 3)**

These discussions have been confined to pressures at 1/250 level, but it should be noted that pressures at more extreme exceedance levels are greater. This is illustrated in Figure 6.46 where the vertical pressure distributions for an impact condition are given for non-exceedance levels of 99.6 and 99.8%, and for 1/250, lying approximately between 99.6 and 99.8%. These confirm that even the use of $p_{1/250}$ may not lead to the highest estimate of local pressures or pressure gradients.

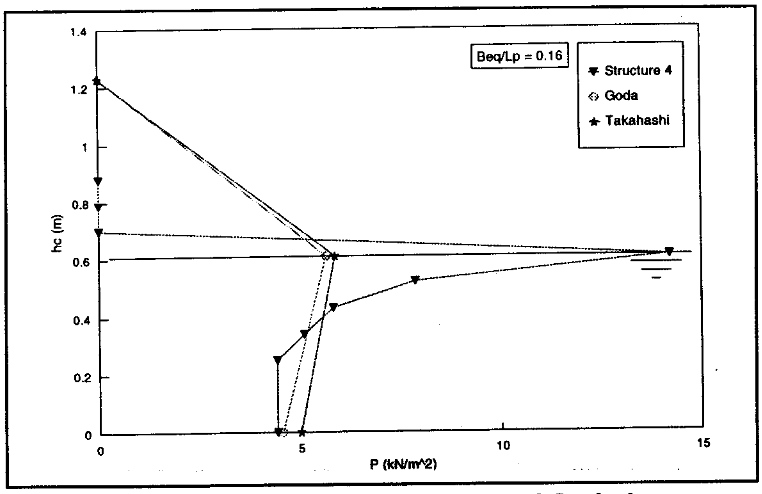

Figure 6.45 Measured distributions and Goda / Takahashi predictions for impact conditions (Structure 4)

6.4.2 Pressure gradients

Analysis by Allsop & Bray (1994) on the stability of blocks in blockwork walls subject to wave action has suggested that large pressure gradients may be particularly important in determining the onset of movement of such blocks. This section considers example pressure gradients calculated from the pressures measured in these model tests.

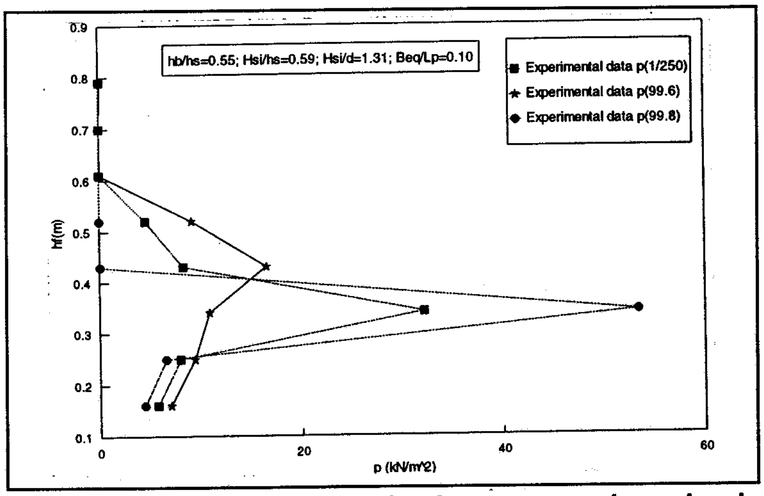

Figure 6.46 Measured distributions at exceedance levels of 1/250, 99.6% and 99.8%, impact conditions (Structure 1)

For ease in scaling and manipulation, the results of calculations of pressure gradients have been expressed as pressure head (in metres of water) divided by the spacing between the measurement points (in this instance between adjacent pressure transducers). Values of the pressure head gradient, dp/dz, discussed below are therefore dimensionless.

The analysis in section 6.4.1 demonstrated that pulsating wave conditions give relatively low absolute values of the wave pressure, so pressure gradients are relatively mild, seldom exceeding values of dp/dz >1. The situation is however dramatically different for impact conditions.

For impact conditions on the simple vertical wall, values of the peak local pressure gradients varied over dp/dz=2 to 70. These values increased slightly for low mounds to dp/dz=5 to 90, and for high mounds to dp/dz=2 to 80. The mean value of these results, the standard deviations (s.d.) and coefficients of variation are summarised below:

Structure	range	mean (dp/dz)	s.d. (dp/dz)	coef. varn. (dp/dz)
Vertical	2 - 70	13.2	15.9	1.19
Low mound	5 - 90	29.5	25.9	0.879
High mound	2 - 80	21.6	17.5	0.814

For impact waves, the greatest relative local pressure measured in these tests was given by:

$$p_{max} / (\rho_w g H_{si}) \leq 50 \quad (6.6a)$$

and the steepest pressure gradient was given by:

$$\max (dp / dz) \leq 90 \quad (6.6b)$$

6.5 Pressure rise times / impulses

The rate at which wave pressures rise is important for two reasons. The first point is that a caisson or related structure will only react to a wave force by moving if the duration of the force impulse is close to or greater than the response period of the structure. At a smaller level, this may also be applied to the component elements of a structure. If the wave impulse is of short duration, as might be characterised by a very short rise time, then the structure or element may respond only slightly to the loading, even if the loading intensity is very high. It is therefore important to characterise wave forces / pressures by their durations. This was not possible directly, but the rise time to peak pressure could be determined from the measurements of pressures, and this was taken as giving a good indication of impulse duration. [It may be useful to note that within the PROVERBS project in early 1996, the working assumption was that the duration of the impact impulse was about 3 Δt.]

The second issue is of scaling from small scale to prototype. It is generally accepted that wave impacts in small scale models may be greater in magnitude, but shorter in duration than their equivalents at full scale. Despite significant programmes of research, at for instance University of Plymouth or Hannover / Braunschweig Universities, researchers there have not yet been able to develop reliable or robust scaling methods. This issue will be discussed further in Chapter 7, using information from the field and laboratory on pressures and rise times.

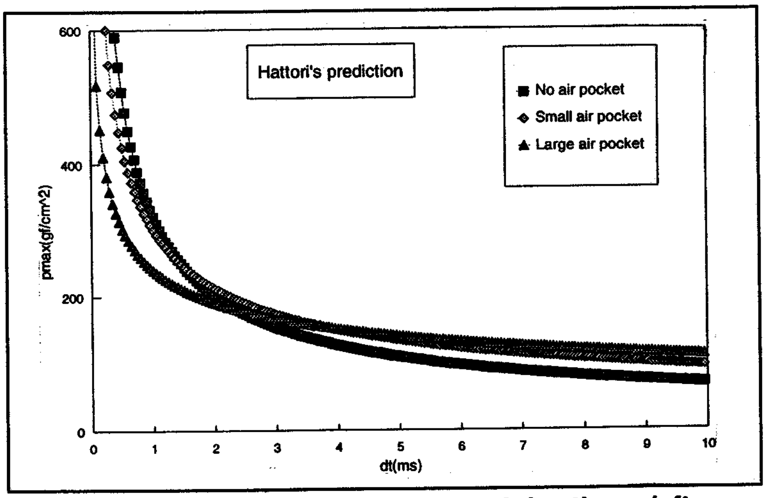

Figure 6.47 Maximum pressures and rise times (after Hattori et al)

The classification of pressure rise times, and the interaction with any limits on pressures have been discussed by Hattori (1994) and Hattori et al (1994) who suggest that, at their particular model scale or size, an upper limit may be applied to individual peak pressures plotted against rise time. These limit curves are summarised in Figure 6.47 where the effects of three different sizes of air pocket between waves and wall are presented by the three limit curves. These curves were derived for regular / single waves, and the units of pressure and rise time are not scaled from Hattori et al's original measurement. For no air pocket, Hattori suggests a limit on p_{max} given by:

$$p_{max} = 320\, \Delta t^{-2/3} \quad (6.7a)$$

whilst for a small air pocket, Hattori suggests:

$$p_{max} = 300\, \Delta t^{-1/2} \quad (6.7b)$$

and for a large air pocket, Hattori suggests:

$$p_{max} = 240\, \Delta t^{-1/3} \quad (6.6c)$$

In each instance, values of p_{max} are in grams force / cm^2, and Δt is in milli-seconds.

These curves are re-presented in Figure 6.48 where some of the shorter rise times measured in the Wallingford experiments are also shown. Hattori et al's measurements covered rise times between 0.2 and 10 milliseconds, whereas the Wallingford results cover from 5 milliseconds to 1 second.

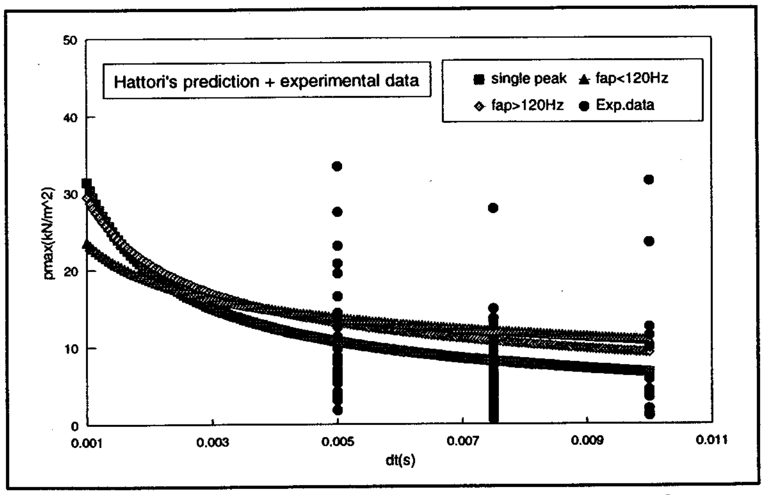

Figure 6.48 Comparison of experimental data and Hattori's predictions for rise times

A fuller set of Wallingford data from an impact condition is shown in Figure 6.49, where Hattori's three limit curves are compared with measurements. There is good agreement at longer rise times, but the measurements appear to lie above Hattori's curves at higher pressures, shorter rise times. In part this will be due to the lower limit to rise times calculated from these test results using 3 points, ie 2 x 1/400s = 5 milliseconds. Some of these records may well relate to rather shorter rise times, which would place the plotted points further to the left on the graph, and thus closer to Hattori's limit. This tendency to give longer rise times may also have been compounded by the somewhat slower response of the transducers used in the Wallingford tests.

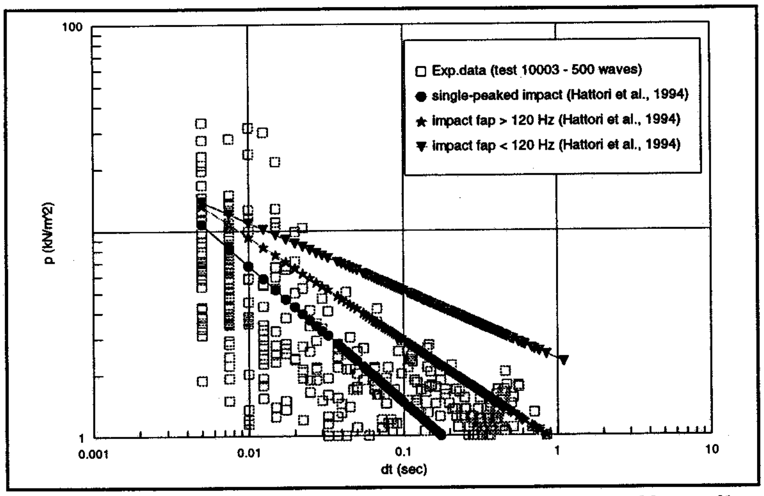

Figure 6.49 Experimental data (this study) and Hattori's prediction lines

It is however most probable that Hattori's limits are themselves strongly influenced by the relatively small wave heights that were used in those experiments, and the scaling of Hattori's limit curves to other model scales, and hence to prototype, have yet to be addressed. The comparisons in Figures 6.47 - 6.49 should therefore be treated with some circumspection.

7 Application of results

The main restrictions to the application of these test results are given by the limits of data covered, distortions of the responses arising from scale effects / uncertainties in scaling from model tests to prototype, and differences in the response characteristics of different structures or elements relative to those used in making / analysing the measurements.

The ranges of parameters, and of the main dimensionless parameter groups covered by these studies have been summarised in earlier chapters of this report. Limits to the application of the design methods are suggested in Chapter 6. Application of the results of this study depend critically on the reliability with which the measurements of pressures made in these model tests may be applied to full scale in sea water. The use of such hydraulic models must therefore be subject to analysis of the influence of scale effects of concern where flows in porous layers may be unrealistically influenced by viscous flow effects, and where the pressures produced by hydro-dynamic actions are themselves influenced by the scale of the experiment. In the studies discussed here, the main influence of scale effects is on the magnitude of the wave impact pressures, and on their durations.

7.1 Influence of scale effects

The principal results of this study are the wave forces / pressures. The analysis of these pressure measurements made at laboratory scale using fresh water has not explicitly assumed any particular scale conversion, but the use of other parameters scaled implicitly by Froude scale has therefore implicitly assumed that the forces / pressures measured here can be so scaled.

In the case of pulsating wave pressures where the relationships between wave momentum, pressure impulse, and total horizontal force are relatively simple, the assumption of Froude scaling is realistic, and will not alter the key conclusions for pulsating load conditions over the range of scales that may be used from these experiments.

For wave impact pressure, scaling is less simple. It has long been argued and is well accepted that wave impacts in small scale hydraulic model tests will be greater in magnitude, but shorter in duration than their equivalents at full scale in (invariably aerated) sea water. It is very probable therefore that the higher impact pressures measured in these model tests can be scaled to lower values, but that the impulse durations must be scaled to longer values. It may be noted in passing that the largest pressures may occur when there is least air entrained or trapped, and these impacts may therefore actually be less influenced by scale effects on air compression.

7.1.1 Studies on scaling

Many of these uncertainties have been studied by researchers working at large scale in the Large Wave Channel (GWK) at Hannover / Braunschweig Universities, and using salt and fresh water in experiments at Plymouth University. It has previously been argued by reference to early work by Bagnold, von Karman, and others, that the addition of only small fractions of air may dramatically change pressure transmission characteristics of the water, thus substantially modifying pressures that might be experienced by the structure. Two studies have however suggested that the effect is very much smaller. There is some indication from studies at Plymouth described by Walkden et al (1995) that even quite high levels of aeration in the model only reduced wave pressures measured in the model by about 20%. Numerical modelling studies by Peregrine and co-workers, see for instance Peregrine & Thais (1996), can be used to suggest that scale errors due to air effects might be limited to about 50%.

In contrast, the results of analysis described in Chapter 6 of this report suggest that even small changes of relative mound level will change wave impact pressures by factors of 5 or more. This suggests that the influences of small changes to relative geometry may be of greater effect than the uncertainties introduced by scale effects. It is however still necessary to assess the likely contribution to overall uncertainties arising from any scale errors.

The argument on scaling wave impact pressures requires information on relative statistics of wave impact pressures, p, impact rise times Δt, and pressure impulses, estimated here perhaps by (p xΔt). These data must be measured in model and field with equivalent definitions of events. If comparative datasets can be compiled, it may then be possible to compare the magnitudes of pressure impulses scaled by Froude. If these show good agreement over the exceedance range of interest, say from 90 or 95% non-exceedance upward, then equivalent comparisons of pressures and rise times will give estimates of the appropriate scale corrections.

7.1.2 Scaling of impacts from HR Wallingford / Bristol studies

Fieldwork measurements on hollow cube concrete armour units have been described by Allsop et al (1995c), who detail four deployments of wave pressure and other recording equipment on La Collette breakwater, Jersey. In the last deployment, wave impact pressures were monitored throughout winter 1993/4 at eight points on a typical Cob concrete armour unit at 500Hz. Intelligent monitoring techniques were used to reduce the volume of data recorded whilst retaining all significant wave impact data. Statistics of wave impact pressures and rise times were retained for the complete winter period, see Allsop et al (1995c). During this deployment, 3270 impact events were recorded, but it was not possible to analyse all of this data. Howarth et al (1996) discuss 15 sets of recordings giving 7417 waves, of which 632 were impacts, so P_i=8.5%. For these 15 storms, values of impact pressure (p), and rise time (Δt) can be plotted for the top 8.5% of waves, that is from 91.5-100%.

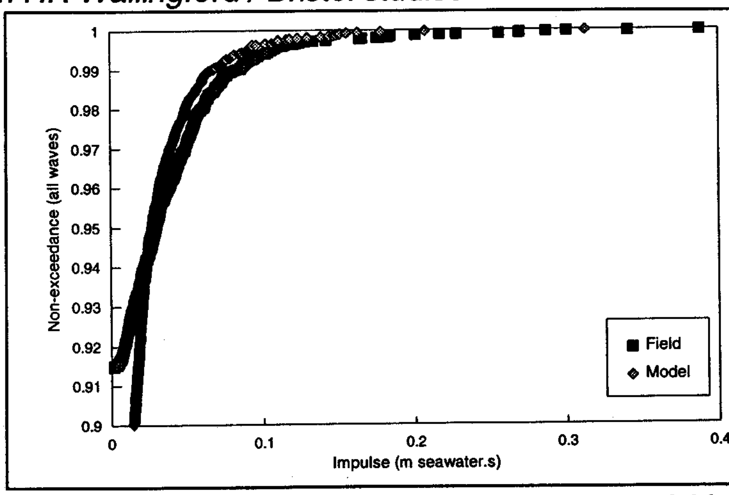

Figure 7.1 Pressure impulses from field and model for wave impacts on armour unit, linear

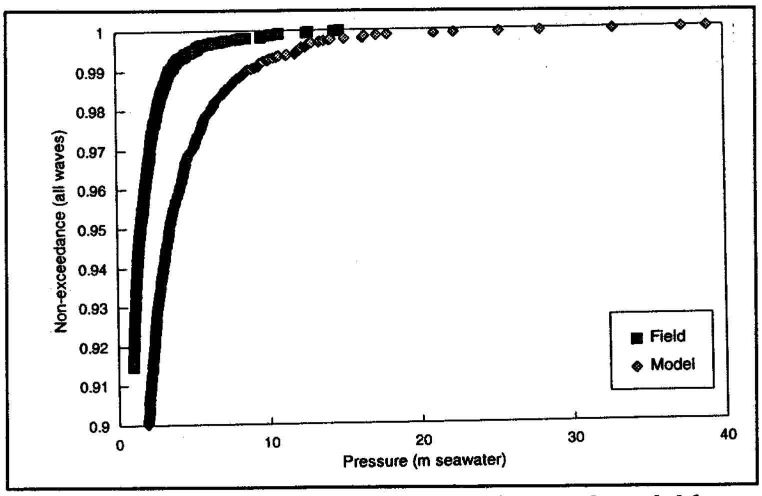

Figure 7.2 Impact pressures from field and model for wave impacts on armour unit, linear

Following previous model tests at Wallingford reported by Herbert & Waldron (1992), a 1:32 model of the breakwater cross-section was tested by Howarth (1996) at Bristol. The model was subjected to tests each of about 200 waves chosen to represent wave conditions / water levels measured in the field at Jersey. Impact pressures were measured on a model Cob unit in the same position as on the instrumented unit. Pressures were collected at 10kHz using a miniature transducer scaled from the prototype transducer size. A total of 37 random wave tests gave 6389 waves of which 1310 gave impacts, so here P_i=20%, thus allowing values of p, and Δt to be plotted for the top 20% of waves, that is from 80-100%.

Comparisons of these statistics give a dataset of impact pressures and rise times for full scale in sea water and small scale (1:32) in fresh water. These may be used to calculate pressure impulse, here estimated by pressure (p) multiplied by the rise time (Δt). Values of this estimate of pressure impulse are compared at the same exceedance levels in Figure 7.1, and show close agreement over the region of 92-99.9% non-exceedance. This agreement supports the thesis that the pressure impulse can be scaled by Froude, even where pressures or rise times cannot be so compared.

Using the same dataset, impact pressures are compared in Figure 7.2, confirming that at the same exceedance levels, wave impact pressures in the field are lower than would be predicted by scaling directly pressures from the model.

The presentation of Figure 7.1 and 7.2 does not easily show the form of the distribution of impulses or pressures, so these data are re-presented on Weibull axes in Figures 7.3 and 7.4. Comparison of impact pressures from field and model in Figure 7.4 suggests that there is a relatively constant relationship between field and laboratory pressures over the exceedance levels studied here. Measurements of impact pressures scaled by Froude need to be corrected by factors between about 0.40 to 0.45 over non-exceedances levels of 92 - 99%, shown in Figure 7.5.

A similar approach may be taken in examining the effect on pressure rise times, taken here to indicate also the effect on impact durations. Impact rise times are plotted on linear axes to the same exceedance levels as before in Figure 7.6, and on Weibull axes in Figure 7.7. The differences here are wider than seen for impact pressures, and more care will be needed in interpreting these results to take account of limitations in the data. For instance, it will be noted that steps are introduced into data on the shortest rise times by the minimum time interval needed to define a rise time, 1-2 sampling intervals. As for wave impact

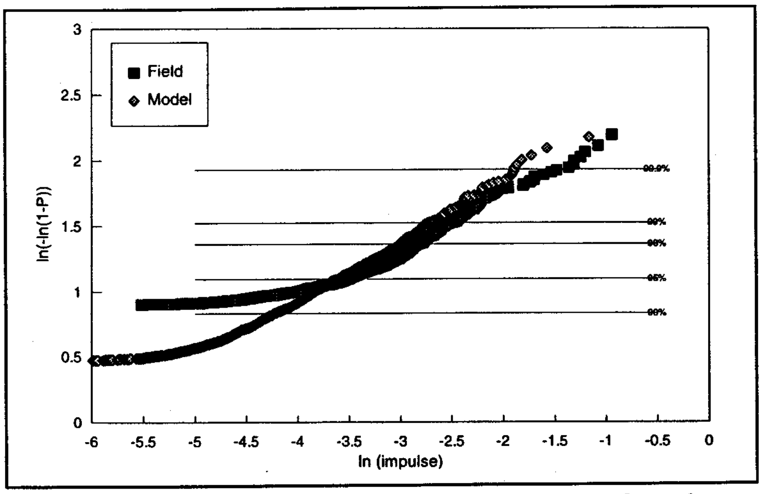

Figure 7.3 **Weibull probabilities for pressure impulses from field and model**

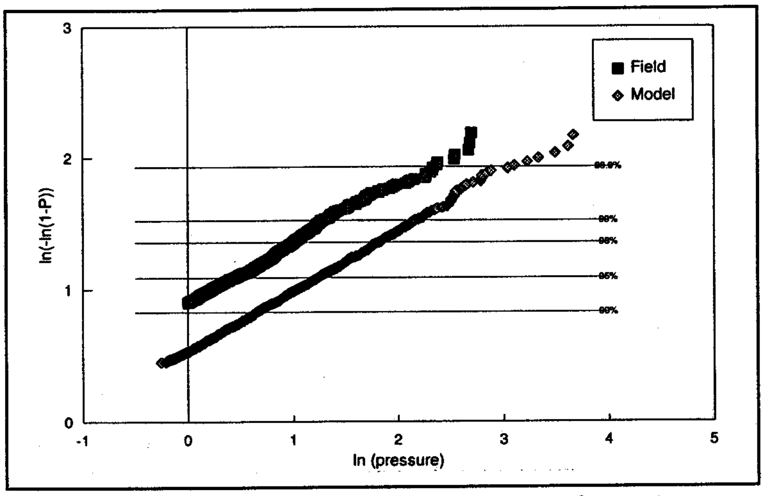

Figure 7.4 **Weibull probabilities for wave impact pressures from field and model**

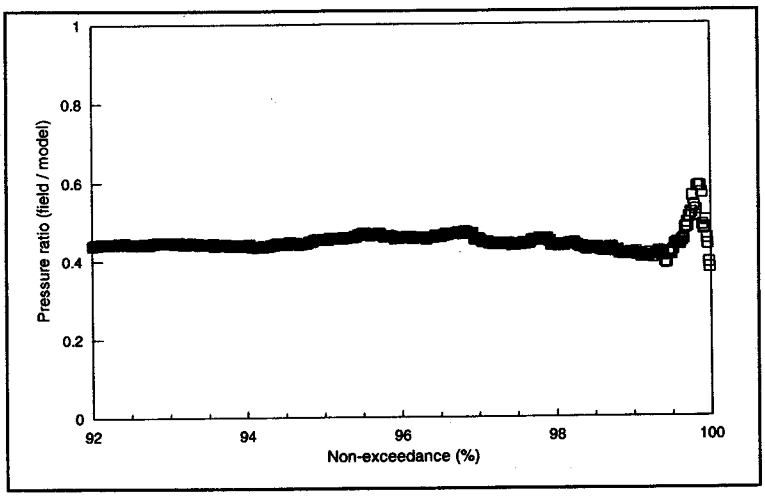

Figure 7.5 **Correction factors for pressures**

pressures, a correction factor may be derived for impact rise times / durations, as in Figure 7.8, but more information will be needed before these correction factors can be applied with the same confidence as can be ascribed to the use of those in Figure 7.5.

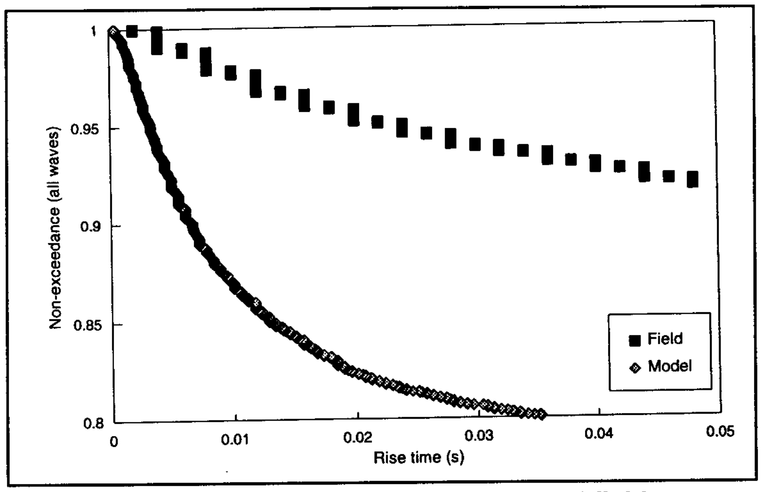

Figure 7.6 **Pressure rise times, model and field measurements**

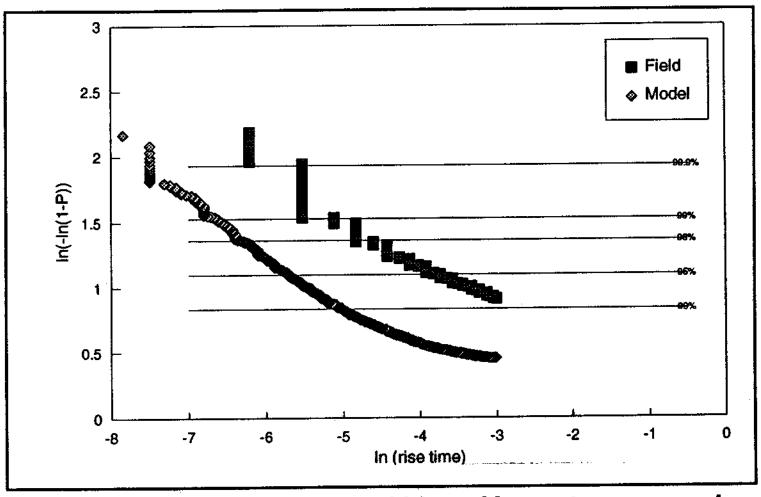

Figure 7.7 **Weibull probabilities of impact pressure rise times from model and field**

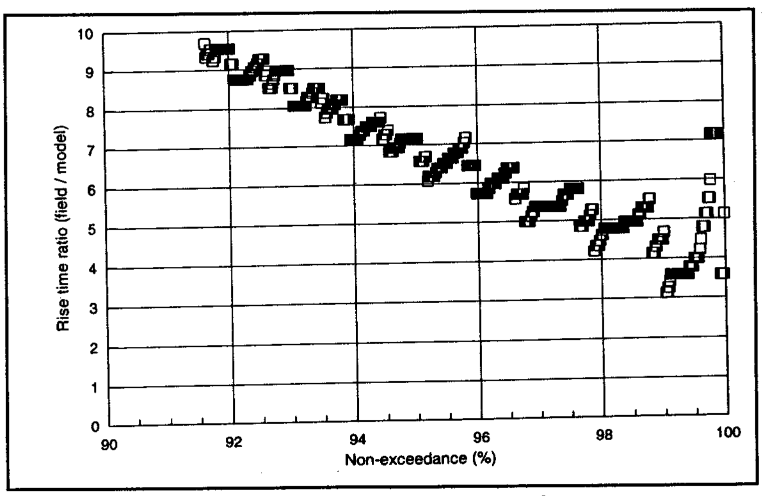

Figure 7.8 **Correction factors for rise times**

The correction factors derived above may be summarised:

Non-exceedance level	Impact pressure correction factor	Rise time / duration correction factor
92%	0.44	9
95%	0.45	6.8
98%	0.43	5
99%	0.41	4.2

7.2 Response periods and impact durations

Another issue in interpreting the use of these measurements is the relationship between the period of the wave loading and the response time of the structure. It has been shown by Muraki (1966) that typical natural periods of oscillation for (Japanese) caissons is 0.2 - 0.4 seconds. It is probable that small elements such as stone or concrete blocks in older walls will respond to much shorter periods, but this has not yet been studied. In experiments at large scale in the GWK at Hannover / Braunschweig, Schmidt et al (1992) measured pressure rise times in the regions of 0.05 -0.02s (sic) in the model. (This may have been mis-typed and should have been 0.005 - 0.02s.) Schmidt et al then suggest that the total wave force rise time is 5-10 times longer at 0.05 to 0.2 seconds, and convert these times by an un-explained scale (of 3) to prototype rise times of 0.15 to 0.6 seconds. They then compare these times and the response periods of caissons to confirm that these measurements of impacts are still able to cause movement of even large caissons.

8 Conclusions and recommendations

8.1 Conclusions

1. Of the prediction methods for wave forces on vertical and composite walls identified in this study, Goda's method is the most reliably based, and generally best accepted. The determination of wave forces in Goda's method was however derived from tests or field data on sliding distances for caissons, and should not necessarily be expected to give accurate estimates of wave pressures. Goda's method has been extended by Takahashi to take greater account of impulsive wave forces.

2. Since its publication in 1951 / 1963, Minikin's method for impact forces has almost always been quoted erroneously (except in British Standard 6349 Pt 1), particularly when the (dimensioned) coefficients have been (mis-) translated from British Imperial units to metric units. The 1963 version to which most later users refer includes a significant error in the example calculations of hydro-static pressures. Many later versions of Minikin's method are dimensionally inconsistent, and this has lead to considerable uncertainties in the values of the dimensioned or dimensionless coefficients. The method given in the Shore Protection Manual departs significantly from Minikin's method, and generally gives substantially greater forces.

3. Wave forces on vertical and composite walls are strongly influenced by the type of wave breaking onto the wall. The forces measured in this study may be divided between pulsating and impact conditions. A response diagram (Fig 6.14) has been developed from these measurements to identify ranges of dimensionless parameters that distinguish the different types of wave breaking, and hence the different types of wave loadings.

4. Pulsating loads are relatively slow-acting. Impact loads are almost always substantially larger than pulsating loads, and of much shorter duration.

5. Analysis of overall stability with a simple model of caisson sliding was used to estimate factors of safety for all configurations tested in these studies. This model identified some cases where simple analysis using $F_{h1/250}$ and $F_{u1/250}$ showed a Factor of Safety above unity, but full time series data showed a Factor of Safety below unity. These cases were however well below the ranges of F_S = 1.5 to 2 suggested by BS6349 Pt 1, and little increase in reliability was given by using loads other than $F_{h1/250}$ and $F_{u1/250}$. Any increase in sophistication of modelling stability is therefore probably not merited unless the full dynamic structure / foundation processes can be reproduced.

6. For pulsating conditions, the vertical distribution of pressures on the front face generally conform to the simple distribution suggested by Goda, but changes dramatically at the onset of impacts. Impact conditions give very intense pressures at or near to the static water level, conforming with the general vertical distribution suggested by Minikin. Impact conditions have less effect on pressures much above or below static water level.

7. Forces on breakwater crown walls are reasonably well described by the simple method developed by Jensen / Bradbury & Allsop and used in the CIRIA / CUR manual.

8. Under impact conditions, local pressure gradients on vertical walls can be very severe, reaching extreme pressure head gradients up to dp/dz = 70 to 90.

9. Pulsating loads may be converted directly from model tests at appropriate scales by Froude scaling without significant scale effects.

10. Impact loads are potentially influenced by scale and other model effects, so impact loads converted directly by Froude scaling will over-estimate prototype loads. A new method has been derived in this study from field and model test data on wave impacts to correct wave impact pressures for scale / model effects.

8.2 Recommendations for design / analysis

1. Combinations of structure configuration and wave / water level conditions that may lead to impact conditions should be identified using the parameter map in Figure 6.14. Where practical, the structure configuration should be revised to reduce the potential for high intensity wave impact loads.

2. For pulsating conditions, the statistics of wave forces fit the Weibull distribution. At the 1/250 level, horizonal wave loads can be predicted by Goda's method with reasonable safety. Goda's method may however over-estimate wave forces for low relative wave heights and large mounds. Up-lift forces are predicted relatively safely by Goda's method

3. For impact conditions, wave forces depart from the Weibull distribution that fits the rest of the (pulsating) forces. Under these conditions, forces at the 1/250 level are substantially greater than would be predicted by Goda's method. Takahashi's extension of Goda's method has little effect in increasing wave impact loads in relation to those measured in these studies. For simple vertical walls and composite structures with low mounds, horizontal forces under impact conditions may be estimated by the simple formula in eqn. 6.1 and up-lift forces by eqn. 6.3b. Methods for other configurations are discussed in Chapter 6, but within this study no general prediction method for impacts has been developed for all structure configurations.

4. Wave forces on breakwater crown walls can generally be estimated safely using the simple prediction method in the CIRIA / CUR manual.

5. The stability of caisson or sections against sliding may be simulated using a simple static analysis provided that: wave forces are predicted at 1/250 level using an appropriate method; and Factors of Safety of at least 1.5 - 2.0 are used.

6. Predictions of pulsating loads derived from hydraulic model tests, therefore including those measured in this study, may be converted to full scale by simple Froude scaling with little scale effect.

7. Predictions of impacts loads derived from hydraulic model studies in fresh water are significantly influenced by model and scale effects, and should be corrected to avoid over-estimating wave loads. A new correction method has been derived here and is presented in Chapter 7.

8.3 Recommendations for future research

Future analysis / design methods for vertical and composite breakwaters are more likely to use probabilistic approaches rather than the deterministic methods used to date. Static stability analysis methods will also be replaced by dynamic analysis of structure and foundation. These new approaches will therefore require substantially greater levels of detail on variabilities / uncertainties in responses than available hitherto. The present study, whilst more comprehensive than any other recent work in this field, has not covered the full range of possible structure configurations or relative wave conditions. Future research studies should therefore include the following:

1. Gaps in the present parameter map should be filled by supplementary testing. Existing and new data should be used to improve the reliability of prediction methods for the onset of impact conditions, and for the prediction of the magnitude and durations of wave impact forces.

2. Further detailed testing and analysis is needed to determine more reliably the spatial extent of high impact pressures, and to describe their spatial variability.

3. The present study was unable to determine correctly the phase lags between horizontal and up-lift forces. Information on these forces and their phasing is needed as input to dynamic modelling of caisson / foundation responses. Future model studies and field measurements should record these forces un-filtered to a common time base to permit phase lags to be determined.

4. These studies have generally supported simple prediction methods for forces on breakwater crown walls, but do not identify the effects of various configuration parameters. Further testing may be

merited to identify more fully the influence of crest geometry and armour configuration on wave loads on the crown wall.

5. Typical time series of pressures on the wall and within the rubble mound / foundation will be required for dynamic structure / foundation simulations. The development of such (standard) time series from the data collected in this study, and from future studies, will require information on typical frequency ranges for the structural responses of caissons, crown walls, and elements of blockwork walls.

6. The development of probabilistic simulations of stability will require more reliable estimates of extreme force statistics. Future tests should be extended to 1000 waves, and additional testing should quantify the effects of long (test or storm) durations on the extreme force statistics.

7. A simple engineering approach to the derivation of scale correction factors for impact pressures has been presented for the first time in this report. the method is relatively simple, and omits some of the more complex aspects of the scaling problem. It is hoped that future studies under the PROVERBS project will refine this approach, and will present more robust methods to scale impact rise times and durations.

9 Acknowledgements

The work discussed here is based in part on studies completed by members of the Coastal and Ports & Estuaries Groups of HR Wallingford for the Construction Sponsorship Directorate of the UK Department of Environment, under research contracts PECD 7/6/263, PECD 7/6/312, and CI 39/5/96; in part under support from the MCS project of the EC's MAST II programme under contract MAS2-CT92-0047, and the PROVERBS project in MAST III under contract MAS3-CT95-0041.

This report also draws on the results of research supported by the MAST I programme of the European Union, and by the Construction Policy Directorate of the UK Department of Environment under contract PECD 7/6/312. The development of the numerical models of internal and external flows used in studies on Alderney breakwater was supported by the Department of Environment under contract PECD 7/6/108.

Substantial additional support to the testing and data analysis has been given by the Queen's University of Belfast; the Department of Hydraulics of the University of Naples; and University of Sheffield. Funding support for visiting researchers at Wallingford from TECHWARE, the international exchange programme of the University of Naples, and the Department of Education NI is also gratefully acknowledged.

The authors are also pleased to acknowledge assistance in testing and analysis by Phil Besley, Daniela Colombo, Chris Jones, and in the compilation of this report by Kirsty McConnell. They are grateful for assistance in processing data by Luca Centurioni, visiting researcher at HR Wallingford, and by Siva Sathiamoorthy of the National University of Singapore.

HR Wallingford are also grateful for advice and assistance provided by Mike Chrimes, librarian of the Institution of Civil Engineers, in researching some of the historical information cited here; to Gerald Müller of Queen's University of Belfast for early discussions on wave impacts, and advice on measurement devices; to Mario Calabrese of the University of Naples for significant assistance in the development of the flow diagram dividing parameter regions and pulsating / impact responses; and to Andreas Kortenhaus of Universities of Hannover and later Braunschweig for advice on analysis and event definition methods.

The senior author is grateful for the interest and support shown by the Port and Harbour Research Institute at Yokosuka, Japan, and to JISTEC for supporting participation in the 1994 Wave Barriers workshop, and to his colleagues in the PROVERBS research project.

10 References

Allsop N.W.H. (1995) "Vertical walls and breakwaters: optimization to improve vessel safety and wave disturbance by reducing wave reflections" Chapter 10 in Wave Forces on Inclined and Vertical Wall Structures, pp 232-258, ed. Kobayashi N. & Demirbilek Z., ASCE, New York.

Allsop N.W.H. & Bray R.N. (1994) "Vertical breakwaters in the United Kingdom: historical and recent experience" Proceedings of Workshop on Wave Barriers in Deep Waters, pp76-100, Port and Harbour Research Institute, Yokosuka, Japan.

Allsop N.W.H., Besley P., McBride M.W., & McKenna J.E. (1994a) "Hydraulic performance of vertical walls: tests on caissons and `low-reflection' walls." Paper 3.7 to 2nd MCS Workshop, Milan, publn University of Hannover.

Allsop N.W.H., MG Briggs, T Denziloe, & AE Skinner (1991) "Alderney breakwater: the quest for a 'final' solution" Conference on Coastal Structures and Breakwaters, Institution of Civil Engineers, London.

Allsop N.W.H., Calabrese M. & Vicinanza D. (1995c) "Analisi dei carichi impulsivi su una diga a paramento verticale" Giornate Italiane di Ingegneria Costiera, Ravenna, Ottobre 1995, Italiana PIANC.

Allsop N.W.H., Calabrese M., Vicinanza D. & Jones R.J. (1996) "Wave impact loads on vertical and composite breakwaters" Proceedings 10th Congress of the Asia and Pacific Division of IAHR, 26-29 August 1996, Langkawi Island, Malaysia

Allsop N.W.H. & McBride M.W. (1994) "Reflections from vertical walls: the potential for improvement in vessel safety and wave disturbance" Proceedings of Workshop on Wave Barriers in Deep Waters, pp101-128, Port and Harbour Research Institute, Yokosuka, Japan.

Allsop N.W.H., McBride M.W., & Colombo D. (1994b) "The reflection performance of vertical walls and `low reflection' alternatives: results of wave flume tests." Paper 3.4 to 3rd MCS Workshop, Emmeloord, publn University of Hannover.

Allsop N.W.H., di Leo M. & McBride M.W. (1995a) "The effect of wave reflections on local wave steepness" Paper II.4.3 to the final MCS Project Workshop, Alderney, publn University of Hannover.

Allsop N.W.H., McBride M.W., & di Leo M. (1995b) "Wave reflections from vertical walls and low reflection alternatives." Paper 4.7 in Final Report of MCS Project, publn University of Hannover.

Allsop N.W.H. & Müller G. (1995) Discn to Technical Note 2575: "Comparative study on breaking wave forces on vertical walls" by Ergin A. & Abdalla S., Proc ASCE, Jo Waterway, Port, Coastal and Ocean Engineering Division, September / October 1995, ASCE, New York

Allsop N.W.H., Vann A.M., Howarth M., Jones R.J. & Davis J.P. (1995c) "Measurements of wave impacts at full scale: results of fieldwork on concrete armour units" pp287-302, Conf. on Coastal Structures and Breakwaters '95, Institution of Civil Engineers / Thomas Telford, London.

Allsop N.W.H. & Vicinanza D. (1996) "Wave impact loadings on vertical breakwaters: development of new prediction formulae " Proceedings of 11th International Harbour Congress, pp 275-284, Royal Flemish Society of Engineers, Antwerp, Belgium.

Allsop N.W.H., Vicinanza D., Calabrese M. & Centurioni L. (1996) "Breaking wave impact loads on vertical faces" Paper to 6th International Offshore and Polar Engineering Conference, Los Angeles, California, USA.

Allsop N.W.H., Vicinanza D, & McKenna JE (1995c). "Wave forces on composite breakwaters and seawalls: analysis of horizontal and up-lift forces and overturning moments" Paper 1.5 in Final Report of MCS Project, publn University of Hannover.

Bagnold (1939) "Interim report on wave pressure research" Jo. Institution of Civil Engineers, Vol 12, pp 202-226, ICE, London.

Banyard L., Calabrese M. & Allsop N.W.H. (1996) "Forces on vertical breakwaters: effects of oblique or short-crested waves" Research Report SR465, HR Wallingford, Wallingford.

Besley P., Allsop N.W.H., Colombo D & Madurini L. (1994). "Overtopping performance of vertical walls and 'low reflection alternatives'- Results of wave flume tests" Paper 4.4 to 3rd MCS Workshop, Emmeloord, publn University of Hannover.

Bennett G.S., McIver P. & Smallman J.V. (1992) "A mathematical model of a slotted wave screen breakwater" Coastal Engineering, Volume 18, Elsevier, Amsterdam.

Blackmore PA & Hewson P (1984) "Experiments on full scale impact pressures" Coastal Engineering, Vol 8, pp 331-346, Elsevier, Amsterdam.

Bishop RW (1950) "Maintenance of some rubble breakwaters: Alderney breakwater" ICE Maritime & Waterways, Paper 16, Session 1950-51, pp 16-35 & 36-53, ICE, London.

Bradbury A.P. & Allsop N.W.H. (1988) "Hydraulic effects of breakwater crown walls" Proceedings Conference on Design of Breakwaters, pp 385-396, Institution of Civil Engineers, London.

Bradbury A.P., Allsop N.W.H. & Stephens R.V. (1988) "Hydraulic performance of breakwater crown walls" HR Report SR 146, Hydraulics Research, Wallingford.

Bray RN & Tatham PFB (1992) "Old waterfront walls: management, maintenance and rehabilitation" CIRIA / E & FN Spon, London.

British Standards Institution (1984) "British Standard Code of practice for Maritime structures, Part 1. General Criteria" BS 6349: Part 1: 1984, and Amendments 5488 and 5942, British Standards Institution, London.

British Standards Institution (1991) "British Standard Code of practice for Maritime structures, Part 7. Guide to the design and construction of breakwaters" BS 6349: Part 7: 1991, British Standards Institution, London.

Bruining J.W. (1994) "Wave forces on vertical breakwaters: reliability of design formulae" MSC thesis, Report H1903, Delft Hydraulics / Delft University of Technology, the Netherlands.

Burcharth H.F., Dalsgaard Sorensen J. & Christiani E (1994) "On the evaluation of failure probability of monolithic vertical wall breakwaters" Proceedings of Workshop on Wave Barriers in Deep Waters, pp 458-469, Port and Harbour Research Institute, Yokosuka, Japan.

Burcharth H.F., Ibsen L.B. (1994) "Response of rubble foundation to dynamic loading" Proceedings of Workshop on Wave Barriers in Deep Waters, pp 402-418, Port and Harbour Research Institute, Yokosuka, Japan.

CERC (1984) "Shore Protection Manual" 4th ed. U.S. Govt. Printing Office, Washington D.C.

Centurioni L., Vicinanza D. & Allsop N.W.H. (1995) "Wave forces on vertical walls: analysis methods for measurements of pressures and forces" Report IT 430, HR Wallingford.

Chan E.S. (1994) "Mechanics of deep water plunging wave impacts on vertical structures" Coastal Engineering, Special Issue on Vertical Breakwaters, Vol 22, pp 115-134, Elsevier Science BV, Amsterdam.

Chan E.S, Cheong H.F. & Gin K.Y.H. (1995) "Breaking wave loads on vertical walls suspended above mean sea level" Jo. Waterway, Port, Coastal, and Ocean Div., ASCE, July / August,

Chan E.S, Cheong H.F. & Tan B.C. (1995) "Laboratory study of plunging wave impacts vertical cylinders" Coastal Engineering Vol 25, pp87-107, Elsevier Science BV, Amsterdam.

Chan E.S, & Melville W.K. (1988) "Deep water plunging wave pressures on a vertical plane wall" Proc. Royal Soc., London.

Chan E.S, & Melville W.K. (1989) "Plunging wave forces on surface-piercing structures" Jo. Offshore Mechanics and Arctic Engineering, Vol 111, May 1989.

Chien C.H., Chiou Y.D. & Lai G.H. (1995) "Irregular impulsive wave forces on solid wall breakwater" Proc. Conf. HYDRA 2000, Vol 3 , pp269-280, Thomas Telford, London.

Cornick HF (1969) "Dock and harbour engineering" Charles Griffin & Co., London.

Crawford A.R, Walkden M.J, Bird P.A.D, Bullock G.N, Hewson P.J. & Griffiths J. "Wave impacts on sea walls & breakwaters" Proc. Conf. Coastal Dynamics '94, Barcelona, ASCE, New York.

Ergin A & Abdalla S (1993) "Comparative study on breaking wave forces on vertical walls" Proc ASCE, Jo Waterway, Port, Coastal and Ocean Engineering Division, Vol. 119, No 5, ASCE, New York

Franco C (1996) "Wave overtopping and loads on caisson breakwater under three-dimensional sea states" MCS / PROVERBS report, Politechnico di Milano, Milan.

Franco L. (1994) "Vertical breakwaters: the Italian experience" Coastal Engineering, Special Issue on Vertical Breakwaters, Vol 22, pp31-55, Elsevier Science BV, Amsterdam.

Franco L., de Gerloni M. & van der Meer J.W. (1994) "Wave overtopping on vertical and composite breakwaters" Proceedings 24th ICCE, Kobe, pp 1030-1045, ASCE, New York.

Franco L & Verdesi G (1993) "Ancient Mediterranean harbours: a heritage to preserve" Med-Coast Conference, Antalya, Turkey.

Funakoshi H., Ohno M. & Tsuda S. (1994) "Survey of long-term deformation of composite breakwaters along the Japan Sea" Proceedings of Workshop on Wave Barriers in Deep Waters, pp239-266, Port and Harbour Research Institute, Yokosuka, Japan.

Ganly P. (1983) Discussion on papers 5 and 6, Proceedings of Conference on Breakwaters: design & construction, pp82-84, Institution of Civil Engineers, publn Thomas Telford, London

Goda Y. (1974) "New wave pressure formulae for composite breakwaters" Proc. 14th ICCE, Copenhagen, ASCE, New York.

Goda Y. (1985) "Random seas and maritime structures" University of Tokyo Press, Tokyo.

Goda Y. (1990) "Random wave interaction with structures" Chapter 16 in Handbook of Coastal and Ocean Engineering, Vol 1, ed. J.B. Herbich, Gulf Publishing Company, Houston.

Goda Y. (1994) "Dynamic response of upright breakwaters to impulsive breaking wave forces" Coastal Engineering, Special Issue on Vertical Breakwaters, Vol 22, pp 135-158, Elsevier Science BV, Amsterdam.

Goda Y. (1995a) "Japan's design practice in assessing wave forces on vertical breakwaters" Chapter 6 in Wave Forces on Inclined and Vertical Wall Structures, pp140-155, ed. Kobayashi N. & Demirbilek Z., ASCE, New York.

Goda Y (1995b) Discn to Technical Note 2575: "Comparative study on breaking wave forces on vertical walls" by Ergin A. & Abdalla S., Proc ASCE, Jo Waterway, Port, Coastal and Ocean Engineering Division, September / October 1995, ASCE, New York.

Hattori M. (1994) "Wave impact pressures on vertical walls and the resulting wall deflections" Proceedings of Workshop on Wave Barriers in Deep Waters, pp 332-346, Port and Harbour Research Institute, Yokosuka.

Hattori M., Arami A. & Yui T. (1994) "Wave impact pressures on vertical walls under breaking waves of various types" Coastal Engineering, Special Issue on Vertical Breakwaters, Vol 22, pp79-115, Elsevier Science BV, Amsterdam.

Herbich J.B. (Ed.) (1990) "Handbook of Coastal and Ocean Engineering" Volume 1 pp1-1155, Gulf Publishing Company, Houston.,

Hitachi S. (1994) "Case study of breakwater damages- Mutsu-Ogawara Port" Proceedings of Workshop on Wave Barriers in Deep Waters, pp 308-331, Port and Harbour Research Institute, Yokosuka.

Hou H.S, Chiou Y.D. & Chien C.H. (1994) "Experimental study and theoretical comparison of irregular wave pressures on deepwater composite breakwaters" Proc. Hydro-Port '94, Yokosuka.

Howarth M. (1996) "Wave impacts on hollow cube breakwater armour units" Ph.D thesis, University of Bristol.

Howarth M.W., Vann A.M., Davis J.P., Allsop N.W.H. & Jones R.J. (1996) "Comparison of wave impact pressures on armour units at prototype and model scale" Paper to 25th International Conference on Coastal Engineering, Orlando, ASCE, New York.

Hunt J.N. (1979) "Direct solution of wave dispersion equation" Jo Waterway and Harbours Division, Proc ASCE, Vol WW4, November, pp 457-459, ASCE, New York

Ito Y. (1971) "Stability of mixed type breakwater - a method of probable sliding distance" Coastal Engineering in Japan, Vol 14, pp53-61, JSCE, Tokyo.

Jensen O.J. (1983) "Breakwater superstructures" Proc. Conf. Coastal structures '83, Arlington, pp272-285, ASCE, New York.

Jensen O.J. (1984) "A monograph on rubble mound breakwaters" Danish Hydraulic Institute, Horsholm.

Johnson J.W, Kondo H. & Wallihan R. (1966) "Scale effects in wave action through porous structures" Proc 10th ICCE, Tokyo, Vol 2 pp 1022-1024, ASCE, New York.

Juhl J. (1994) "Danish experience and recent research on vertical breakwater" Proceedings of Workshop on Wave Barriers in Deep Waters, pp154-171, Port and Harbour Research Institute, Yokosuka, Japan.

Karman von T (1928) "The impact of seaplane floats during landing" NACA Tech Note 321, Washington.

Kirkgoz M.S. (1995) "Breaking wave impact on vertical and sloping coastal structures" Ocean Engineering, Vol 22, No 1, pp 35-48, Elsevier Science, Oxford.

Kobayashi N. (1994) "Breakwaters in USA and Canada, and review of composite breakwater design" Proceedings of Workshop on Wave Barriers in Deep Waters, pp184-198, Port and Harbour Research Institute, Yokosuka, Japan.

Kortenhaus A., Oumeraci H., Kohlhase S. & Klammer P (1994) "Wave induced up-lift loading of caisson breakwaters" Proceedings 24th ICCE, Kobe, pp 1298-1311, ASCE, New York.

Kuo C.T. (1994) "Recent researches and experiences on composite breakwaters in Taiwan" Proceedings of Workshop on Wave Barriers in Deep Waters, pp217-238, Port and Harbour Research Institute, Yokosuka, Japan.

Lamberti A. & Franco L. (1994) "Italian experience on upright breakwaters" Proceedings of Workshop on Wave Barriers in Deep Waters, pp25-75, Port and Harbour Research Institute, Yokosuka, Japan.

Lee D.S. & Hong G.P. "Korean experience on composite breakwaters" Proceedings of Workshop on Wave Barriers in Deep Waters, pp172-183, Port and Harbour Research Institute, Yokosuka, Japan.

Ligteringen H. (1994) "Other European experience on deep water breakwaters" Proceedings of Workshop on Wave Barriers in Deep Waters, pp199-216, Port and Harbour Research Institute, Yokosuka, Japan.

Lundgren H. & Juhl J. (1995) "Optimization of caisson breakwater design" Chapter 8 in Wave Forces on Inclined and Vertical wall Structures, pp 181-204, ed. Kobayashi N. & Demirbilek Z., ASCE, New York.

Madurini L. & Allsop N.W.H. (1995) "Overtopping performance of vertical and composite breakwaters and seawalls: results of wave flume tests" Paper II.4.2 to the Final MCS Project Workshop, Alderney, publn University of Hannover.

Meer JW van der, d'Angremond K & Juhl J (1994) "Probabilistic calculations of wave forces on vertical structures" Proceedings 24th ICCE, Kobe, pp 1754-1767, ASCE, New York.

Meer JW van der, Juhl J, & Driel G van (1992) "Probabilistic calculations of wave forces on vertical structures" In Proceedings of Final Overall Workshop, MAST G6-S, Lisbon, publn University of Hannover.

McBride M.W., Allsop N.W.H., Besley P., Colombo D. & Madurini L. (1995a) "Vertical walls and low reflection alternatives: results of wave flume tests on reflections and overtopping" Report IT 417, HR Wallingford, Wallingford.

McBride M.W., Hamer B.A., Besley P., Smallman J.V. & Allsop N.W.H. (1993) "The hydraulic design of harbour entrances: a pilot study" Report SR 338, HR Wallingford, Wallingford.

McBride M.W., Smallman J.V. & Allsop N.W.H. (1994) "Design of harbour entrances: breakwater design and vessel safety" Proceedings of Hydro-port '94, pp525-541, Port and Harbour Research Institute, Yokosuka, Japan.

McBride M.W., Smallman J.V. & Allsop N.W.H. (1995b) "Vertical walls and low reflection alternatives: numerical modelling of absorbing wave screens" Report IT 400, HR Wallingford, Wallingford.

McBride M.W., Smallman J.V. & Allsop N.W.H. (1996) "Guidelines for the hydraulic design of harbour entrances" Report SR 430, HR Wallingford, Wallingford.

McBride M.W., & Watson G.M. (1995c) "Vertical walls and low reflection alternatives: results of 3-d physical model tests" Report IT 425, HR Wallingford, Wallingford.

McKenna J.E. (1996) "Wave forces on caissons and breakwater crown walls" Ph.D thesis, Queen's University of Belfast, Belfast.

McKenna J.E., Besley P., Allsop N.W.H., Whittaker T.J.T. (1994) "Wave pressures on caisson breakwaters: preliminary results of parametric flume tests." Paper 1.4 to 3rd MCS Workshop, Emmeloord, publn University of Hannover.

Minikin R.R. (1963) "Winds, Waves and Maritime Structures" 2nd ed., Griffin, London.

Müller G.U. & Whittaker T.J.T. (1995) "On the vertical distribution of wave impact pressures" Proc 5th ISOPE conf., The Hague, The Netherlands.

Müller G.U. (1993) "A study of breaking wave loads on a shoreline wave power station" Ph.D thesis, Queen's University of Belfast, Belfast

Muraki Y. (1966) "Field investigations on the oscillations of breakwaters caused by wave action" Coastal Engineering In Japan, Vol 9, JSCE, Tokyo.

Noli A., Franco L., Tomassi S., Verni R. & Mirri F. (1995) "The new Porto Torres breakwater, Italy" Proc. Instn. Civ. Engrs., Civil Engineering, Vol 108, pp 17-27, ICE, London.

Owen M.W. & Allsop N.W.H. (1983) "Hydraulic modelling of rubble mound breakwaters" Proceedings Conference on Breakwater: Design and Construction, ICE, London.

Owen M.W. & Briggs M.G. (1985) "Limitations of modelling" Proceedings Conference on Breakwater '85, ICE, publn Thomas Telford, London.

Oumeraci H. (1994a) "Scour in front of vertical breakwaters - review of problems" Proceedings of Workshop on Wave Barriers in Deep Waters, pp 281-307, Port and Harbour Research Institute, Yokosuka, Japan.

Oumeraci H. (1994b) "Multi-disciplinary research experience in Europe on vertical breakwaters" Proceedings of Workshop on Wave Barriers in Deep Waters, pp 267-280, Port and Harbour Research Institute, Yokosuka, Japan.

Oumeraci H. (1994c) "Review and analysis of vertical breakwater failures - lessons learned" Coastal Engineering, Special Issue on Vertical Breakwaters, Vol 22, pp3-30, Elsevier Science BV, Amsterdam.

Oumeraci H. (1995a) "Vertical breakwaters: a plea for an integrated design approach" Chapter 9 in Wave Forces on Inclined and Vertical wall Structures, pp 205-231, ed. Kobayashi N. & Demirbilek Z., ASCE, New York.

Oumeraci H. (1995b) "European multi-disciplinary research experience on vertical breakwaters: the MCS project" Second MAST Days and EUROMAR market, 7-10 November 1995, pp 737-762, Directorate General of Science, Research and Development, European Commission, Brussels.

Oumeraci H. & Kortenhaus A. (1994) "Analysis of the dynamic response of caisson breakwaters" Coastal Engineering, Special Issue on Vertical Breakwaters, Vol 22, pp159-183, Elsevier Science BV, Amsterdam.

Oumeraci H., Klammer P. & Kortenhaus A. (1994a) "Impact loading and dynamic response of vertical breakwaters: review of experimental results" Proceedings of Workshop on Wave Barriers in Deep Waters, pp347-361, Port and Harbour Research Institute, Yokosuka, Japan.

Oumeraci H., Kortenhaus A. & Klammer P. (1994b) "Caisson breakwaters: integrated design and wave load specification" Proc. Conf. Hydro-Port '94, Yokosuka, Japan.

Oumeraci H., Kortenhaus A. & Klammer P. (1995) "Displacement of caisson breakwaters induced by breaking wave impacts." Conference of Institution of Civil Engineers on coastal structures and breakwaters '95, ICE, London.

Oumeraci H. & Lundgren H. (1992) "Some remarks on design guidelines for monolithic structures" In Proceedings of Final Overall Workshop, MAST G6-S, Lisbon, publn HR Wallingford.

Oumeraci H., Partenscky H-W. & Tautenhain E. (1992) "Breaking wave loads on vertical gravity structures" Proc. 2nd ISOPE conf., San Francisco.

Partenscky H-W. (1988) "Dynamic forces due to waves breaking at vertical coastal structures" Proc 2nd Int Symposium on Wave Research and Coastal Engineering, University of Hannover.

Peregrine D.H. (1994) "Pressure on breakwater: a forward look" Coastal Engineering, Special Issue on Vertical Breakwaters, Vol 22, pp553-573, Elsevier Science BV, Amsterdam.

Peregrine D.H. (1995) "Water wave impact on walls and the associated hydro-dynamic pressure field" Chapter 11 in Wave Forces on Inclined and Vertical Wall Structures, pp 259-281, ed. Kobayashi N. & Demirbilek Z., ASCE, New York.

Rennie Sir J (1854) "The theory, formation, and construction of British and foreign harbours" John Weale, High Holborn, London.

Routh EMG (1912) "Tangier: England's lost Atlantic outpost, 1661-1684" (Chapter 17: The Mole and Harbour), John Murray, Albemarle St, London.

Rouville MA, Besson P, & Petry P (1938) "Etudes internationales sur les efforts dus aux lames" Vol 108, pp 5-113, Annales des Ponts et Chaussees, Paris.

Sainflou G (1928) "Essai sur les digues maritimes verticales" Vol 98, Annales des Ponts et Chaussees, Paris.

Schmidt R., Oumeraci H. & Partenscky H-W (1992) "Impact loads induced by plunging breakers on vertical structures" Proceedings of 23rd ICCE, Venice, publn. ASCE, New York.

Simm JD (Ed) (1991) "Manual on the use of rock in coastal and shoreline engineering" CIRIA / CUR, Special Publication 83, CIRIA, London.

Shield W (1895) "Principles and practice of harbour construction" Longmans, Green & Co., London

Smeaton J (1837) "Reports of the late John Smeaton FRS" 2nd Edition, M Taylor, Strand, London.

Soler W. (1996) "Grand Harbour breakwater in Malta, 1903-09" Proc. Institution of Civil Engineers, Civil Engineering, Vol 114, pp 81-91, Thomas Telford for ICE, London

Stevenson T (1874) "The design and construction of harbours: a treatise on maritime engineering" 2nd edition, Adam & Charles Black, Edinburgh.

Stoney BB (1874) "On the construction of harbour and marine works with artificial blocks of large size" Paper 1376, Institution of Civil Engineers, London.

Takahashi S. Tanimoto K. & Shimosako K. (1992) "Experimental study of impulsive pressures on composite breakwaters" Report of Port & Harbour Research Institute, Vol 31, No 5, pp 35-74, PHRI, Yokosuka.

Takahashi S. Tanimoto K. & Shimosako K. (1994) "Dynamic response and sliding of breakwater caissons against impulsive breaking wave forces" Proceedings of Workshop on Wave Barriers in Deep Waters, pp362-401, Port and Harbour Research Institute, Yokosuka, Japan.

Takahashi S. Tanimoto K. & Shimosako K. (1994) "A proposal of impulsive pressure coefficient for the design of composite breakwaters" Proc. Conf. Hydro-Port '94, Yokosuka, Japan.

Takayama T. "Development of new caisson type breakwater in Japan, and probabalistic design approach for composite breakwaters" Chapter 7 in Wave Forces on Inclined and Vertical Wall Structures, pp 156-180, ed. Kobayashi N. & Demirbilek Z., ASCE, New York.

Tanimoto K. & Takahashi S. (1994a) "Japanese experiences on composite breakwaters" Proceedings of Workshop on Wave Barriers in Deep Waters, pp1-24, Port and Harbour Research Institute, Yokosuka, Japan.

Tanimoto K. & Takahashi S. (1994b) "Design and construction of caisson breakwaters - the Japanese experience" Coastal Engineering, Special Issue on Vertical Breakwaters, Vol 22, pp57-78, Elsevier Science BV, Amsterdam.

Thomas RS & Hall B (1991) "Sea wall design guidelines" CIRIA / Butterworths, London.

Townshend BO'D (1898) "Repairs at Alderney breakwater" Paper 3006, Proc Institution of Civil Engineers, pp 307-310, London.

Vernon-Harcourt LF (1873) "Account of the construction and maintenance of the harbour at Braye Bay, Alderney" Paper 1347, Institution of Civil Engineers, London.

Vernon-Harcourt LF (1885) "Harbours and docks: their physical features, history, construction equipment, and maintenance" Clarendon Press Series, Oxford University Press, Oxford.

Vicinanza D. (1997) "Pressioni e forze di impatto di onde frangenti su dighe a paramento verticale e composte" Ph.D thesis, University of Naples, Naples.

Vicinanza D., Allsop N.W.H. & Centurioni L. (1995) "Horizontal forces on composite breakwaters: initial analysis" Paper II.1.1 to the final MCS Project Workshop, Alderney, May 1995, publn University of Hannover.

Waldron P & Herbert DM. (1992) "Wave induced stresses in hollow cube armour units" Coastal Structures and Breakwaters, pp285-303, Thomas Telford, London.

Walkden M.J.A., Crawford A.R., Bullock G.N., Hewson P.J. & Bird P.A.D. "Wave impact loading on vertical structures" Conference of Institution of Civil Engineers on coastal structures and breakwaters '95, ICE, London.

Xie S.L. (1994) "Recent research and experience on vertical and composite breakwaters in China" Proceedings of Workshop on Wave Barriers in Deep Waters, pp129-153, Port and Harbour Research Institute, Yokosuka, Japan.

Appendix

Summary of test conditions, structural configurations and results

Str.	Test No.	hs	hb	d	hc	hcals	hf	Rc	Bb	Bt	Beq	α	Hso	Hsi	Tmo	Tmi	Tpi	smo	smi	smp	Lmo	Lmi	Lpi	Bb/Lpi	Beq/Lpi	Hsi/hs	Hsi/d	hb/hs	Pi (%)	Fh1/250(st.)
0	20001	0.340	0.000	0.340	-	0.691	0.803	0.463	0.000	0.000	0.00	0.0	0.20	0.16	1.79	1.70	1.95	0.04	0.05	0.05	5.00	3.04	3.35	0.00	0.00	0.47	0.47	0.00	8.60	1.678
0	20002	0.340	0.000	0.340	-	0.691	0.803	0.463	0.000	0.000	0.00	0.0	0.20	0.15	1.46	1.59	1.83	0.06	0.06	0.05	3.33	2.38	3.11	0.00	0.00	0.44	0.44	0.00	7.00	0.981
0	20003	0.340	0.000	0.340	-	0.691	0.803	0.463	0.000	0.000	0.00	0.0	0.25	0.18	2.00	1.98	2.28	0.04	0.05	0.05	6.25	3.44	3.97	0.00	0.00	0.53	0.53	0.00	7.00	2.813
0	20004	0.340	0.000	0.340	-	0.691	0.803	0.463	0.000	0.000	0.00	0.0	0.25	0.17	1.63	1.76	2.02	0.06	0.06	0.05	4.15	2.72	3.49	0.00	0.00	0.50	0.50	0.00	8.55	2.167
0	20005	0.340	0.000	0.340	-	0.691	0.803	0.463	0.000	0.000	0.00	0.0	0.30	0.20	2.19	2.20	2.53	0.04	0.05	0.04	7.49	3.81	4.45	0.00	0.00	0.59	0.59	0.00	5.00	2.967
0	20006	0.340	0.000	0.340	-	0.691	0.803	0.463	0.000	0.000	0.00	0.0	0.30	0.18	1.79	1.90	2.18	0.06	0.06	0.05	5.00	3.04	3.80	0.00	0.00	0.53	0.53	0.00	7.00	1.859
0	20100	0.430	0.000	0.430	-	0.691	0.803	0.373	0.000	0.000	0.00	0.0	0.10	0.08	1.79	1.70	1.95	0.02	0.02	0.02	5.00	3.34	3.71	0.00	0.00	0.19	0.19	0.00	0.00	0.414
0	20102	0.430	0.000	0.430	-	0.691	0.803	0.373	0.000	0.000	0.00	0.0	0.20	0.19	2.53	2.50	2.87	0.02	0.04	0.03	9.99	4.96	5.70	0.00	0.00	0.44	0.44	0.00	0.40	3.091
0	20103	0.430	0.000	0.430	-	0.691	0.803	0.373	0.000	0.000	0.00	0.0	0.20	0.16	1.79	1.70	1.95	0.04	0.05	0.04	5.00	3.34	3.71	0.00	0.00	0.37	0.37	0.00	2.00	1.420
0	20104	0.430	0.000	0.430	-	0.691	0.803	0.373	0.000	0.000	0.00	0.0	0.20	0.14	1.46	1.50	1.72	0.06	0.05	0.04	3.33	2.59	3.20	0.00	0.00	0.33	0.33	0.00	1.00	1.252
0	20105	0.430	0.000	0.430	-	0.691	0.803	0.373	0.000	0.000	0.00	0.0	0.25	0.20	2.00	1.90	2.18	0.04	0.05	0.05	6.25	3.81	4.21	0.00	0.00	0.47	0.47	0.00	8.50	3.233
0	20106	0.430	0.000	0.430	-	0.691	0.803	0.373	0.000	0.000	0.00	0.0	0.25	0.18	1.63	1.70	1.95	0.06	0.06	0.05	4.17	2.99	3.71	0.00	0.00	0.42	0.42	0.00	5.00	2.021
0	20200	0.610	0.000	0.610	-	0.691	0.803	0.193	0.000	0.000	0.00	0.0	0.10	0.07	1.79	1.6	1.84	0.02	0.02	0.02	5.00	3.82	3.95	0.00	0.00	0.11	0.11	0.00	0.00	1.452
0	20201	0.610	0.000	0.610	-	0.691	0.803	0.193	0.000	0.000	0.00	0.0	0.10	0.08	1.27	1.2	1.38	0.04	0.03	0.03	2.52	2.34	2.66	0.00	0.00	0.13	0.13	0.00	0.00	0.401
0	20203	0.610	0.000	0.610	-	0.691	0.803	0.193	0.000	0.000	0.00	0.0	0.20	0.15	1.79	1.6	1.84	0.04	0.04	0.04	5.00	3.82	3.95	0.00	0.00	0.25	0.25	0.00	0.00	1.081
0	20204	0.610	0.000	0.610	-	0.691	0.803	0.193	0.000	0.000	0.00	0.0	0.20	0.15	1.46	1.4	1.61	0.06	0.05	0.05	3.33	2.89	3.31	0.00	0.00	0.25	0.25	0.00	0.00	0.888
0	20205	0.610	0.000	0.610	-	0.691	0.803	0.193	0.000	0.000	0.00	0.0	0.25	0.19	2.00	1.9	2.18	0.04	0.04	0.04	6.25	4.39	4.88	0.00	0.00	0.31	0.31	0.00	0.00	1.591
0	20206	0.610	0.000	0.610	-	0.691	0.803	0.193	0.000	0.000	0.00	0.0	0.25	0.18	1.63	1.6	1.84	0.06	0.05	0.05	4.15	3.37	3.95	0.00	0.00	0.30	0.30	0.00	0.00	1.264
0	20207	0.610	0.000	0.610	-	0.691	0.803	0.193	0.000	0.000	0.00	0.0	0.30	0.26	2.19	2.10	2.41	0.04	0.05	0.05	7.49	4.90	5.49	0.00	0.00	0.43	0.43	0.00	0.00	2.795
0	20208	0.610	0.000	0.610	-	0.691	0.803	0.193	0.000	0.000	0.00	0.0	0.30	0.23	1.79	1.80	2.07	0.06	0.06	0.05	5.00	3.82	4.58	0.00	0.00	0.38	0.38	0.00	2.00	1.909
0	20209	0.610	0.000	0.610	-	0.691	0.803	0.193	0.000	0.000	0.00	0.0	0.35	0.26	1.93	2	2.30	0.06	0.06	0.05	5.82	4.20	5.19	0.00	0.00	0.43	0.43	0.00	1.00	2.653
0	20300	0.700	0.000	0.700	-	0.691	0.803	0.103	0.000	0.000	0.00	0.0	0.10	0.07	1.79	1.6	1.84	0.02	0.02	0.02	5.00	4.00	4.15	0.00	0.00	0.10	0.10	0.00	0.00	0.578
0	20301	0.700	0.000	0.700	-	0.691	0.803	0.103	0.000	0.000	0.00	0.0	0.10	0.08	1.27	1.20	1.38	0.04	0.03	0.03	2.52	2.39	2.74	0.00	0.00	0.11	0.11	0.00	0.00	0.412
0	20302	0.700	0.000	0.700	-	0.691	0.803	0.103	0.000	0.000	0.00	0.0	0.20	0.15	2.53	2.40	2.76	0.02	0.02	0.02	9.99	6.14	6.78	0.00	0.00	0.21	0.21	0.00	0.00	1.250
0	20303	0.700	0.000	0.700	-	0.691	0.803	0.103	0.000	0.000	0.00	0.0	0.20	0.15	1.79	1.60	1.84	0.04	0.04	0.04	5.00	4.00	4.15	0.00	0.00	0.21	0.21	0.00	0.00	1.001
0	20304	0.700	0.000	0.700	-	0.691	0.803	0.103	0.000	0.000	0.00	0.0	0.20	0.15	1.46	1.40	1.61	0.06	0.05	0.04	3.33	2.99	3.46	0.00	0.00	0.21	0.21	0.00	0.00	0.773
0	20305	0.700	0.000	0.700	-	0.691	0.803	0.103	0.000	0.000	0.00	0.0	0.25	0.20	2.00	1.80	2.07	0.04	0.04	0.04	6.25	4.62	4.82	0.00	0.00	0.29	0.29	0.00	0.00	1.664
0	20306	0.700	0.000	0.700	-	0.691	0.803	0.103	0.000	0.000	0.00	0.0	0.25	0.19	1.63	1.60	1.84	0.06	0.05	0.05	4.15	3.52	4.15	0.00	0.00	0.27	0.27	0.00	0.60	1.289
0	20307	0.700	0.000	0.700	-	0.691	0.803	0.103	0.000	0.000	0.00	0.0	0.30	0.23	2.19	2.00	2.30	0.04	0.04	0.04	7.49	5.17	5.49	0.00	0.00	0.33	0.33	0.00	0.00	1.597
0	20308	0.700	0.000	0.700	-	0.691	0.803	0.103	0.000	0.000	0.00	0.0	0.30	0.23	1.79	1.8	2.07	0.06	0.06	0.05	5.00	4.00	4.82	0.00	0.00	0.33	0.33	0.00	0.00	1.454
0	20400	0.520	0.000	0.520	-	0.691	0.803	0.283	0.000	0.000	0.00	0.0	0.10	0.07	1.79	1.6	1.84	0.02	0.02	0.02	5.00	3.60	3.72	0.00	0.00	0.13	0.13	0.00	0.00	0.508
0	20401	0.520	0.000	0.520	-	0.691	0.803	0.283	0.000	0.000	0.00	0.0	0.10	0.08	1.27	1.2	1.38	0.04	0.04	0.03	2.52	2.26	2.55	0.00	0.00	0.15	0.15	0.00	0.00	0.376
0	20402	0.520	0.000	0.520	-	0.691	0.803	0.283	0.000	0.000	0.00	0.0	0.20	0.17	2.53	2.4	2.76	0.02	0.03	0.03	9.99	5.40	5.94	0.00	0.00	0.33	0.33	0.00	0.00	1.891
0	20403	0.520	0.000	0.520	-	0.691	0.803	0.283	0.000	0.000	0.00	0.0	0.20	0.15	1.79	1.60	1.84	0.04	0.04	0.04	5.00	3.60	3.72	0.00	0.00	0.29	0.29	0.00	0.00	1.028
0	20404	0.520	0.000	0.520	-	0.691	0.803	0.283	0.000	0.000	0.00	0.0	0.20	0.14	1.27	1.5	1.72	0.06	0.06	0.04	2.52	2.26	3.44	0.00	0.00	0.27	0.27	0.00	0.00	0.928
0	20405	0.520	0.000	0.520	-	0.691	0.803	0.283	0.000	0.000	0.00	0.0	0.25	0.20	2.00	1.90	2.18	0.04	0.05	0.04	6.25	4.12	4.57	0.00	0.00	0.38	0.38	0.00	4.00	2.260
0	20406	0.520	0.000	0.520	-	0.691	0.803	0.283	0.000	0.000	0.00	0.0	0.25	0.18	1.63	1.7	1.95	0.06	0.06	0.04	4.15	3.20	4.01	0.00	0.00	0.35	0.35	0.00	0.00	1.383
1	10003	0.340	0.187	0.153	0.112	0.691	0.616	0.463	0.250	0.624	0.44	2.0	0.20	0.16	1.79	1.7	1.95	0.04	0.05	0.05	5.00	3.03	3.35	0.07	0.13	0.47	1.05	0.55	26.00	4.96393
1	10004	0.340	0.187	0.153	0.112	0.691	0.616	0.463	0.250	0.624	0.44	2.0	0.20	0.15	1.46	1.6	1.83	0.06	0.06	0.05	3.33	2.38	3.11	0.08	0.14	0.44	0.98	0.55	51.00	4.07307
1	10005	0.340	0.187	0.153	0.112	0.691	0.616	0.463	0.250	0.624	0.44	2.0	0.25	0.18	2.00	2.0	2.28	0.04	0.05	0.05	6.25	3.45	3.97	0.06	0.11	0.53	1.18	0.55	64.00	5.71696
1	10006	0.340	0.187	0.153	0.112	0.691	0.616	0.463	0.250	0.624	0.44	2.0	0.25	0.17	1.63	1.8	2.02	0.06	0.06	0.05	4.17	2.73	3.49	0.07	0.13	0.50	1.11	0.55	44.00	6.2036
1	10007	0.340	0.187	0.153	0.112	0.691	0.616	0.463	0.250	0.624	0.44	2.0	0.30	0.20	2.19	2.2	2.52	0.04	0.05	0.05	7.50	3.81	4.43	0.06	0.10	0.59	1.31	0.55	26.00	5.29671
1	10008	0.340	0.187	0.153	0.112	0.691	0.616	0.463	0.250	0.624	0.44	2.0	0.30	0.18	1.79	1.9	2.18	0.06	0.06	0.05	5.00	3.03	3.80	0.07	0.12	0.53	1.18	0.55	26.00	5.66992
1	10009	0.430	0.187	0.243	0.112	0.691	0.616	0.373	0.250	0.624	0.44	2.0	0.20	0.19	2.53	2.5	2.87	0.02	0.04	0.03	10.00	4.96	5.70	0.04	0.08	0.44	0.78	0.43	5.00	5.45858
1	10010	0.430	0.187	0.243	0.112	0.691	0.616	0.373	0.250	0.624	0.44	2.0	0.20	0.16	1.79	1.7	1.95	0.04	0.05	0.04	5.00	3.34	3.71	0.07	0.12	0.37	0.66	0.43	5.00	1.64023
1	10011	0.430	0.187	0.243	0.112	0.691	0.616	0.373	0.250	0.624	0.44	2.0	0.20	0.14	1.46	1.5	1.72	0.06	0.05	0.04	3.33	2.59	3.20	0.08	0.14	0.33	0.58	0.43	5.00	1.58091
1	10012	0.430	0.187	0.243	0.112	0.691	0.616	0.373	0.250	0.624	0.44	2.0	0.25	0.20	2.00	1.9	2.18	0.04	0.05	0.05	6.25	3.81	4.21	0.06	0.10	0.47	0.82	0.43	11.00	3.66387
1	10013	0.430	0.187	0.243	0.112	0.691	0.616	0.373	0.250	0.624	0.44	2.0	0.25	0.18	1.63	1.7	1.95	0.06	0.06	0.05	4.17	2.99	3.71	0.07	0.12	0.42	0.74	0.43	10.00	4.9028
1	10014	0.520	0.187	0.333	0.112	0.691	0.616	0.283	0.250	0.624	0.44	2.0	0.20	0.17	2.53	2.4	2.76	0.02	0.03	0.03	10.00	5.40	5.94	0.04	0.07	0.33	0.51	0.36	0.00	2.53642
1	10015	0.520	0.187	0.333	0.112	0.691	0.616	0.283	0.250	0.624	0.44	2.0	0.20	0.15	1.79	1.6	1.84	0.04	0.04	0.04	5.00	3.60	3.72	0.07	0.12	0.29	0.45	0.36	0.00	1.25408

Str.	Test No.	hs	hb	d	hc	hcais	hf	Rc	Bb	Bt	Beq	α	Hso	Hsi	Tmo	Tmi	Tpi	smo	smi	smp	Lmo	Lmi	Lpi	Bb/Lpi	Beq/Lpi	Hsi/hs	Hsi/d	hb/hs	Pi (%)	Fh1/250(st.)
1	10016	0.520	0.187	0.333	0.112	0.691	0.616	0.283	0.250	0.624	0.44	2.0	0.25	0.20	2.00	1.9	2.18	0.04	0.05	0.04	6.25	4.12	4.57	0.05	0.10	0.38	0.60	0.36	2.00	3.25774
1	10017	0.430	0.187	0.243	0.112	0.691	0.616	0.373	0.250	0.624	0.44	2.0	0.10	0.08	1.79	1.7	1.95	0.02	0.02	0.02	5.00	3.34	3.71	0.07	0.12	0.18	0.31	0.43	0.00	0.442765
1	10018	0.430	0.187	0.243	0.112	0.691	0.616	0.373	0.250	0.624	0.44	2.0	0.10	0.08	1.27	1.2	1.38	0.04	0.04	0.03	2.50	2.13	2.40	0.10	0.18	0.18	0.31	0.43	0.00	0.413415
2	10019	0.340	0.367	-0.027	0.112	0.691	0.436	0.463	0.250	0.984	0.62	2.0	0.20	0.16	1.79	1.70	1.95	0.04	0.05	0.05	5.00	3.03	3.35	0.07	0.18	0.47	-5.93	1.08	11.00	2.66636
2	10020	0.340	0.367	-0.027	0.112	0.691	0.436	0.463	0.250	0.984	0.62	2.0	0.25	0.18	2.00	1.98	2.28	0.04	0.05	0.05	6.25	3.45	3.97	0.06	0.16	0.53	-6.67	1.08	4.00	5.36281
2	10021	0.340	0.367	-0.027	0.112	0.691	0.436	0.463	0.250	0.984	0.62	2.0	0.20	0.15	1.46	1.59	1.83	0.06	0.06	0.05	3.33	2.38	3.11	0.08	0.20	0.44	-5.56	1.08	2.00	1.30282
2	10022	0.340	0.367	-0.027	0.112	0.691	0.436	0.463	0.250	0.984	0.62	2.0	0.25	0.17	1.63	1.76	2.02	0.06	0.06	0.05	4.17	2.73	3.49	0.07	0.18	0.50	-6.30	1.08	6.00	2.85785
2	10024	0.430	0.367	0.063	0.112	0.691	0.436	0.373	0.250	0.984	0.62	2.0	0.20	0.19	2.53	2.50	2.87	0.02	0.04	0.03	10.00	4.96	5.70	0.04	0.11	0.44	3.02	0.85	6.00	4.62849
2	10025	0.430	0.367	0.063	0.112	0.691	0.436	0.373	0.250	0.984	0.62	2.0	0.20	0.16	1.79	1.70	1.95	0.04	0.05	0.04	5.00	3.34	3.71	0.07	0.17	0.37	2.54	0.85	12.00	2.55273
2	10026	0.430	0.367	0.063	0.112	0.691	0.436	0.373	0.250	0.984	0.62	2.0	0.20	0.14	1.46	1.50	1.72	0.06	0.05	0.04	3.33	2.59	3.20	0.08	0.19	0.33	2.22	0.85	26.00	3.26294
2	10027	0.430	0.367	0.063	0.112	0.691	0.436	0.373	0.250	0.984	0.62	2.0	0.25	0.2	2.00	1.90	2.18	0.04	0.05	0.05	6.25	3.81	4.21	0.06	0.15	0.47	3.17	0.85	24.00	4.34904
2	10028	0.520	0.367	0.153	0.112	0.691	0.436	0.283	0.250	0.984	0.62	2.0	0.10	0.08	1.27	1.20	1.38	0.04	0.04	0.03	2.50	2.24	2.55	0.10	0.24	0.16	0.54	0.71	2.00	0.561175
2	10029	0.520	0.367	0.153	0.112	0.691	0.436	0.283	0.250	0.984	0.62	2.0	0.20	0.17	2.53	2.40	2.76	0.02	0.03	0.03	10.00	5.40	5.94	0.04	0.10	0.33	1.11	0.71	2.50	2.24552
2	10030	0.520	0.367	0.153	0.112	0.691	0.436	0.283	0.250	0.984	0.62	2.0	0.20	0.15	1.79	1.60	1.84	0.04	0.04	0.04	5.00	3.60	3.72	0.07	0.17	0.29	0.98	0.71	10.00	3.43767
2	10031	0.520	0.367	0.153	0.112	0.691	0.436	0.283	0.250	0.984	0.62	2.0	0.20	0.14	1.46	1.50	1.72	0.06	0.05	0.04	3.33	2.76	3.44	0.07	0.18	0.27	0.92	0.71	24.00	4.09518
2	10032	0.520	0.367	0.153	0.112	0.691	0.436	0.283	0.250	0.984	0.62	2.0	0.25	0.20	2.00	1.90	2.18	0.04	0.05	0.04	6.25	4.12	4.57	0.05	0.14	0.38	1.31	0.71	9.00	6.34245
2	10033	0.610	0.367	0.243	0.112	0.691	0.436	0.193	0.250	0.984	0.62	2.0	0.10	0.08	1.27	1.20	1.38	0.04	0.04	0.03	2.50	2.32	2.66	0.09	0.23	0.14	0.34	0.60	0.00	0.468435
2	10034	0.610	0.367	0.243	0.112	0.691	0.436	0.193	0.250	0.984	0.62	2.0	0.20	0.15	2.53	2.30	2.64	0.02	0.03	0.02	10.00	5.79	6.09	0.04	0.10	0.25	0.62	0.60	0.00	1.63816
2	10035	0.610	0.367	0.243	0.112	0.691	0.436	0.193	0.250	0.984	0.62	2.0	0.20	0.15	1.79	1.60	1.84	0.04	0.04	0.04	5.00	3.82	3.95	0.06	0.16	0.25	0.62	0.60	0.90	1.64311
2	10036	0.610	0.367	0.243	0.112	0.691	0.436	0.193	0.250	0.984	0.62	2.0	0.20	0.15	1.46	1.40	1.61	0.06	0.05	0.05	3.33	2.89	3.31	0.08	0.19	0.25	0.62	0.60	4.00	1.64091
2	10037	0.610	0.367	0.243	0.112	0.691	0.436	0.193	0.250	0.984	0.62	2.0	0.25	0.19	2.00	1.90	2.18	0.04	0.04	0.04	6.25	4.39	4.88	0.05	0.13	0.31	0.78	0.60	7.50	3.64128
2	10038	0.700	0.367	0.333	0.112	0.691	0.436	0.103	0.250	0.984	0.62	2.0	0.10	0.08	1.27	1.20	1.38	0.04	0.03	0.03	2.50	2.38	2.74	0.09	0.23	0.11	0.24	0.52	0.00	0.454175
2	10039	0.700	0.367	0.333	0.112	0.691	0.436	0.103	0.250	0.984	0.62	2.0	0.20	0.15	2.53	2.40	2.76	0.02	0.02	0.02	10.00	6.14	6.78	0.04	0.09	0.21	0.45	0.52	0.00	1.30008
2	10040	0.700	0.367	0.333	0.112	0.691	0.436	0.103	0.250	0.984	0.62	2.0	0.20	0.15	1.79	1.60	1.84	0.04	0.04	0.04	5.00	4.00	4.15	0.06	0.15	0.21	0.45	0.52	0.40	1.27972
2	10041	0.700	0.367	0.333	0.112	0.691	0.436	0.103	0.250	0.984	0.62	2.0	0.20	0.15	1.46	1.40	1.61	0.06	0.05	0.04	3.33	3.00	3.46	0.07	0.18	0.21	0.45	0.52	0.00	1.23873
2	10042	0.700	0.367	0.333	0.112	0.691	0.436	0.103	0.250	0.984	0.62	2.0	0.25	0.20	2.00	1.80	2.07	0.04	0.04	0.04	6.25	4.63	4.82	0.05	0.13	0.29	0.60	0.52	0.00	2.17053
3	10043	0.340	0.367	-0.027	0.202	0.691	0.526	0.553	0.250	0.984	0.62	2.0	0.20	0.16	1.79	1.70	1.95	0.04	0.05	0.05	5.00	3.03	3.35	0.07	0.18	0.47	-5.93	1.08	3.00	4.85781
3	10044	0.340	0.367	-0.027	0.202	0.691	0.526	0.553	0.250	0.984	0.62	2.0	0.25	0.18	2.00	1.98	2.28	0.04	0.05	0.05	6.25	3.45	3.97	0.06	0.16	0.53	-6.67	1.08	9.00	5.35173
3	10045	0.340	0.367	-0.027	0.202	0.691	0.526	0.553	0.250	0.984	0.62	2.0	0.20	0.15	1.46	1.59	1.83	0.06	0.06	0.05	3.33	2.38	3.11	0.08	0.20	0.44	-5.56	1.08	2.00	2.52797
3	10046	0.340	0.367	-0.027	0.202	0.691	0.526	0.553	0.250	0.984	0.62	2.0	0.25	0.17	2.00	1.76	2.02	0.04	0.05	0.05	6.25	3.45	3.49	0.07	0.18	0.50	-6.30	1.08	4.00	3.4563
3	10047	0.430	0.367	0.063	0.202	0.691	0.526	0.463	0.250	0.984	0.62	2.0	0.10	0.08	1.27	1.20	1.38	0.04	0.04	0.03	2.50	2.13	2.40	0.10	0.26	0.19	1.27	0.85	10.00	0.699575
3	10048	0.430	0.367	0.063	0.202	0.691	0.526	0.463	0.250	0.984	0.62	2.0	0.20	0.19	2.53	2.50	2.87	0.02	0.04	0.03	10.00	4.96	5.70	0.04	0.11	0.44	3.02	0.85	11.00	5.57761
3	10049	0.430	0.367	0.063	0.202	0.691	0.526	0.463	0.250	0.984	0.62	2.0	0.20	0.16	1.79	1.70	1.95	0.04	0.05	0.04	5.00	3.34	3.71	0.07	0.17	0.37	2.54	0.85	48.00	4.91693
3	10050	0.430	0.367	0.063	0.202	0.691	0.526	0.463	0.250	0.984	0.62	2.0	0.20	0.14	1.46	1.50	1.72	0.06	0.05	0.04	3.33	2.59	3.20	0.08	0.19	0.33	2.22	0.85	29.50	4.26068
3	10051	0.430	0.367	0.063	0.202	0.691	0.526	0.463	0.250	0.984	0.62	2.0	0.25	0.2	2.00	1.90	2.18	0.04	0.05	0.05	6.25	3.81	4.21	0.06	0.15	0.47	3.17	0.85	33.00	5.95371
3	10052	0.520	0.367	0.153	0.202	0.691	0.526	0.373	0.250	0.984	0.62	2.0	0.10	0.08	1.27	1.20	1.38	0.04	0.04	0.03	2.50	2.24	2.55	0.10	0.24	0.16	0.54	0.71	0.00	0.37737
3	10053	0.520	0.367	0.153	0.202	0.691	0.526	0.373	0.250	0.984	0.62	2.0	0.20	0.17	2.53	2.40	2.76	0.02	0.03	0.03	10.00	5.40	5.94	0.04	0.10	0.33	1.11	0.71	0.00	1.88558
3	10054	0.520	0.367	0.153	0.202	0.691	0.526	0.373	0.250	0.984	0.62	2.0	0.20	0.15	1.79	1.70	1.95	0.04	0.04	0.04	5.00	3.60	4.01	0.06	0.15	0.29	0.98	0.71	5.50	3.41507
3	10055	0.520	0.367	0.153	0.202	0.691	0.526	0.373	0.250	0.984	0.62	2.0	0.20	0.14	1.46	1.50	1.72	0.06	0.05	0.04	3.33	2.76	3.44	0.07	0.18	0.27	0.92	0.71	13.00	2.58232
3	10056	0.520	0.367	0.153	0.202	0.691	0.526	0.373	0.250	0.984	0.62	2.0	0.25	0.20	2.00	1.90	2.18	0.04	0.05	0.04	6.25	4.12	4.57	0.05	0.14	0.38	1.31	0.71	12.00	7.33561
3	10057	0.610	0.367	0.243	0.202	0.691	0.526	0.283	0.250	0.984	0.62	2.0	0.10	0.08	1.27	1.20	1.38	0.04	0.04	0.03	2.50	2.32	2.66	0.09	0.23	0.14	0.34	0.60	0.00	0.407895
3	10058	0.610	0.367	0.243	0.202	0.691	0.526	0.283	0.250	0.984	0.62	2.0	0.20	0.15	2.53	2.30	2.64	0.02	0.03	0.02	10.00	5.79	6.09	0.04	0.10	0.25	0.62	0.60	0.00	1.48845
3	10059	0.610	0.367	0.243	0.202	0.691	0.526	0.283	0.250	0.984	0.62	2.0	0.20	0.15	1.79	1.60	1.84	0.04	0.04	0.04	5.00	3.82	3.95	0.06	0.16	0.25	0.62	0.60	0.40	1.38961
3	10060	0.610	0.367	0.243	0.202	0.691	0.526	0.283	0.250	0.984	0.62	2.0	0.20	0.15	1.46	1.40	1.61	0.06	0.05	0.05	3.33	2.89	3.31	0.08	0.19	0.25	0.62	0.60	2.00	1.40749
3	10061	0.610	0.367	0.243	0.202	0.691	0.526	0.283	0.250	0.984	0.62	2.0	0.25	0.19	2.00	1.90	2.18	0.04	0.04	0.04	6.25	4.39	4.88	0.05	0.13	0.31	0.78	0.60	0.00	1.79136
3	10062	0.700	0.367	0.333	0.202	0.691	0.526	0.193	0.250	0.984	0.62	2.0	0.10	0.08	1.27	1.20	1.38	0.04	0.03	0.03	2.50	2.38	2.74	0.09	0.23	0.11	0.24	0.52	0.00	0.853495
3	10063	0.700	0.367	0.333	0.202	0.691	0.526	0.193	0.250	0.984	0.62	2.0	0.20	0.15	2.53	2.40	2.76	0.02	0.02	0.02	10.00	6.14	6.78	0.04	0.09	0.21	0.45	0.52	0.00	1.27301
3	10064	0.700	0.367	0.333	0.202	0.691	0.526	0.193	0.250	0.984	0.62	2.0	0.20	0.15	1.79	1.60	1.84	0.04	0.04	0.04	5.00	4.00	4.15	0.06	0.15	0.21	0.45	0.52	1.00	1.35203
3	10065	0.700	0.367	0.333	0.202	0.691	0.526	0.193	0.250	0.984	0.62	2.0	0.20	0.15	1.46	1.40	1.61	0.06	0.05	0.04	3.33	3.00	3.46	0.07	0.18	0.21	0.45	0.52	0.00	1.2811
3	10066	0.700	0.367	0.333	0.202	0.691	0.526	0.193	0.250	0.984	0.62	2.0	0.25	0.20	2.00	1.80	2.07	0.04	0.04	0.04	6.25	4.63	4.82	0.05	0.13	0.29	0.60	0.52	0.00	2.25873

Str.	Test No.	hs	hb	d	hc	hcals	hf	Rc	Bb	Bt	Beq	α	Hso	Hsi	Tmo	Tmi	Tpi	smo	smi	smp	Lmo	Lmi	Lpi	Bb/Lpi	Beq/Lpi	Hsi/hs	Hsi/d	hb/hs	Pi (%)	Fh1/250(st.)
4	10067	0.520	0.367	0.153	0.202	0.691	0.526	0.373	0.250	1.351	0.80	3.0	0.10	0.08	1.27	1.20	1.38	0.04	0.04	0.03	2.50	2.24	2.55	0.10	0.31	0.16	0.54	0.71	4.00	0.42714
4	10068	0.520	0.367	0.153	0.202	0.691	0.526	0.373	0.250	1.351	0.80	3.0	0.20	0.17	2.53	2.40	2.76	0.02	0.03	0.03	10.00	5.40	5.94	0.04	0.13	0.33	1.11	0.71	13.00	3.12482
4	10069	0.520	0.367	0.153	0.202	0.691	0.526	0.373	0.250	1.351	0.80	3.0	0.20	0.15	1.79	1.60	1.84	0.04	0.04	0.04	5.00	3.60	3.72	0.07	0.21	0.29	0.98	0.71	29.00	7.25832
4	10070	0.520	0.367	0.153	0.202	0.691	0.526	0.373	0.250	1.351	0.80	3.0	0.20	0.14	1.46	1.50	1.72	0.06	0.05	0.04	3.33	2.76	3.44	0.07	0.23	0.27	0.92	0.71	19.00	3.3294
4	10071	0.520	0.367	0.153	0.202	0.691	0.526	0.373	0.250	1.351	0.80	3.0	0.25	0.20	2.00	1.90	2.18	0.04	0.05	0.04	6.25	4.12	4.57	0.05	0.18	0.38	1.31	0.71	26.00	9.60443
4	10072	0.610	0.367	0.243	0.202	0.691	0.526	0.283	0.250	1.351	0.80	3.0	0.10	0.08	1.27	1.20	1.38	0.04	0.04	0.03	2.50	2.32	2.66	0.09	0.30	0.14	0.34	0.60	0.00	0.41868
4	10073	0.610	0.367	0.243	0.202	0.691	0.526	0.283	0.250	1.351	0.80	3.0	0.20	0.15	2.53	2.30	2.64	0.02	0.03	0.02	10.00	5.79	6.09	0.04	0.13	0.25	0.62	0.60	0.00	1.65524
4	10074	0.610	0.367	0.243	0.202	0.691	0.526	0.283	0.250	1.351	0.80	3.0	0.20	0.15	1.79	1.60	1.84	0.04	0.04	0.04	5.00	3.82	3.95	0.06	0.20	0.25	0.62	0.60	16.00	1.73487
4	10075	0.610	0.367	0.243	0.202	0.691	0.526	0.283	0.250	1.351	0.80	3.0	0.20	0.15	1.46	1.40	1.61	0.06	0.05	0.05	3.33	2.89	3.31	0.08	0.24	0.25	0.62	0.60	2.00	1.84799
4	10076	0.610	0.367	0.243	0.202	0.691	0.526	0.283	0.250	1.351	0.80	3.0	0.25	0.19	2.00	1.90	2.18	0.04	0.04	0.04	6.25	4.39	4.88	0.05	0.16	0.31	0.78	0.60	9.00	3.36402
5	10077	0.520	0.367	0.153	0.202	0.691	0.526	0.373	0.250	0.801	0.53	1.5	0.10	0.08	1.27	1.20	1.38	0.04	0.04	0.03	2.50	2.24	2.55	0.10	0.21	0.16	0.54	0.71	0.00	0.42565
5	10078	0.520	0.367	0.153	0.202	0.691	0.526	0.373	0.250	0.801	0.53	1.5	0.20	0.17	2.53	2.40	2.76	0.02	0.03	0.03	10.00	5.40	5.94	0.04	0.09	0.33	1.11	0.71	0.00	1.13273
5	10079	0.520	0.367	0.153	0.202	0.691	0.526	0.373	0.250	0.801	0.53	1.5	0.20	0.15	1.79	1.60	1.84	0.04	0.04	0.04	5.00	3.60	3.72	0.07	0.14	0.29	0.98	0.71	0.00	1.50765
5	10080	0.520	0.367	0.153	0.202	0.691	0.526	0.373	0.250	0.801	0.53	1.5	0.20	0.14	1.46	1.50	1.72	0.06	0.05	0.04	3.33	2.76	3.44	0.07	0.15	0.27	0.92	0.71	8.00	1.55965
5	10081	0.520	0.367	0.153	0.202	0.691	0.526	0.373	0.250	0.801	0.53	1.5	0.25	0.20	2.00	1.90	2.18	0.04	0.05	0.04	6.25	4.12	4.57	0.05	0.11	0.38	1.31	0.71	6.60	3.64933
5	10082	0.610	0.367	0.243	0.202	0.691	0.526	0.283	0.250	0.801	0.53	1.5	0.10	0.08	1.27	1.20	1.38	0.04	0.04	0.03	2.50	2.32	2.66	0.09	0.20	0.14	0.34	0.60	0.00	0.41084
5	10083	0.610	0.367	0.243	0.202	0.691	0.526	0.283	0.250	0.801	0.53	1.5	0.20	0.15	2.53	2.30	2.64	0.02	0.03	0.02	10.00	5.79	6.09	0.04	0.09	0.25	0.62	0.60	0.00	1.46282
5	10084	0.610	0.367	0.243	0.202	0.691	0.526	0.283	0.250	0.801	0.53	1.5	0.20	0.15	1.79	1.60	1.84	0.04	0.04	0.04	5.00	3.82	3.95	0.06	0.13	0.25	0.62	0.60	0.00	1.09035
5	10085	0.610	0.367	0.243	0.202	0.691	0.526	0.283	0.250	0.801	0.53	1.5	0.20	0.15	1.46	1.40	1.61	0.06	0.05	0.05	3.33	2.89	3.31	0.08	0.16	0.25	0.62	0.60	0.60	1.3028
5	10086	0.610	0.367	0.243	0.202	0.691	0.526	0.283	0.250	0.801	0.53	1.5	0.25	0.19	2.00	1.90	2.18	0.04	0.04	0.04	6.25	4.39	4.88	0.05	0.11	0.31	0.78	0.60	0.90	1.75991
6	10087	0.430	0.367	0.063	0.202	0.691	0.526	0.463	0.375	1.109	0.74	2.0	0.10	0.08	1.27	1.20	1.38	0.04	0.04	0.03	2.50	2.13	2.40	0.16	0.31	0.19	1.27	0.85	26.00	2.98383
6	10088	0.430	0.367	0.063	0.202	0.691	0.526	0.463	0.375	1.109	0.74	2.0	0.20	0.19	2.53	2.50	2.87	0.02	0.04	0.03	10.00	4.96	5.70	0.07	0.13	0.44	3.02	0.85	6.50	7.69626
6	10089	0.430	0.367	0.063	0.202	0.691	0.526	0.463	0.375	1.109	0.74	2.0	0.20	0.16	1.79	1.70	1.95	0.04	0.05	0.04	5.00	3.34	3.71	0.10	0.20	0.37	2.54	0.85	18.00	4.96482
6	10090	0.430	0.367	0.063	0.202	0.691	0.526	0.463	0.375	1.109	0.74	2.0	0.20	0.14	1.46	1.50	1.72	0.06	0.05	0.04	3.33	2.59	3.20	0.12	0.23	0.33	2.22	0.85	65.00	3.85405
6	10091	0.430	0.367	0.063	0.202	0.691	0.526	0.463	0.375	1.109	0.74	2.0	0.25	0.2	2.00	1.90	2.18	0.04	0.05	0.05	6.25	3.81	4.21	0.09	0.18	0.47	3.17	0.85	25.00	6.0763
6	10092	0.520	0.367	0.153	0.202	0.691	0.526	0.373	0.375	1.109	0.74	2.0	0.10	0.08	1.27	1.20	1.38	0.04	0.04	0.03	2.50	2.24	2.55	0.15	0.29	0.16	0.54	0.71	0.00	0.399305
6	10093	0.520	0.367	0.153	0.202	0.691	0.526	0.373	0.375	1.109	0.74	2.0	0.20	0.17	2.53	2.40	2.76	0.02	0.03	0.03	10.00	5.40	5.94	0.06	0.12	0.33	1.11	0.71	0.40	2.20601
6	10094	0.520	0.367	0.153	0.202	0.691	0.526	0.373	0.375	1.109	0.74	2.0	0.20	0.15	1.79	1.60	1.84	0.04	0.04	0.04	5.00	3.60	3.72	0.10	0.20	0.29	0.98	0.71	16.00	3.67254
6	10095	0.520	0.367	0.153	0.202	0.691	0.526	0.373	0.375	1.109	0.74	2.0	0.20	0.14	1.46	1.50	1.72	0.06	0.05	0.04	3.33	2.76	3.44	0.11	0.22	0.27	0.92	0.71	16.00	3.79742
6	10096	0.520	0.367	0.153	0.202	0.691	0.526	0.373	0.375	1.109	0.74	2.0	0.25	0.20	2.00	1.90	2.18	0.04	0.05	0.04	6.25	4.12	4.57	0.08	0.16	0.38	1.31	0.71	16.00	8.07913
6	10097	0.610	0.367	0.243	0.202	0.691	0.526	0.283	0.375	1.109	0.74	2.0	0.10	0.08	1.27	1.20	1.38	0.04	0.04	0.03	2.50	2.32	2.66	0.14	0.28	0.14	0.34	0.60	0.00	0.40554
6	10098	0.610	0.367	0.243	0.202	0.691	0.526	0.283	0.375	1.109	0.74	2.0	0.20	0.15	2.53	2.30	2.64	0.02	0.03	0.02	10.00	5.79	6.09	0.06	0.12	0.25	0.62	0.60	0.00	1.54676
6	10099	0.610	0.367	0.243	0.202	0.691	0.526	0.283	0.375	1.109	0.74	2.0	0.20	0.15	1.79	1.60	1.84	0.04	0.04	0.04	5.00	3.82	3.95	0.09	0.19	0.25	0.62	0.60	1.00	1.29005
6	10100	0.610	0.367	0.243	0.202	0.691	0.526	0.283	0.375	1.109	0.74	2.0	0.20	0.15	1.46	1.40	1.61	0.06	0.05	0.05	3.33	2.89	3.31	0.11	0.22	0.25	0.62	0.60	2.00	1.69816
6	10101	0.610	0.367	0.243	0.202	0.691	0.526	0.283	0.375	1.109	0.74	2.0	0.25	0.19	2.00	1.90	2.18	0.04	0.04	0.04	6.25	4.39	4.88	0.08	0.15	0.31	0.78	0.60	8.50	1.80386
7	10102	0.430	0.367	0.063	0.202	0.691	0.526	0.463	0.500	1.234	0.87	2.0	0.10	0.08	1.27	1.20	1.38	0.04	0.04	0.03	2.50	2.13	2.40	0.21	0.36	0.19	1.27	0.85	44.00	0.81365
7	10103	0.430	0.367	0.063	0.202	0.691	0.526	0.463	0.500	1.234	0.87	2.0	0.20	0.19	2.53	2.50	2.87	0.02	0.04	0.03	10.00	4.96	5.70	0.09	0.15	0.44	3.02	0.85	9.00	3.71007
7	10104	0.430	0.367	0.063	0.202	0.691	0.526	0.463	0.500	1.234	0.87	2.0	0.20	0.16	1.79	1.70	1.95	0.04	0.05	0.04	5.00	3.34	3.71	0.13	0.23	0.37	2.54	0.85	3.00	2.19782
7	10105	0.430	0.367	0.063	0.202	0.691	0.526	0.463	0.500	1.234	0.87	2.0	0.20	0.14	1.46	1.50	1.72	0.06	0.05	0.04	3.33	2.59	3.20	0.16	0.27	0.33	2.22	0.85	3.00	2.55593
7	10106	0.430	0.367	0.063	0.202	0.691	0.526	0.463	0.500	1.234	0.87	2.0	0.25	0.2	2.00	1.90	2.18	0.04	0.05	0.05	6.25	3.81	4.21	0.12	0.21	0.47	3.17	0.85	7.00	5.48271
7	10107	0.520	0.367	0.153	0.202	0.691	0.526	0.373	0.500	1.234	0.87	2.0	0.10	0.08	1.27	1.20	1.38	0.04	0.04	0.03	2.50	2.24	2.55	0.20	0.34	0.16	0.54	0.71	3.00	0.545005
7	10108	0.520	0.367	0.153	0.202	0.691	0.526	0.373	0.500	1.234	0.87	2.0	0.20	0.17	2.53	2.40	2.76	0.02	0.03	0.03	10.00	5.40	5.94	0.08	0.15	0.33	1.11	0.71	17.00	5.075
7	10109	0.520	0.367	0.153	0.202	0.691	0.526	0.373	0.500	1.234	0.87	2.0	0.20	0.15	1.79	1.60	1.84	0.04	0.04	0.04	5.00	3.60	3.72	0.13	0.23	0.29	0.98	0.71	29.00	5.51695
7	10110	0.520	0.367	0.153	0.202	0.691	0.526	0.373	0.500	1.234	0.87	2.0	0.20	0.14	1.46	1.50	1.72	0.06	0.05	0.04	3.33	2.76	3.44	0.15	0.25	0.27	0.92	0.71	28.00	3.32427
7	10111	0.520	0.367	0.153	0.202	0.691	0.526	0.373	0.500	1.234	0.87	2.0	0.25	0.20	2.00	1.90	2.18	0.04	0.05	0.04	6.25	4.12	4.57	0.11	0.19	0.38	1.31	0.71	33.00	5.62908
7	10112	0.610	0.367	0.243	0.202	0.691	0.526	0.283	0.500	1.234	0.87	2.0	0.10	0.08	1.27	1.20	1.38	0.04	0.04	0.03	2.50	2.32	2.66	0.19	0.33	0.14	0.34	0.60	0.00	0.45024
7	10113	0.610	0.367	0.243	0.202	0.691	0.526	0.283	0.500	1.234	0.87	2.0	0.20	0.15	2.53	2.30	2.64	0.02	0.03	0.02	10.00	5.79	6.09	0.08	0.14	0.25	0.62	0.60	2.00	2.41539
7	10114	0.610	0.367	0.243	0.202	0.691	0.526	0.283	0.500	1.234	0.87	2.0	0.20	0.15	1.79	1.60	1.84	0.04	0.04	0.04	5.00	3.82	3.95	0.13	0.22	0.25	0.62	0.60	11.00	4.20843
7	10115	0.610	0.367	0.243	0.202	0.691	0.526	0.283	0.500	1.234	0.87	2.0	0.20	0.15	1.46	1.40	1.61	0.06	0.05	0.05	3.33	2.89	3.31	0.15	0.26	0.25	0.62	0.60	5.50	4.08799
7	10116	0.610	0.367	0.243	0.202	0.691	0.526	0.283	0.500	1.234	0.87	2.0	0.25	0.19	2.00	1.90	2.18	0.04	0.04	0.04	6.25	4.39	4.88	0.10	0.18	0.31	0.78	0.60	16.00	6.61492

Str.	Test No.	hs	hb	d	hc	hcais	hf	Rc	Bb	Bt	Beq	α	Hso	Hsi	Tmo	Tmi	Tpi	smo	smi	smp	Lmo	Lmi	Lpi	Bb/Lpi	Beq/Lpi	Hsi/hs	Hsi/d	hb/hs	Pi (%)	Fh1/250(st.)
8	10121	0.430	0.457	-0.027	0.202	0.691	0.436	0.463	0.250	1.164	0.71	2.0	0.10	0.08	1.27	1.20	1.38	0.04	0.04	0.03	2.50	2.13	2.40	0.10	0.29	0.19	-2.96	1.06	6.50	0.47977
8	10122	0.430	0.457	-0.027	0.202	0.691	0.436	0.463	0.250	1.164	0.71	2.0	0.20	0.19	2.53	2.50	2.87	0.02	0.04	0.03	10.00	4.96	5.70	0.04	0.12	0.44	-7.04	1.06	5.00	2.69534
8	10123	0.430	0.457	-0.027	0.202	0.691	0.436	0.463	0.250	1.164	0.71	2.0	0.20	0.16	1.79	1.70	1.95	0.04	0.05	0.04	5.00	3.34	3.71	0.07	0.19	0.37	-5.93	1.06	15.00	1.53602
8	10124	0.430	0.457	-0.027	0.202	0.691	0.436	0.463	0.250	1.164	0.71	2.0	0.20	0.14	1.46	1.50	1.72	0.06	0.05	0.04	3.33	2.59	3.20	0.08	0.22	0.33	-5.19	1.06	3.50	1.03771
8	10125	0.430	0.457	-0.027	0.202	0.691	0.436	0.463	0.250	1.164	0.71	2.0	0.25	0.2	2.00	1.90	2.18	0.04	0.05	0.05	6.25	3.81	4.21	0.06	0.17	0.47	-7.41	1.06	1.50	3.93762
8	10126	0.520	0.457	0.063	0.202	0.691	0.436	0.373	0.250	1.164	0.71	2.0	0.10	0.08	1.27	1.20	1.38	0.04	0.04	0.03	2.50	2.24	2.55	0.10	0.28	0.15	1.27	0.88	36.00	0.979485
8	10127	0.520	0.457	0.063	0.202	0.691	0.436	0.373	0.250	1.164	0.71	2.0	0.20	0.17	2.53	2.40	2.76	0.02	0.03	0.03	10.00	5.40	5.94	0.04	0.12	0.33	2.70	0.88	12.00	3.34028
8	10128	0.520	0.457	0.063	0.202	0.691	0.436	0.373	0.250	1.164	0.71	2.0	0.20	0.15	1.79	1.60	1.84	0.04	0.04	0.04	5.00	3.60	3.72	0.07	0.19	0.29	2.38	0.88	23.50	4.62458
8	10129	0.520	0.457	0.063	0.202	0.691	0.436	0.373	0.250	1.164	0.71	2.0	0.20	0.14	1.46	1.50	1.72	0.06	0.05	0.04	3.33	2.76	3.44	0.07	0.21	0.27	2.22	0.88	66.00	4.43884
8	10130	0.520	0.457	0.063	0.202	0.691	0.436	0.373	0.250	1.164	0.71	2.0	0.25	0.2	2.00	1.90	2.18	0.04	0.05	0.04	6.25	4.12	4.57	0.05	0.15	0.38	3.17	0.88	19.50	5.73294
8	10131	0.610	0.457	0.153	0.202	0.691	0.436	0.283	0.250	1.164	0.71	2.0	0.10	0.08	1.27	1.20	1.38	0.04	0.04	0.03	2.50	2.32	2.66	0.09	0.27	0.14	0.54	0.75	4.00	0.542285
8	10132	0.610	0.457	0.153	0.202	0.691	0.436	0.283	0.250	1.164	0.71	2.0	0.20	0.15	2.53	2.30	2.64	0.02	0.03	0.02	10.00	5.79	6.09	0.04	0.12	0.25	0.98	0.75	0.90	2.85792
8	10133	0.610	0.457	0.153	0.202	0.691	0.436	0.283	0.250	1.164	0.71	2.0	0.20	0.18	1.79	1.70	1.95	0.04	0.05	0.04	5.00	3.82	4.27	0.06	0.17	0.30	1.18	0.75	11.50	4.65405
8	10134	0.610	0.457	0.153	0.202	0.691	0.436	0.283	0.250	1.164	0.71	2.0	0.20	0.15	1.46	1.40	1.61	0.06	0.05	0.05	3.33	2.89	3.31	0.08	0.21	0.25	0.98	0.75	18.00	3.61553
8	10135	0.610	0.457	0.153	0.202	0.691	0.436	0.283	0.250	1.164	0.71	2.0	0.25	0.19	2.00	1.90	2.18	0.04	0.04	0.04	6.25	4.39	4.88	0.05	0.14	0.31	1.24	0.75	19.00	6.44278
8	10136	0.700	0.457	0.243	0.202	0.691	0.436	0.193	0.250	1.164	0.71	2.0	0.10	0.08	1.27	1.20	1.38	0.04	0.03	0.03	2.50	2.38	2.74	0.09	0.26	0.11	0.33	0.65	0.00	0.42276
8	10137	0.700	0.457	0.243	0.202	0.691	0.436	0.193	0.250	1.164	0.71	2.0	0.20	0.15	2.53	2.40	2.76	0.02	0.02	0.02	10.00	6.14	6.78	0.04	0.10	0.21	0.62	0.65	0.00	1.33133
8	10138	0.700	0.457	0.243	0.202	0.691	0.436	0.193	0.250	1.164	0.71	2.0	0.20	0.15	1.79	1.60	1.84	0.04	0.04	0.04	5.00	4.00	4.15	0.06	0.17	0.21	0.62	0.65	1.00	1.98349
8	10139	0.700	0.457	0.243	0.202	0.691	0.436	0.193	0.250	1.164	0.71	2.0	0.20	0.15	1.46	1.40	1.61	0.06	0.05	0.04	3.33	3.00	3.46	0.07	0.20	0.21	0.62	0.65	4.50	2.02125
8	10140	0.700	0.457	0.243	0.202	0.691	0.436	0.193	0.250	1.164	0.71	2.0	0.25	0.20	2.00	1.80	2.07	0.04	0.04	0.04	6.25	4.63	4.82	0.05	0.15	0.29	0.82	0.65	4.50	4.35814
9	10141	0.340	0.367	-0.027	0.292	0.691	0.616	0.643	0.250	0.984	0.62	2.0	0.20	0.16	1.79	1.70	1.95	0.04	0.05	0.05	5.00	3.03	3.35	0.07	0.18	0.47	-5.93	1.08	23.00	1.41531
9	10142	0.340	0.367	-0.027	0.292	0.691	0.616	0.643	0.250	0.984	0.62	2.0	0.25	0.18	2.00	1.98	2.28	0.04	0.05	0.05	6.25	3.45	3.97	0.06	0.16	0.53	-6.67	1.08	7.50	3.67893
9	10143	0.340	0.367	-0.027	0.292	0.691	0.616	0.643	0.250	0.984	0.62	2.0	0.20	0.15	1.46	1.59	1.83	0.06	0.06	0.05	3.33	2.38	3.11	0.08	0.20	0.44	-5.56	1.08	0.00	1.00744
9	10144	0.340	0.367	-0.027	0.292	0.691	0.616	0.643	0.250	0.984	0.62	2.0	0.25	0.17	2.00	1.76	2.02	0.04	0.05	0.05	6.25	3.45	3.49	0.07	0.18	0.50	-6.30	1.08	8.50	2.27725
9	10145	0.430	0.367	0.063	0.292	0.691	0.616	0.553	0.250	0.984	0.62	2.0	0.10	0.08	1.27	1.20	1.38	0.04	0.04	0.03	2.50	2.13	2.40	0.10	0.26	0.19	1.27	0.85	28.00	1.25232
9	10146	0.430	0.367	0.063	0.292	0.691	0.616	0.553	0.250	0.984	0.62	2.0	0.20	0.19	2.53	2.50	2.87	0.02	0.04	0.03	10.00	4.96	5.70	0.04	0.11	0.44	3.02	0.85	30.00	3.01606
9	10147	0.430	0.367	0.063	0.292	0.691	0.616	0.553	0.250	0.984	0.62	2.0	0.20	0.16	1.79	1.70	1.95	0.04	0.05	0.04	5.00	3.34	3.71	0.07	0.17	0.37	2.54	0.85	71.00	2.61276
9	10148	0.430	0.367	0.063	0.292	0.691	0.616	0.553	0.250	0.984	0.62	2.0	0.20	0.14	1.46	1.50	1.72	0.06	0.05	0.04	3.33	2.59	3.20	0.08	0.19	0.33	2.22	0.85	49.00	4.04697
9	10149	0.430	0.367	0.063	0.292	0.691	0.616	0.553	0.250	0.984	0.62	2.0	0.25	0.2	2.00	1.90	2.18	0.04	0.05	0.05	6.25	3.81	4.21	0.06	0.15	0.47	3.17	0.85	33.00	4.35532
9	10150	0.520	0.367	0.153	0.292	0.691	0.616	0.463	0.250	0.984	0.62	2.0	0.10	0.08	1.27	1.20	1.38	0.04	0.04	0.03	2.50	2.24	2.55	0.10	0.24	0.16	0.54	0.71	0.00	0.34104
9	10151	0.520	0.367	0.153	0.292	0.691	0.616	0.463	0.250	0.984	0.62	2.0	0.20	0.17	2.53	2.40	2.76	0.02	0.03	0.03	10.00	5.40	5.94	0.04	0.10	0.33	1.11	0.71	26.50	1.61999
9	10152	0.520	0.367	0.153	0.292	0.691	0.616	0.463	0.250	0.984	0.62	2.0	0.20	0.15	1.79	1.60	1.84	0.04	0.04	0.04	5.00	3.60	3.72	0.07	0.17	0.29	0.98	0.71	5.00	3.15216
9	10153	0.520	0.367	0.153	0.292	0.691	0.616	0.463	0.250	0.984	0.62	2.0	0.20	0.14	1.46	1.50	1.72	0.06	0.05	0.04	3.33	2.76	3.44	0.07	0.18	0.27	0.92	0.71	16.00	2.45427
9	10154	0.520	0.367	0.153	0.292	0.691	0.616	0.463	0.250	0.984	0.62	2.0	0.25	0.20	2.00	1.90	2.18	0.04	0.05	0.04	6.25	4.12	4.57	0.05	0.14	0.38	1.31	0.71	11.00	4.76602
9	10155	0.610	0.367	0.243	0.292	0.691	0.616	0.373	0.250	0.984	0.62	2.0	0.10	0.08	1.27	1.20	1.38	0.04	0.04	0.03	2.50	2.32	2.66	0.09	0.23	0.14	0.34	0.60	0.00	0.35912
9	10156	0.610	0.367	0.243	0.292	0.691	0.616	0.373	0.250	0.984	0.62	2.0	0.20	0.15	2.53	2.30	2.64	0.02	0.03	0.02	10.00	5.79	6.09	0.04	0.10	0.25	0.62	0.60	0.00	1.34588
9	10157	0.610	0.367	0.243	0.292	0.691	0.616	0.373	0.250	0.984	0.62	2.0	0.20	0.15	1.79	1.60	1.84	0.04	0.04	0.04	5.00	3.82	3.95	0.06	0.16	0.25	0.62	0.60	0.00	1.03446
9	10158	0.610	0.367	0.243	0.292	0.691	0.616	0.373	0.250	0.984	0.62	2.0	0.20	0.15	1.46	1.40	1.61	0.06	0.05	0.05	3.33	2.89	3.31	0.08	0.19	0.25	0.62	0.60	1.50	1.08353
9	10159	0.610	0.367	0.243	0.292	0.691	0.616	0.373	0.250	0.984	0.62	2.0	0.25	0.19	2.00	1.90	2.18	0.04	0.04	0.04	6.25	4.39	4.88	0.05	0.13	0.31	0.78	0.60	0.00	1.5819
9	10160	0.700	0.367	0.333	0.292	0.691	0.616	0.283	0.250	0.984	0.62	2.0	0.10	0.08	1.27	1.20	1.38	0.04	0.03	0.03	2.50	2.38	2.74	0.09	0.23	0.11	0.24	0.52	0.00	0.39466
9	10161	0.700	0.367	0.333	0.292	0.691	0.616	0.283	0.250	0.984	0.62	2.0	0.20	0.15	2.53	2.40	2.76	0.02	0.02	0.02	10.00	6.14	6.78	0.04	0.09	0.21	0.45	0.52	0.00	1.13688
9	10162	0.700	0.367	0.333	0.292	0.691	0.616	0.283	0.250	0.984	0.62	2.0	0.20	0.15	1.79	1.60	1.84	0.04	0.04	0.04	5.00	4.00	4.15	0.06	0.15	0.21	0.45	0.52	0.70	1.24267
9	10163	0.700	0.367	0.333	0.292	0.691	0.616	0.283	0.250	0.984	0.62	2.0	0.20	0.15	1.46	1.40	1.61	0.06	0.05	0.04	3.33	3.00	3.46	0.07	0.18	0.21	0.45	0.52	2.00	1.0657
9	10164	0.700	0.367	0.333	0.292	0.691	0.616	0.283	0.250	0.984	0.62	2.0	0.25	0.20	2.00	1.80	2.07	0.04	0.04	0.04	6.25	4.63	4.82	0.05	0.13	0.29	0.60	0.52	0.00	1.82849
10	10165	0.340	0.457	-0.117	0.292	0.691	0.526	0.643	0.250	1.164	0.71	2.0	0.20	0.16	1.79	1.70	1.95	0.04	0.05	0.05	5.00	3.03	3.35	0.07	0.21	0.47	-1.37	1.34	46.00	0.85848
10	10166	0.340	0.457	-0.117	0.292	0.691	0.526	0.643	0.250	1.164	0.71	2.0	0.25	0.18	2.00	1.98	2.28	0.04	0.05	0.05	6.25	3.45	3.97	0.06	0.18	0.53	-1.54	1.34	44.00	1.52498
10	10167	0.340	0.457	-0.117	0.292	0.691	0.526	0.643	0.250	1.164	0.71	2.0	0.20	0.15	1.46	1.59	1.83	0.06	0.06	0.05	3.33	2.38	3.11	0.08	0.23	0.44	-1.28	1.34	37.00	0.60687
10	10168	0.340	0.457	-0.117	0.292	0.691	0.526	0.643	0.250	1.164	0.71	2.0	0.25	0.17	2.00	1.76	2.02	0.04	0.05	0.05	6.25	3.45	3.49	0.07	0.20	0.50	-1.45	1.34	78.50	1.08051
10	10169	0.430	0.457	-0.027	0.292	0.691	0.526	0.553	0.250	1.164	0.71	2.0	0.10	0.08	1.27	1.20	1.38	0.04	0.04	0.03	2.50	2.13	2.40	0.10	0.29	0.19	-2.96	1.06	6.50	0.443445
10	10170	0.430	0.457	-0.027	0.292	0.691	0.526	0.553	0.250	1.164	0.71	2.0	0.20	0.19	2.53	2.50	2.87	0.02	0.04	0.03	10.00	4.96	5.70	0.04	0.12	0.44	-7.04	1.06	26.00	2.48799

Str.	Test No.	hs	hb	d	hc	hcais	hf	Rc	Bb	Bt	Beq	α	Hso	Hsi	Tmo	Tmi	Tpi	smo	smi	smp	Lmo	Lmi	Lpi	Bb/Lpi	Beq/Lpi	Hsi/hs	Hsi/d	hb/hs	Pi (%)	Fh1/250(st.)
10	10171	0.430	0.457	-0.027	0.292	0.691	0.526	0.553	0.250	1.164	0.71	2.0	0.20	0.16	1.79	1.70	1.95	0.04	0.05	0.04	5.00	3.34	3.71	0.07	0.19	0.37	-5.93	1.06	14.00	1.27641
10	10172	0.430	0.457	-0.027	0.292	0.691	0.526	0.553	0.250	1.164	0.71	2.0	0.20	0.14	1.46	1.50	1.72	0.06	0.05	0.04	3.33	2.59	3.20	0.08	0.22	0.33	-5.19	1.06	19.50	1.5838
10	10173	0.430	0.457	-0.027	0.292	0.691	0.526	0.553	0.250	1.164	0.71	2.0	0.25	0.2	2.00	1.90	2.18	0.04	0.05	0.05	6.25	3.81	4.21	0.06	0.17	0.47	-7.41	1.06	40.50	2.79928
10	10174	0.520	0.457	0.063	0.292	0.691	0.526	0.463	0.250	1.164	0.71	2.0	0.10	0.08	1.27	1.20	1.38	0.04	0.04	0.03	2.50	2.24	2.55	0.10	0.28	0.15	1.27	0.88	60.00	1.5018
10	10176	0.520	0.457	0.063	0.292	0.691	0.526	0.463	0.250	1.164	0.71	2.0	0.20	0.15	1.79	1.60	1.84	0.04	0.04	0.04	5.00	3.60	3.72	0.07	0.19	0.29	2.38	0.88	4.00	3.59402
10	10177	0.520	0.457	0.063	0.292	0.691	0.526	0.463	0.250	1.164	0.71	2.0	0.20	0.14	1.46	1.50	1.72	0.06	0.05	0.04	3.33	2.76	3.44	0.07	0.21	0.27	2.22	0.88	67.00	2.05002
10	10178	0.520	0.457	0.063	0.292	0.691	0.526	0.463	0.250	1.164	0.71	2.0	0.25	0.20	2.00	1.90	2.18	0.04	0.05	0.04	6.25	4.12	4.57	0.05	0.15	0.38	3.17	0.88	11.00	4.03505
10	10179	0.610	0.457	0.153	0.292	0.691	0.526	0.373	0.250	1.164	0.71	2.0	0.10	0.08	1.27	1.20	1.38	0.04	0.04	0.03	2.50	2.32	2.66	0.09	0.27	0.14	0.54	0.75	4.00	0.49371
10	10180	0.610	0.457	0.153	0.292	0.691	0.526	0.373	0.250	1.164	0.71	2.0	0.20	0.15	2.53	2.30	2.64	0.02	0.03	0.02	10.00	5.79	6.09	0.04	0.12	0.25	0.98	0.75	0.00	2.4862
10	10181	0.610	0.457	0.153	0.292	0.691	0.526	0.373	0.250	1.164	0.71	2.0	0.20	0.15	1.79	1.60	1.84	0.04	0.04	0.04	5.00	3.82	3.95	0.06	0.18	0.25	0.98	0.75	14.00	3.40488
10	10183	0.610	0.457	0.153	0.292	0.691	0.526	0.373	0.250	1.164	0.71	2.0	0.25	0.19	2.00	1.90	2.18	0.04	0.04	0.04	6.25	4.39	4.88	0.05	0.14	0.31	1.24	0.75	61.50	5.41317
10	10184	0.700	0.457	0.243	0.292	0.691	0.526	0.283	0.250	1.164	0.71	2.0	0.10	0.08	1.27	1.20	1.38	0.04	0.03	0.03	2.50	2.38	2.74	0.09	0.26	0.11	0.33	0.65	0.00	0.40998
10	10185	0.700	0.457	0.243	0.292	0.691	0.526	0.283	0.250	1.164	0.71	2.0	0.20	0.15	2.53	2.40	2.76	0.02	0.02	0.02	10.00	6.14	6.78	0.04	0.10	0.21	0.62	0.65	0.00	1.24335
10	10186	0.700	0.457	0.243	0.292	0.691	0.526	0.283	0.250	1.164	0.71	2.0	0.20	0.15	1.79	1.60	1.84	0.04	0.04	0.04	5.00	4.00	4.15	0.06	0.17	0.21	0.62	0.65	2.00	1.92518
10	10187	0.700	0.457	0.243	0.292	0.691	0.526	0.283	0.250	1.164	0.71	2.0	0.20	0.15	1.46	1.40	1.61	0.06	0.05	0.04	3.33	3.00	3.46	0.07	0.20	0.21	0.62	0.65	5.00	1.99422
10	10188	0.700	0.457	0.243	0.292	0.691	0.526	0.283	0.250	1.164	0.71	2.0	0.25	0.20	2.00	1.80	2.07	0.04	0.04	0.04	6.25	4.63	4.82	0.05	0.15	0.29	0.82	0.65	6.00	5.45358